The vaccinia virus N2 protein associates with karyopherins α2 and α4 and reduces the turnover rate of karyopherin α2

by

Megan Amanda Desaulniers

A thesis submitted in partial fulfillment of the requirements for the degree of

Master of Science

in

Virology

Department of Medical Microbiology and Immunology
University of Alberta

**ABSTRACT**

Due to their large genomes, poxviruses encode a number of enzymes, including a DNA polymerase and a DNA-dependent RNA polymerase, and therefore require few host gene factors for their replication. Several studies have shown several host nuclear factors are in fact recruited to viral sites of replication. Using bioinformatics we identified a putative bipartite nuclear localization signal in vaccinia virus N2L. Through immuno-precipitation, we were able to show that N2 interacts with two nuclear import proteins, karyopherins (KPN) alpha 2 and alpha 4. Immunofluorescence analysis indicated that in the presence of N2, KPNα2 was found evenly dispersed throughout the cell. However, when N2 is absent from the infection, KPNα2 accumulates at the nuclear periphery. Using Fluorescence Recovery After Photobleaching (FRAP), we show that the presence of N2 retards the nuclear turnover rate of KPNα2. Taken together, we suggest that N2 is competing for available KPNα2 to modulate nuclear transport thus promoting virulence.

**PREFACE**

The animal studies were approved by the Animal Care and Use Committee (ACUC) and the Research Ethics Office (University of Alberta) under the title "Vaccinia virus virulence determination". The approval date was the 21 of May, 2013 and the study ID number is AUP00000506.

**ACKNOWLEDGEMENTS**

**TABLE OF CONTENTS**

## LIST OF TABLES

## LIST OF FIGURES

## LIST OF ABBREVIATIONS

| | |
|---|---|
| 6-TG | 6-thioguanine |
| AraC | cytosine arabinoside |
| BFP | blue fluorescent protein |
| BSA | bovine serum albumin |
| CEV | cell-associated enveloped virus |
| CMPV | camelpox virus |
| CMV | cytomegalovirus |
| CPVX | cowpox virus |
| C-terminal | carboxy terminal |
| DAPI | 4', 6'-diamidino-2-phenylindole |
| DISC | death-inducing signaling complex |
| DMEM | Dulbecco's modified Eagle's medium |
| DNA | deoxyribonucleic acid |
| ds | double stranded |
| DUBs | deubiquitinases |
| EBV | Epstein-Barr virus |
| ECTV | ectromelia virus |
| EDTA | ethylenediamine tetraacetic acid |
| EFC | entry/fusion complex |
| E/L | early/late |
| EMCV | encephalomyocarditis virus |
| ER | endoplasmic reticulum |
| EV | extracellular virions |
| FBS | fetal bovine serum |
| FRAP | fluorescence recovery after photobleaching |
| GAGs | glycosaminoglycans |
| GFP | green fluorescent protein |
| hnRNP C1/C2 | heterogenous nuclear riboprotein complex C1/C2 |
| His or His$_6$ | hexahistidine epitope tag |
| HSV | herpes simplex virus |
| i.d. | intradermal |
| IFN | interferon |
| I$\kappa$B | inhibitor of $\kappa$B |
| IKK | I$\kappa$B kinase |
| i.n. | intranasal |
| IP | immunoprecipitation |
| IRF | interferon regulatory transcription factor |
| ISG | interferon stimulated genes |
| KPN | karyopherin |
| MEM | minimum essential medium |
| MOI | multiplicity of infection |
| MPA | mycophenolic acid |
| MPVX | monkeypox virus |
| mRNA | messenger RNA |

| | |
|---|---|
| MV | mature virions |
| NFκB | nuclear factor κB |
| NPC | nuclear pore complex |
| NLS | nuclear localization signal |
| N-terminal | amino terminal |
| OPV | Orthopoxvirus |
| PBS | phosphate buffered saline |
| PBS-T | PBS with 0.1% tween |
| PCR | polymerase chain reaction |
| PFU | plaque forming unit |
| PHD2 | prolyl hydroxylase domain-containing protein 2 |
| PKR | protein kinase R |
| RE | restriction enzyme |
| RNA | ribonucleic acid |
| RT | room temperature |
| SIAS | Sequences Identities and Similarities |
| SARS-CoV | severe acute respiratory syndrome coronavirus |
| SDS | sodium dodecyl sulfate |
| SSB | single stranded binding protein |
| ssDNA | single-stranded DNA |
| TAE | Tris/Acetate/EDTA |
| TAGC | The Applied Genomics Core |
| TCA | trichloroacetic acid |
| TLR | toll-like receptor |
| TNF | tumor necrosis factor |
| TRAF | TNF receptor associated factors |
| *ts* | temperature-sensitive |
| VACV | vaccinia virus |
| VARV | variola virus |
| VETF | virus early transcription factor |
| VSV | varicella-zoster virus |
| WB | western blot |
| WHO | World Health Organization |
| WR | western reserve |
| YFP | yellow fluorescent protein |

**CHAPTER 1 - INTRODUCTION**

**1.1. POXVIRUSES**

**1.1.1. Smallpox**

Smallpox is an infectious disease that devastated mankind for centuries [1]. The disease is caused by either Variola major or Variola minor [2, 3]. Variola major is the more common strain and it produces a more serious disease with mortality rates as high as 30 to 35% [3, 4]. Variola minor produces a milder disease with a mortality rate of 1% or less [3, 4]. Humans are the only reservoir for smallpox and thus the virus has to spread from one individual to another for continuous survival [5]. The virus is spread by direct contact with an infected individual or bodily fluid, or contaminated items such as bedding [3, 6]. It is estimated that in the twentieth century, smallpox was responsible for 300-500 million deaths [7].

The earliest method of prevention was called variolation which involved deliberate infection of an individual with live variola virus [1]. Those who were treated by variolation developed a milder form of the disease [1]. However, because the individual was infected with live variola virus, there was a chance that a severe infection would result which could then be transmitted to others [1]. The mortality rate of variolation was approximately 2%, which was one tenth of the mortality rate of the disease [1]. When variolation was successful, it produced lasting immunity to subsequent smallpox infections [8]. Thanks to the earlier work done by Edward Jenner (1749-1823) [9] and eventually an aggressive

vaccination campaign, the World Health Organization (WHO) declared the eradication of smallpox in 1979 [10].

### 1.1.2. History of vaccination

Edward Jenner was an English physician and a scientist who is credited for pioneering the world's first vaccine, the smallpox vaccine, which eventually led to the eradication of smallpox [11]. Hearing tales of dairymaids being naturally protected against smallpox once they have been infected with cowpox led Jenner to believe that cowpox can effectively protect against the smallpox disease [1, 6, 12]. Furthermore, Jenner noted that cowpox could be deliberately transmitted from one person to another as a mechanism of protection [1]. He hypothesized that if cowpox could provide protection against smallpox, then immunity to smallpox can be produced more safely than through variolation [6]. His work demonstrated the first scientific attempt to manage an infectious disease by means of vaccination [1].

The thought of using cowpox as a protective measure against smallpox excited Jenner, and in May of 1796, Jenner took matter from a cowpox lesion formed on a dairymaid (Sarah Nelms) and used it to deliberately inoculate an 8 year old boy (James Phipps) [1, 6, 12]. Phipps developed a mild fever however he recovered from the infection [12]. Two months later, Jenner inoculated Phipps with matter from a smallpox lesion, and was elated to discover that Phipps did not develop smallpox [1, 6]. In fact, the cowpox infection had induced immunity to smallpox and provided the boy with complete protection [1, 10]. Jenner called this new

prevention technique "vaccination" (the Latin word for cow is *vacca* and cowpox is *vaccinia*) and it eventually replaced the practice of variolation [1]. During some point in the nineteenth century, the virus used for smallpox vaccinations switched from cowpox virus to vaccinia virus (VACV) [13]. VACV is related to both variola virus and cowpox virus, all belonging to the Orthopoxvirus genus [3], however the origin of VACV is unknown [14].

### 1.1.3. Orthopoxviruses

Both variola (VARV) and VACV along with a number of animal poxviruses belong to the Orthopoxvirus (OPV) genus (**Figure 1-1**), which is part of the subfamily Chordopoxvirinae and the Poxviridae family [3]. VARV is arguably the most famous member of OPV genus, as it is the causative agent of smallpox [15]. VACV is also a well known member of this family, as it was used as the vaccine to eradicate VARV [3, 15]. Other members of OPV include cowpox (CPVX), monkeypox (MPVX), ectromelia (ECTV), camelpox (CMPV), and taterapox [15]. Although humans are a natural host for VARV, we are susceptible to incidental infection with other OPVs [16, 17]. These zoonotic OPVs include MPVX [16, 17], CPXV [16, 17], CMPX [16], and VACV [16, 17].

The members of the OPV genus all share common characteristics. These viruses are large, enveloped brick-shaped viruses with the capsid measuring around 270X350 nm in size [3]. They have a double stranded DNA (dsDNA) genome that is approximately 200 kb in size with AT-rich hairpins [3, 18]. The different viruses encode 150-200 genes, with VARV having the smallest genome

| Family | Subfamily | Genus | Species |
|---|---|---|---|
| *Poxviridae* | *Chordopox virinae* | *Avipoxvirus* *Capripoxvirus* *Leporipoxvirus* *Molluscipoxvirus* | |
| | | *Orthopoxvirus* | *Camelpox virus* *Cowpox virus* *Ectromelia virus* *Monkeypox virus* *Taterapox virus* *Vaccinia virus* *Variola virus* |
| | | *Parapoxvirus* *Suipoxvirus* *Yatapoxvirus* | |
| | *Entomopox virinae* | | |

**Figure 1-1: Poxvirus classification.** Poxviruses can be divided into two subfamilys, *Chordopoxvirinae* which infect vertebrates, and *Entomopoxvirinae* which infect invertebrates. The *Chordopoxvirinae* subfamily can be further divided into eight genera. *Vaccinia virus* falls under the *Orthopoxvirus* genus.

and CPVX having the largest [3, 16, 17]. Unlike most DNA viruses, poxvirus replication is unique in that they exclusively replicate in the cytoplasm of the host cell in structures called "viral factories" [3].

The replication cycle of poxviruses can be separated into the following steps: entry, early gene expression, uncoating, DNA replication, intermediate and late gene expression, and finally morphogenesis (see **Figure 1-2**) (reviewed in [19]).

The mechanism in which poxviruses enter the cell is poorly understood [3]. This in part is due to the presence of two structurally different virions, mature virions (MVs) and extracellular virions (EVs), the later having an additional membrane with at least six unique proteins [20, 21]. As a result of EVs additional membrane, the two types of virions don't share any common viral proteins, therefore each type uses different attachment factors [20]. Two different entry pathways have been described for both virions, which are direct fusion with the plasma membrane or entry by macropinocytosis [20, 21].

Both types of virions are capable of entering the cell through fusion with the plasma membrane [21]. The MV particles are thought to interact with cellular glycosaminoglycans (GAGs) as well as additional surface molecules [20, 21]. Three viral proteins have been identified to bind to GAGs. A27 [22] and H3 [23] bind to heparin sulfate and D8 binds to chondroitin sulfate [24]. Two other viral proteins, A26 and L1, are implicated in host cell binding through a GAG-independent mechanism [20]. A26 binds to laminin [25] whereas L1 doesn't have a known cellular factor [26]. An entry/fusion complex (EFC), involving 11 viral
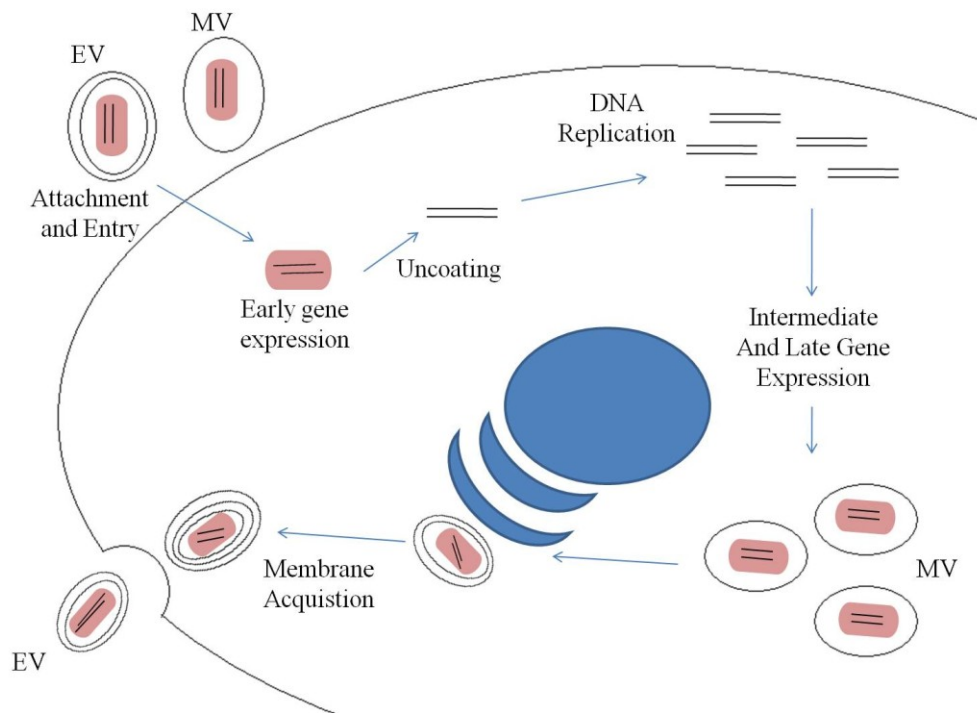
**Figure 1-2: Poxvirus Replication cycle.** The replication cycle of poxviruses can be broken down into several steps. First the virus particle enters the cell. Once the virus core reaches the cytoplasm it immediately begins early gene expression. After early gene expression, the virus uncoats and DNA replication begins. Intermediate and late gene expression follow DNA replication. The last step is viral morphogenesis where newly formed virions are wrapped with membrane(s).

proteins (8 transmembrane proteins and 3 viral membrane proteins), mediates the fusion of the viral envelope with the plasma membrane, allowing the viral core to enter the cytoplasm [20]. For EVs, it is thought that the GAGs disrupt the fragile outer membrane, which exposes the inner MV particle and the EFC which then fuses to the plasma membrane [20].

Alternatively, both MV and EVs can enter the cells through macropinocytosis [20]. This mechanism provides several benefits to the virus, including avoiding the cytoskeleton barrier, lack of viral components left at the plasma membrane that could be recognized by the innate immune system, and the acidic environment and/or proteases present in the endosome may activate the viral membrane fusion process to release the core at the appropriate cytoplasmic location [20]. Electron micrographs have depicted virus particles bound to the plasma membrane, as well as being internalized by macropinocytosis [20]. In this scenario, the EVs second membrane is thought to be disrupted by the acidic environment of the endosome, exposing the MV particle [20]. The MV particle can fuse to the endosomal membrane through the EFC, releasing the viral core into the cytoplasm [20].

As the virus core is released into the cytoplasm, it immediately activates early gene transcription [27, 28]. This is possible because the virus core itself contains a number of viral enzymes and associated proteins that are necessary for the start of early gene synthesis which occurs inside the viral capsid [29, 30]. These enzymes include a RNA polymerase, a virus early transcription factor (VETF), a capping enzyme and a poly (A) polymerase [28, 30]. The viral mRNA

of the early genes is synthesized inside the capsid and exported through pores before the uncoating process begins [30]. Early genes encode proteins needed for DNA replication, intermediate gene transcription, as well as immune evasion proteins [31, 32]. Approximately half of VACV genes are classified as early genes [30]. Interestingly, all the early genes are transcribed by the VETF, which is a heterodimer of the D6R and A7L gene products, and the RNA polymerase [30].

Once the early gene expression reaches its peak, the virus starts replicating its genome [29]. The majority of genes required for replication are expressed early, with only a few exceptions of replication proteins packaged inside the virion [31]. Four of the viral early proteins that are necessary for the release of the genomic DNA are B1R, I3L, H5R, and E8R [29]. The B1 protein is a protein kinase [33] and is known to phosphorylate the H5 protein [34], which binds to the double stranded DNA [29]. The I3 protein is the viral single stranded DNA binding protein [35], and is involved in replication as well as organization of the early DNA factories [36]. The E8 protein also binds to the genome DNA [37]. More interesting, the E8 membrane protein has two putative transmembrane domains [29]. It has been speculated that E8, which localizes to the ER during infection [38], may mediate the association of the viral genome with the ER [29]. Once E8 becomes phosphorylated by the viral late protein kinase (F10L) [31, 37], E8 loses its DNA binding properties [29]. Interestingly, the B1 protein kinase is unable to phosphorylate E8 [29]. The viral DNA polymerase is encoded by the E9L gene which possesses polymerase as well as the 3' to 5' proofreading exonuclease activites [27].

Only full replicated genomes can serve as templates for intermediate and late gene expression [38]. Once DNA replication reached a threshold, intermediate gene expression can occur [19]. Intermediate genes encode for late gene transcription factors [19]. This ensures that the genes are expressed in succession [31]. Structural proteins that make up the new virus particles as well as the enzymes that are packaged in the core that initiate transcription upon infection are encoded by the late genes [19].

The final step in the lifecycle is the assembly of the structural proteins and packaging of the genome [39]. These newly formed immature viruses undergo the process of morphogenesis and acquire a membrane envelope to form MVs (reviewed in [39]). The majority of the newly synthesized virions end morphogenesis at this stage and are released upon cell lysis [19]. However, a small proportion, approximately 1% [39], of the MVs undergo further morphogenesis, acquiring two additional membranes (thought to be obtained from the Golgi) as they move to the cell periphery [19]. These viruses exit the cell by fusing their outer most membrane with the cell membrane, producing cell-associated enveloped virus (CEV), which once released from the cell will become EVs [40]. These two forms have different purposes, with MVs believed to play apart in transmission between hosts whereas EVs are important for viral spread within the host [19, 40].

It was previously thought that poxviruses could replicate independently of the host nucleus since they encode enzymes that are required for DNA replication, transcription, and modification [41]. However, early studies had already shown

that poxviruses were capable of early and late gene expression in the absence of the host cell nucleus, yet the newly synthesized virions were not infectious [41], implying that the nucleus is needed for a productive infection [42]. Consistently, more recent finding from Sivan *et al*. demonstrated that siRNAs targeting the nuclear pore genes, specifically Nup62, reduced VACV replication and spread, as a result of a delay in virion morphogenesis [43]. Furthermore, certain host proteins, such as topoisomerase II$\alpha$/$\beta$ [44], are recruited from the nucleus to sites of viral replication [45]. Finally, there are multiple examples of VACV proteins that locate to the nucleus during infection including C4 [46], C6 [47], C16 [48], B14 [49], E3 [50], and F16 [51]. The theme of the nuclear involvement in VACV infection will be discussed in later sections.

## 1.2. OVERVIEW OF INNATE IMMUNE RESPONSE TO VIRUSES

### 1.2.1. Viruses vs host

Viruses are small infectious particles that require a living host to replicate and spread. Upon infection, the virus triggers the host cells innate immune system, which under normal circumstances will eliminate the infection [52]. Some viral infections are unfavorable for the host. As a defense mechanism, the host has evolved sophisticated antiviral mechanisms to eliminate the virus and prevent the spread to uninfected cells. However, viruses have evolved counter mechanisms to target the host innate immune response and guarantee survival [53]. The co-evolution of the host and pathogen results in novel cellular antiviral mechanisms as well as novel viral inhibitors to target these mechanisms [54].

One line of cellular defense is apoptosis, a conserved process of programmed cell death [55]. Hosts cells use apoptosis to limit viral replication and spread [56]. It is not surprising that viruses have evolved complex strategies to inhibit apoptosis to allow for their continued proliferation [55]. Signals that initiate apoptosis can be detected by internal sensors, triggering the intrinsic pathway, or can be activated through an external stimulus, such as death receptors at the cell surface, triggering the extrinsic pathway [55]. Both pathways involve two apoptotic protein families [55], caspases and Bcl-2 proteins. The caspase proteases are necessary to coordinate proteolytic events during apoptosis [55]. The Bcl-2 protein family regulates the events of apoptosis [55]. The Bcl-2 family can be further divided into two groups, the anti-apoptotic (Bcl-2 and Bcl-X$_1$) and the pro-apoptotic (Bax, Bak, and Bid) members [55]. The intrinsic pathway is initiated by the BH3 domain-only internal sensors [57]. The BH3 domain-only proteins activate the pro-apoptotic members of Bcl-2 family [57]. Once activated, the pro-apoptotic members form pores in the outer mitochondrial membrane resulting in the release of compounds such as cytochrome c [57]. The loss of mitochondrial integrity is prevented by the anti-apoptotic family members [57]. Once in the cytoplasm, cytochrome c activates the apoptosome, which includes Apaf1 and pro-caspase 9 [57]. Pro-caspase 9 in the complex is self cleaved into its active form, caspase 9, which then initiates the effector caspase cascade (includes caspases 2, 3, 6, and 7) [57]. The extrinsic pathway is triggered by the death receptors binding to the TNF family death ligands [57]. Following activation of the death receptor, pro-caspase 8 (or pro-caspase 10) is recruited to form a death-

inducing signaling complex (DISC) [57]. This recruitment results in the cleavage of pro-caspases into their active forms which then function as initiator caspases that activate the effector caspase cascade [57]. The intrinsic pathway is also triggered by caspase 8 or caspase 10, which cleave the pro-apoptotic protein Bid into t-Bid [55, 57]. In order to escape apoptosis, viruses inhibit the activation of death receptors, inhibit caspases, or encode for homologs of the anti-apoptotic Bcl-2 proteins [58]. These mechanisms allow the virus to prevent premature cell death, which would have detrimental effects on virus production [58].

In addition to apoptosis, viruses also target the NFκB signaling pathway. Activation of the apoptotic pathway through tumor necrosis factor (TNF) receptors simultaneously activates TNF receptor associated factors (TRAFs) which results in the activation the NFκB signaling cascade. NFκB is an important regulator of the cells fate. It is the factor deciding whether the cell undergoes apoptosis or proliferation [59]. NFκB is a major transcription factor composed of hetero- or homodimers of the Rel protein family (RelA (p65), RelB, c-Rel, NFκB1 (p50), and NFκB2 (p52)) [60]. The transcription factor complex is held in an inactive state in the cytoplasm by inhibitor proteins called inhibitors of kappa B (IkBs) [60]. The IκB proteins mask the NLS signal of NFκB transcription factors, preventing their translocation into the nucleus [60]. The NFκB pathway is activated by two different mechanisms, one being the canonical pathway, which is triggered through toll-like receptors and TNFα and is crucial for innate immunity and cell survival [60]. The alternate pathway is not activated by TNFα and is required for adaptive immunity [60]. In both pathways, the IκB protein is

phosphorylated and degraded, releasing the NFκB transcription factor [60]. Once released, the NFκB transcription factor translocates to the nucleus and induces expression of inflammatory cytokines, chemokines, immunoreceptors, and others [60]. Because of its extensive role in the host immune response, the NFκB pathway is often targeted by viruses.

Interferons (IFNs) are another host immune defense mechanism [54]. IFNs are a family of soluble proteins secreted from the cell. They are involved in inhibition of cell growth, promotion of apoptosis, and induction of an antiviral state [54]. Once secreted, IFNs bind to specific receptors on the other cells Binding activates a signaling cascade, resulting in the production of antiviral and immune modulatory proteins through members of the interferon regulatory transcription factor (IRF) family [61]. Interferon stimulated genes (ISGs) induce expression of additional IFN, and proteins that target viral replication [62]. Upon viral infection, dsRNA begins to appear within the cell. The dsRNA-dependent protein kinase R (PKR) binds to this dsRNA and as a result, it activates the IFN system [54]. Many examples exist of viral inhibitors possessing dsRNA binding properties to prevent the activation of IFN. The influenza protein NS1 is a dsRNA binding protein that functions to prevent the expression of IFNα and IFNβ by inhibiting the activation of IRF3 [63]. The ebola virus protein VP25 also acts in a similar manner by binding dsRNA and blocking IRF3 activation [64]. The NFκB pathway is also activated in the presence of dsRNA through PKR [54]. Upon translocation to the nucleus, NFκB binds to the IFN-β promoter as part of an enhanceasome (multi-protein transcription complex) [54]. This example

demonstrates how complex and intertwined the different host defense mechanisms are.

## 1.2.2. Immune evasion strategies of vaccinia virus

VACV is a remarkable virus when one considers the number of virulence factors it encodes to modulate the hosts immune response (reviewed in [32, 65, 66]). In fact, VACV dedicates between 33-50% of its genome to these genes [13, 32]. The majority of these proteins are expressed early in infection to suppress the host innate immune system quickly [32]. These genes have diverse functions, yet there are several examples where the same cellular pathway is targeted by multiple proteins acting in a non-redundant fashion [32].

As discussed earlier, the NFκB pathway is an important target to viruses as it is a key transcription factor that controls the fate of the cell. The NFκB pathway is complex and different viruses manipulate it differently. Some viruses, such as the Epstein-Barr virus (EBV), for example, rely on the constitutive activity of this pathway [67]. In cases where it is blocked, the cells undergo apoptosis [67]. However other viruses, such as varicella-zoster virus (VZV), inhibit the NFκB pathway to inhibit the cellular antiviral responses [68]. VACV is no different in its attempt to inhibit the NFκB pathway. Ten intracellular VACV proteins are known to inhibit NFκB activation (**Figure 1-3**) [32]. The A46 protein inhibits the activation NFκB (and IRF3 activation (discussed later in this section)) by binding to the adaptor molecules (TRIM, TRAM, TIRAP, MyD88) associated with TLRs and IL-1R [69]. This association prevents the activation of MAP
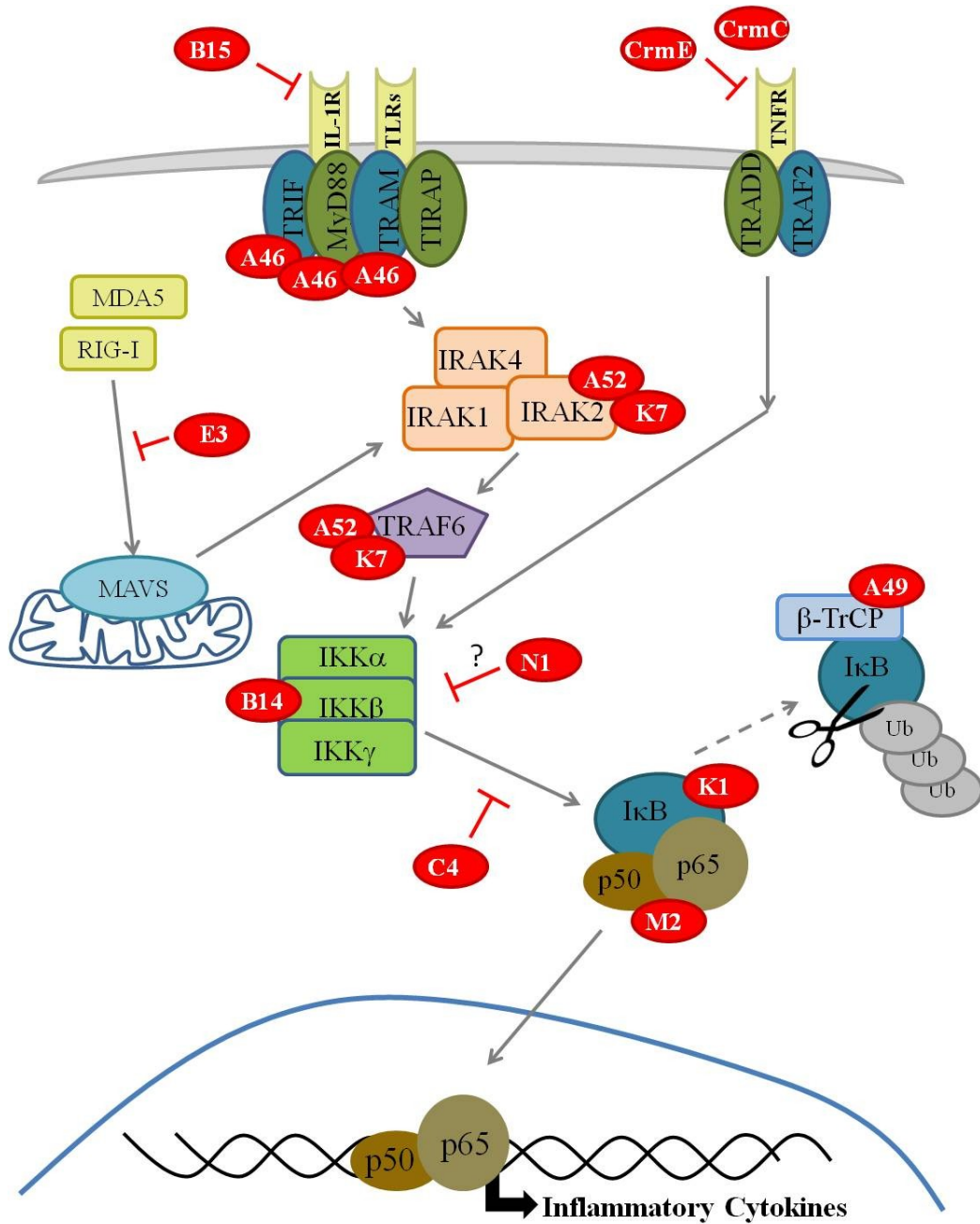
**Figure 1-3: Vaccinia inhibitors of NFκB.** Vaccinia encodes for multiple proteins that inhibit NFκB activation. The vaccinia proteins are depicted in red.

kinases which act in the signaling cascade [69]. The A52 [70] and K7 [71] proteins bind to both IRAK2 and TRAF6. These three proteins act early in the pathway, but they only act on signals generated from TLRs and IL-1β, and not from TNFα signals [32]. The remaining proteins all act downstream of where these two pathways converge, therefore inhibiting NFκB activation through either pathway [32]. The N1 and C4 block NFκB activation, but their mechanisms of action are still under examination or unknown [32]. The N1 protein was originally reported to bind to the IKK complex [72], but this finding has been disputed [73]. In a separate study, immunoprecipitations with N1 detected no interaction between N1 and IKKα, IKKβ, or IKKγ [73]. Furthermore, a luciferase reporter assay showed that N1 did not inhibit IL-1 induced NFκB dependent gene expression during a VACV infection [74]. The C4 protein, however, is thought to act at or downstream of the IKK complex through an unknown mechanism [46]. B14 prevents the phophorylation of IκBα by binding the IKKβ [73]. The E3 protein binds to dsRNA, preventing activation of the PKR pathway [75, 76]. E3 also prevents activation of NFκB by disrupting the RNA polymerase III dsDNA sensing pathway [77]. Both A49 and K1 proteins prevent the degradation of IκBα [32]. A49 binds to the β-TrCP protein, which is an E3 ubiquitin ligase [78]. Even if IκBα is phosphorylated, IκBα is not ubiquinated or targeted for degradation in the presence of A49 [78]. The mechanism in which the K1 protein prevents IκBα from being degraded is still unknown [79]. Finally, the M2 protein prevents the nuclear translocation of p65 [80]. Clearly, VACV employs several diverse strategies to nullify the NFκB pathway.

VACV significantly reduces the amount of IFN-β production by blocking NFκB activation. VACV also encodes multiple proteins that block IRF3 activation [32], including A46, E3, K7, C6, C16, and N2 [32]. As mentioned earlier, A46 can bind to adaptor molecules (TRIM, TRAP, TIRAP, and MyD88) and therefore prevents the signaling cascade that inhibits both NFκB and IRF3 activity [69]. As previously discussed, the E3 protein prevents the activation of the PKR system by binding to dsRNA in the cytoplasm [76]. K7 binds to DDX3 [71] and C6 binds to NAP1 and SINTBAD [47], which are scaffold adaptor proteins that prevent the TBK1/IKKε activation of IRF3 (as well as IRF7) [47]. The C16 protein binds to the prolyl hydroxylase domain-containing protein 2 (PHD2), which is an oxygen sensor. This interaction prevents HIF-1α from degradation, allowing it to translocate into the nucleus and activate the HIF response [32]. Recently, the N2 protein was shown to inhibit IRF3 downstream of its translocation into the nucleus through an unknown mechanism (**Figure 1-4**) [81].

These are just two examples of how VACV evades the host immune response. VACV encodes additional proteins that target complement, block apoptosis, bind chemokines, or restrict IFN production and secrete decoy IFN receptors (reviewed in [32]). However, these proteins fan outside the scope of this thesis.

A common mechanism of regulation of the host innate immune system is holding transcription factors (ex. NFκB and IRF3) in an inactive state in the
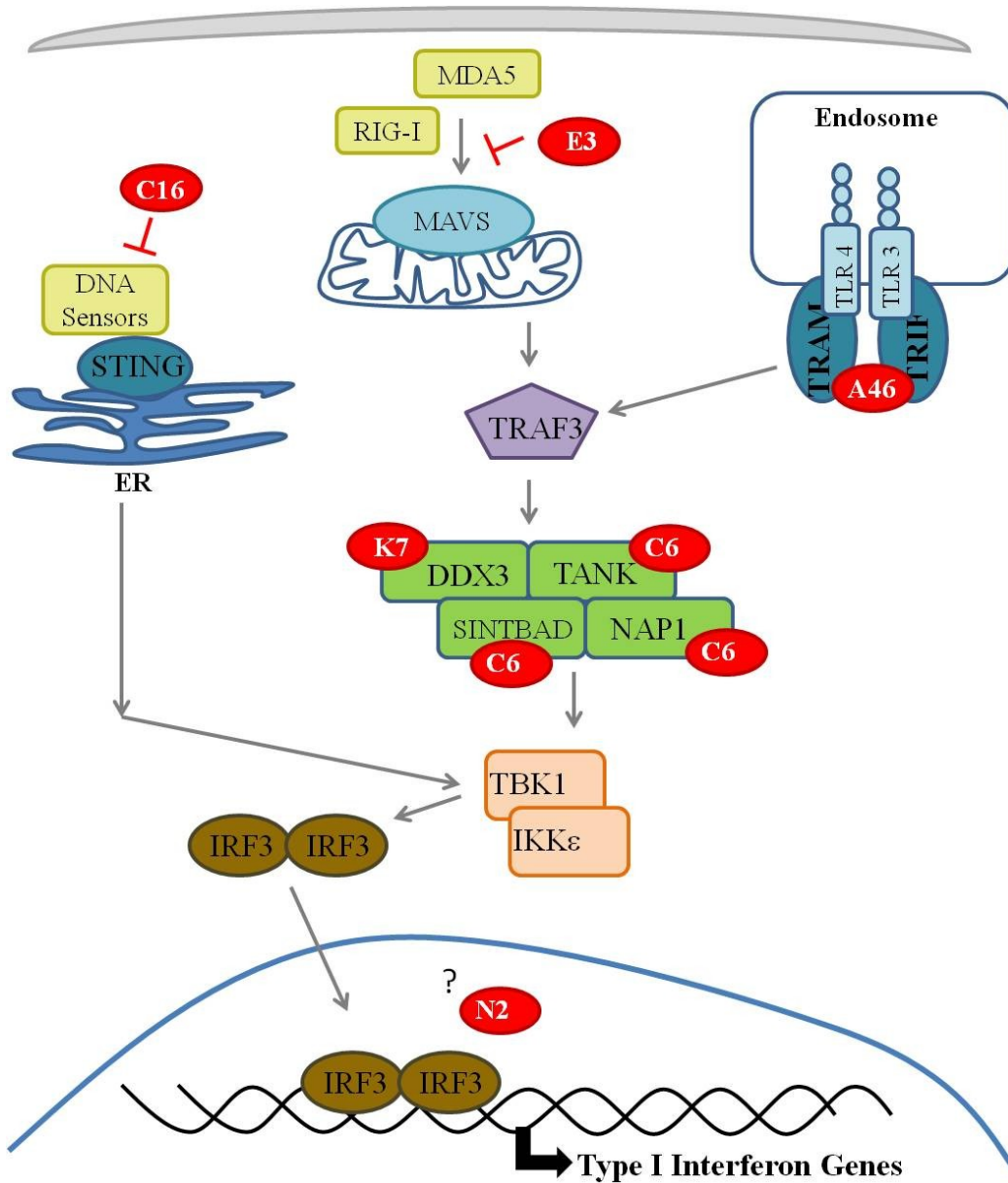
**Figure 1-4: Vaccinia inhibitors of IRF3 activation.** Target sites where vaccinia proteins (shown in red) inhibit the IRF3 pathway. The protein functions are discussed further in the text.

cytoplasm. Transduction of these factors into the nucleus is a critical step in mounting an effective immune response.

## 1.3. NUCLEAR TRANSPORT

### 1.3.1. Host nuclear transport system

The nucleus is separated from the cytoplasm by the nuclear envelope [82, 83]. The nuclear envelope consists of a double bilayer and functions as a barrier to prevent the free passage of molecules between the nucleus and cytoplasm [84]. However, proteins and RNAs need to traffic across the nuclear membrane [85]. The transport process is tightly regulated by the nuclear pore complex (NPC) [86]. The NPC is comprised of ~50-100 different proteins [84]. Small molecules, such as ions and metabolites, and small proteins (>60 kDa) passively diffuse through the nuclear membrane through the open channels intrinsic to the NPC [85, 86]. However, larger proteins and RNAs unable to pass through these open channels require an active process to cross the nuclear membrane [83].

Proteins requiring access to the nucleus usually contain a specific amino acid sequence called nuclear localization signals (NLS) [87]. Most of these sequences are characterized by short stretches of basic amino acids (ex. lysine and arginine) [86, 87]. NLSs are recognized by importin α proteins (also called karyopherins (KPNs)) [86]. Once bound to its respective KPNα subunit, the receptor-substrate complex binds to a KPNβ subunit. This complex is targeted to the nuclear pore by binding to the NPC [86, 87]. The following step, translocation of the substrate through the NPC, is energy-dependent [84]. This step involves another protein,

called Ran, which is a small GTP-binding protein [84, 87]. A high concentration of Ran-GDP is required on the cytosolic side of the nuclear membrane for KPNβ to form a complex with KPNα and its substrate [82, 84]. The complex is then transported through the NPC into the nucleus, where there is a high concentration of Ran-GTP [84]. Ran-GTP then binds to KPNβ, releasing KPNα and its substrate [84, 86]. The Ran-GTP complexed with KPNβ is immediately exported back into the cytoplasm [86]. The GTP is hydrolyzed to GDP and releases the KPNβ which then repeats the process (see **Figure 1-5**) [84].

Nuclear protein import is a tightly regulated cellular process [84, 88]. Transcription factors are often held in an inactive state in the cytoplasm [84]. The regulation transcription factor import into the nucleus is therefore a mechanism the cell uses to control gene expression [82, 84]. As a cell undergoes stress, such as a viral infection, a signaling cascades are initiated that leads to the activation of these transcription factors [84]. Activated transcription factors are imported into the nucleus to transcribe sets of antiviral genes [84]. These responses threaten virus survival. Many, if not all, viruses have therefore developed mechanisms to inhibit nuclear transport [89, 90].

## 1.3.2. Viral mechanisms targeting nucleocytoplasmic trafficking

In light of the importance the nucleus plays in many cellular processes, including cell survival, viruses have evolved to target the nuclear pore complex as well as import proteins (KPNs) to ensure virus replication and virulence [89, 90]. Some viruses target protein import to prevent activation of the innate immune
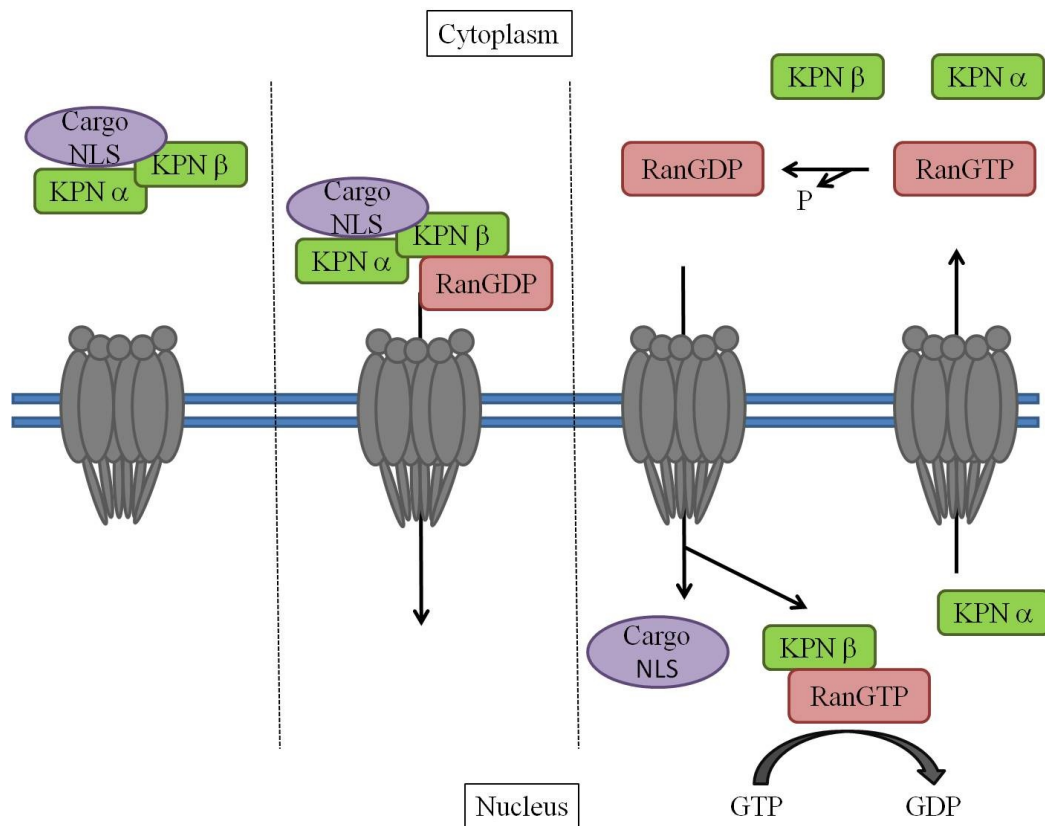
**Figure 1-5: The host nuclear transport system.** A protein requiring access to the nucleus requires a nuclear localization signal (NLS) (depicted in purple). The NLS on the protein is then recognized by the nuclear import protein karyopherin (KPN) α subunit (green). This complex then binds to a KPN β subunit (green) and is brought to the nuclear pore (grey) (Panel A). Ran-GDP (red) binds the newly formed complex which is then transported into the nucleus (Panel B). Inside the nucleus, Ran-GTP (red) complexes with KPN β, releasing the KPN α subunit and the protein cargo. The KPN α and β subunits are then recycled to the cytoplasm where Ran-GTP is hydrolyzed to Ran-GDP (Panel C).

system whereas others target mRNA nuclear export [90]. In contrast, some viruses utilize the nuclear transport system to transport viral mRNAs or proteins into the nucleus to complete their lifecycle [90].

Poliovirus is a positive stranded RNA virus that replicates exclusively in the cytoplasm of infected cells [91]. Even though its entire lifecycle occurs in the cytoplasm, poliovirus proteins still interact with nuclear proteins in order to shut down cellular processes [91]. Certain host nuclear proteins are found in the cytoplasm during poliovirus infection, and some viral proteins get into the nucleus [91]. For example, three normally nuclear host proteins (Sam68, La, and nucleolin) are relocated to the cytoplasm during infection. However, it is unclear if or how these proteins are involved in poliovirus infection [89, 91]. During infection with poliovirus, reporter proteins containing an NLS relocalize from the nucleus to the cytoplasm, therefore suggesting a general inhibition of nuclear trafficking [91]. Additionally, poliovirus degrades nuclear pore proteins (Nup62, Nup 98, and Nup 153) [89-91]. These same results were observed during infection with the related human rhinovirus, which is also a positive stranded RNA virus [90, 92]. It was hypothesized that these cytoplasmic RNA viruses disrupt the nuclear import pathway to prevent the start of an antiviral response [90].

The encephalomyocarditis virus (EMCV) is yet another member of the *Picornaviridae* family [90]. It demonstrates yet another way to inhibit nuclear protein import. EMCV lack the proteases used by polioviruses to degrade the nuclear pore proteins. Instead, they encode for a protein, EMCV L, which is responsible for hyperphosphorylation of the same group of nuclear pore proteins

[90, 93]. Moreover, EMCV L also binds to Ran-GTPase, which is required for both the release and binding of cargos to KPNs [90, 94].

The severe acute respiratory syndrome coronavirus (SARS-CoV) is an enveloped positive single stranded RNA virus [90]. The SARS-CoV employs a different mechanism to inhibit the nuclear transport system. The ORF6 protein, which localizes to the ER and Golgi membrane, binds to KPNα2 and KPNβ1 and sequesters them there [90, 95]. The retention of these transport molecules at the ER and Golgi membranes prevents the transcription factor STAT1 from being translocated into the nucleus, thus preventing an antiviral response [90].

Ebola virus is negative single stranded RNA virus that causes an extremely severe disease in humans [90]. This virus successfully blocks the host IFN response [96]. It encodes for two proteins, VP35 and VP24, that block IFN production and inhibit the downstream signaling of the IFN pathway [97]. VP35 is a multifunction protein that acts upstream of the IFN pathway [97], interfering at multiple steps. VP24 inhibits IFN signaling by interacting with KPNα2 [98]. This latter interaction, similarly to that of SARS-CoV ORF6, prevents the nuclear translocation of STAT1 [98]. VP24 was also shown to interact with KPNα1 [90, 99]. It is thought that VP24 outcompetes the host heterogenous nuclear ribonuclear protein complex C1/C2 (hnRNP C1/C2) protein for KPNα1 binding [90, 98]. As a result, the hnRNP C1/C2 protein, which is involved in host mRNA transcript processing, remains in the cytoplasm [90, 98]. The hnRNP C1/C2 protein is also retained in the cytoplasm during poliovirus infection, as a result of

poliovirus targeting components of the nuclear pore complex for degradation (discussed earlier) [90].

The herpes simplex virus (HSV) is a double stranded DNA virus that replicates in the nucleus of infected cells [100]. The HSV ICP27 protein has been shown to directly interact with the nuclear pore protein, Nup62, blocking nuclear import of both KPNα/KPNβ1 and KPNβ2 cargos [90, 100].

As discussed above, various viruses have evolved unique ways to inhibit the nuclear transport system to promote virulence (reviewed in [89, 90]). This led us to ask if there is a gene or subset of genes in VACV that target nuclear import pathway. To determine if any VACV proteins contained a nuclear localization signal, we performed a bioinformatic search which identified two VACV proteins, one of which was N2.

### 1.3.3. Vaccinia N2

VACV is a large DNA virus that encodes approximately 200 genes [101, 102]. Many of these genes have unknown functions or remain to be characterized [101]. When we began this project, VACV N2 was a protein still in need of further characterization. Early publications had claimed that a single G to T transversion mutation at the -10 position of the N2L gene was responsible for the resistance to α-amanitin and temperature sensitivity phenotypes [103]. The α-amanitin toxin is potent inhibitor of the host RNA polymerase II [103]. In the presence of α-amanitin, the host transcription process is inhibited [104]. However viral transcription is unaffected [104]. This observation that N2 is responsible for

resistance to α-amanitin led Tamin *et al.* to suggest that N2 was linked to the nucleus [103]. For some time it was thought that VACV could replicate independently of the cell nucleus until experiments showed that VACV was capable of initiating infection but was unable to assemble infectious progeny in the absence of the nucleus [103-105].

Bioinformatics analyses show that there are no non-poxvirus homologs to the N2 protein and that this protein is highly conserved in the Orthopoxvius genus. Further analysis revealed that N2 has a potential bipartite NLS signal. This finding is consistent with the claim that N2 was a VACV protein involved with the host cell nucleus [103].

It was recently published that VACV N2 is a nuclear protein that inhibits IRF3 downstream of IRF3 phosphorylation via unknown mechanisms [81]. Through luciferase reporter assays, N2 was shown to inhibit the activation of the IFNβ promoter [81]. Luciferase reporter assays provided evidence that N2 may inhibit the activation of IRF3. It was hypothesized that N2 may be preventing IRF3 phosphorylation or its translocation into the nucleus [81]. However, IRF3 was still phosphorylated and translocated into the nucleus during an infection in the presence of N2 [81]. A second hypothesis proposed that once in the nucleus, N2 prevented IRF3 from assembling into an active transcription complex [81].

By examining the virulence properties of the mutant viruses it was concluded that N2 is a virulence factor [81]. Two animal models were tested. With an intranasal (i.n.) mouse model where they infected the mice at $5 \times 10^3$ pfu [81], and an intradermal (i.d.) model where the mice were injected with $10^4$ pfu.

The study indicated that the N2L deletion mutant showed less signs of infection and caused less weight loss than the control groups [81]. Furthermore, although the deletion mutant grew to the same extent initially in the lungs of the mice, the N2L deletion mutant grew to lower titers than the control viruses at days 5 and 7 p.i. suggesting the mice were able to clear the N2L deletion mutant infection more rapidly [81]. Virulence in the i.d. model was determined by the size of the lesion and the time it took for the lesion to heal [81]. The conclusions were consistent with the results obtained from the i.n. infection [81]. Again, the results indicated that the N2L deletion virus formed smaller lesions and the lesions took less time to heal [81].

## 1.4. GOALS OF THIS THESIS PROJECT

The main goal of this thesis project was to determine the functional role of VACV N2 during infection. When I started this research, little was known about N2. This protein was of interest to our lab after the observation made by Lin *et al.* that the cellular topoisomerase II$\alpha$/$\beta$ is recruited to sites of viral replication [44]. It was hypothesized that VACV may encode for a protein that actively recruits host cell nuclear proteins to the viral factories. The VACV genome was screened for proteins that contained putative nuclear localization signals. This search returned two proteins, VACV O1 and N2. Both of these proteins were tagged at the C-terminus and their localization was determined by immunofluorescence. The O1 protein was found throughout the cytoplasm, while the N2 protein was found to localize to the nucleus. Although we found that N2 did not affect the

localization of cellular topoisomerase IIα/β, we decided to further investigate its function.

Because N2 localized to the nucleus, we hypothesized that N2 could inhibit or regulate host nuclear transport during infection. Regulation of host nuclear transport during infection could be essential to transport viral proteins into the nucleus or transport host factors out of the nucleus to viral sites of replication. It may also prevent the nuclear translocation of transcription factors essential for amounting effective innate immune responses. Various viruses have demonstrated the ability to interfere with host nuclear transport to promote virulence (reviewed in [89, 90]). However, nuclear transport has yet to be studied during a VACV infection.

**CHAPTER 2 – MATERIALS AND METHODS**

**2.1. MOLECULAR CLONING TECHNIQUES**

**2.1.1. Polymerase chain reaction**

The polymerase chain reaction (PCR) was used to amplify a specific region of DNA. This technique was also used to perform diagnostic analysis on the N2L recombinant viruses, as well as for amplifying DNAs for cloning. Two different heat stable DNA polymerases were used in these experiments. *Taq* polymerase (Fermentas) was used when the PCR product was less than 1 kb in length. Reactions using *Taq* polymerase were performed in 1X *Taq* buffer, 2.5mM MgCl$_2$, 100μm of each dNTP, 20pmol of each primer, 25ng template DNA. For PCR products larger than 1 kb, the *Pfu* high fidelity polymerase (Roche) was used to decrease the likelihood of errors being introduced. In this case, PCR was carried out using 1X high fidelity buffer, 100μm of each dNTP, 20pmol of each primer, 25ng genomic DNA and 1 unit of *Pfu* high fidelity polymerase. Amplification was carried out following these steps: initial denaturation at 94˚C for 2-3 minutes, then 30 cycles of denaturation at 94˚C for 30 seconds, primer annealing for 30 seconds, and primer extension at 72˚C for 2 minutes. The final cycle was followed by a 7 minute extension at 72˚C. The primer annealing temperature was determined from the melting temperatures of the primer set and subtracting 5°C.

**2.1.2. Restriction enzyme (RE) digests**

Diagnostic digests to confirm the presence, size, or orientation of a DNA were typically performed in 20 μL reactions, which consisted of the appropriate buffer, 0.5-1.0 μg of plasmid DNA, and 1-5 U of the restriction enzyme. Sub cloning digests were done in 50 μL reactions, with the appropriate buffer diluted to 1X, 5-10 μg of plasmid DNA and the amount of enzyme ranging from 2-10 U. Digests were incubated at 37°C for 1-3 hrs, with the occasional digests running overnight. All restriction enzymes used were purchased from Fermentas.

### 2.1.3. Agarose gel electrophoresis and gel-purification

PCR products and restriction enzyme digests were analyzed by agarose gel electrophoresis. Gel loading buffer (10X concentration) (60% glycerol (v/v); 50mM Tris HCl pH 7.5) was added to the DNA to a final concentration of 1X (6% glycerol (v/v); 5mM Tris HCl pH 7.5), which was then loaded onto a TAE agarose gel. Depending on the size of the DNA fragments to be resolved, the concentration of UltraPure Agarose (Invitrogen) ranged from 0.8-1.2%. SYBR safe DNA stain (Invitrogen), provided at a 10,000X concentrate, was added directly to the gel at a final concentration of 1X. The gel was then imaged using a Kodak Gel Logic 200L imager.

If a fragment of DNA was to be gel purified, the desired band was cut from the agarose gel using a razor blade and a UV light box. The gel slices were then purified using a GeneJET Gel Extraction kit (Thermo Scientific).

### 2.1.4. TOPO TA cloning and DNA ligations

If a PCR product was to be ligated into the TOPO TA cloning vector, 0.1 Units of *Taq* polymerase was added following the PCR reaction and incubated at 72˚C for 20 minutes to add an overhanging 5'A. The PCR product was then ligated into the pCR2.1-TOPO vector (Invitrogen) by mixing 4μL of the PCR product, 1μL of ¼ diluted salt solution, and 1μL of the pCR2.1-TOPO vector. The TOPO reaction was incubated at room temperature for 20 minutes and then 1μL was electroporated into electrocompetent *E. coli* (Invitrogen).

DNAs were ligated together in a 3:1 ratio of insert to vector using T4 DNA ligase (Fermentas). The ligation reactions were allowed to proceed for 2-4 hours at room temperature or they were incubated at 16°C overnight. A 1 μL aliquot of the ligation reaction was then used to transform electrocompetent bacteria (described in **section 2.1.5.**).

## 2.1.5. Bacteria transformations

Electroporation was used to transform plasmid DNA into electrocompetent *E. coli* strains. Unless otherwise stated, plasmid DNAs were electroporated into either DH10B (*F⁻ mcrA Δ(mrr-hsdRMS-mcrBC) φ80lacZΔM15ΔlacX74 recA1 endA1 araD139Δ(ara, leu)7697 galUgalK λ⁻ rpsL nupG*) *E. coli* or DH5α (F- φ80*lacZ*ΔM15 Δ(*lacZ*Y-*arg*F) U169 *recA1 endA1 hsd*R17 (rK-, mK+) *pho*A *sup*E44 λ- *thi*-1 *gyr*A96 *rel*A1) *E. coli*.

Following the 1.80kV pulse, SOC recovery media (Invitrogen) was immediately added to the cells. Bacteria were incubated at 37˚C for 1 hour in a horizontal shaker to allow for recovery. If blue/white selection was being used,

then 40 μL of UltraPure X-Gal (Invitrogen) at a concentration of 40 mg/mL was added to the LB plates. An aliquot of bacteria was then spread onto LB plates containing the appropriate antibiotic (and/or X-Gal) and incubated overnight at 37˚C. Colonies were picked and grown up in LB broth supplemented with the appropriate antibiotic.

### 2.1.6. Plasmid isolation

Plasmid DNA was isolated from overnight bacterial cultures using a GeneJET Plasmid Mini-prep Kit (Thermo Scientific). Large scale plasmid purification used the Qiagen Midi-Prep Kit, as per the manufacturer's instructions.

### 2.1.7. DNA sequencing and vector map construction

All final constructs were sequenced by The Applied Genomics Centre (TAGC) at the University of Alberta. Sequences were compared to a reference sequence using either Sequencher (v4) or CLC Genomics Workbench (v6.5.1.). Plasmid maps were generated for all final plasmids (**Table 2-2**) using MacVector (v11.0).

### 2.2. GENERATION OF PLASMIDS

### 2.2.1. C-terminal MYC tagged N2L

The VACV N2L gene was amplified by PCR from genomic DNA using the N2L C-term Tag FWD (*Sal*1) and N2L C-term Myc tag REV (*Not*1) primers

(**Table 2-1**). Following PCR, the product size was confirmed by agarose gel electrophoresis and incubated with the pCR2.1-TOPO vector. The mixture was then transformed into DH10B *E. coli*. Plasmid DNA was isolated and then digested with *Eco*R1. Clones with the correct restriction digest pattern were then sequenced using the M13 forward and M13 reverse primers.

One clone that had the correct sequence was digested with *Sal*1 and *Not*1 using ~5μg of DNA. At the same time, the pSC66 vector which encode a pox virus early late (E/L) promoter was digested with the same enzymes [106]. Both restriction digests were run out on an agarose gel and gel purified. Finally, the two pieces of DNA were ligated together and then transformed into DH5α *E. coli*. Transformants were analyzed by plasmid restriction digest with *Sal*1 and *Not*1.

### 2.2.2. N-terminal MYC and N-terminal FLAG tagged N2L

The N-terminal MYC and FLAG tags were also cloned using the techniques mentioned in **section 2.2.1**. To generate the N-terminal MYC tagged N2L, the N2L N-term Myc Tag FWD and N2L N-term Tag REV primers (**Table 2-1**) were used to amplify the N2L gene from VACV genomic DNA. The N-terminal FLAG tag N2L was amplified from VACV genomic DNA using the N2L N-term Flag Tag FWD and N2L N-term Tag REV primers (**Table 2-1**).

PCR was carried out for both reactions using the *Pfu* high fidelity polymerase. The PCR product was then topo-cloned (**section 2.1.4.**) and transformed into DH10B *E. coli*. Plasmid DNA was isolated and subjected to restriction digests with *Not*1 and *Sal*1. Positive clones were confirmed by DNA

sequencing using the M13 forward and M13 reverse primers (TAGC University of Alberta). Digested DNA fragments were gel purified and then ligated into pSC66 as described in **section 2.2.1.**. The ligated plasmids were then transformed into DH10B *E. coli.* Transformants were analyzed by restriction digests with *Sal*1 and *Not*1.

### 2.2.3. Construction of C-terminal N2-MYC under CMV promoter control

The pcDNA3.0 vector was received from Dr. Michele Barry (University of Alberta). Both the pcDNA3.0 vector and the C-terminal N2-MYC tag construct (described in **section 2.2.1.**) were digested with *Not*1 and *Hind*III and then gel purified. The fragments were ligated together and then the ligated plasmid was transformed into DH10B *E. coli.* Transformants were confirmed by restriction digests with *Not*1 and *Hind*III. Expression of the protein was tested by western blot. Human 293T cells were transfected with the plasmid and total protein was extracted with RIPA buffer (50mM Tris HCl pH 8.0; 0.1% SDS; 150mM NaCl; 0.5% sodium deoxycholate; 1% NP-40). The lysates were western blotted with the anti-MYC antibody (**Table 2-3**) and then imaged using a Li-Cor Odyssey scanner (Li-Cor, NE). No expression was detected.

Because the C-terminal N2-MYC construct did not express in the pcDNA3.0, it was re-synthesized by GeneArt (Regensburg, Germany) and codon optimized for mammalian expression. The plasmid DNA was then resuspended in distilled water and then both the codon optimized C-terminal N2-MYC and pcDNA3.0 vector were digested with *Not*1 and *Hind*III. The DNA fragments were

gel purified and ligated together. The ligation product was then transformed into DH10B *E. coli*. Conformational digests with *Not*1 and *Hind*III were performed to identify positive clones. Expression was then tested by western blotting and immunofluorescence.

### 2.2.4. pDGloxPΔN2 plasmid

To delete the N2L gene, two arms of homology were amplified by PCR and cloned into the pDGloxPKO$^{DEL}$ [107] vector flanking the EcoGPT/YFP cassette. Both the right arm of homology, nucleotides 22047 to 22353 (GenBank entry AY243312.1), and the left arm of homology, nucleotides 22875 to 23303, were amplified by PCR from VACV WR genomic DNA using *Taq* polymerase (primers summarized in **Table 2-1**). Following the PCR, the PCR products were each inserted into pCR2.1-TOPO vector and then electroporated into DH10B *E. coli*. Plasmid DNA was isolated from white colonies which were then analyzed by restriction digests using *Eco*R1, *Bam*H1, *Sac*1, and *Bam*H1/*Sac*1 for the right arm of homology and *Eco*R1, *Sal*1, *Spe*1, and *Sal*1/*Spe*1 were used for the left arm of homology. Positive clones were confirmed by DNA sequencing using the M13 forward and M13 reverse primers (TAGC University of Alberta).

The pCR2.1-TOPO vector which contained the right arm of homology and the pDGloxPKO$^{DEL}$ vector were both digested with *Bam*H1. The digests were gel purified and then ligated together. The ligation reaction was then electroporated into DH10B *E. coli.* Transformants were picked and analyzed by plasmid restriction digest with *Bam*H1, *Dra*1, and *Hind*III/*Pst*1.

To clone the left arm of homology to N2L into the pDGloxP$^{DEL}$ plasmid already containing the right arm of homology to N2L, the pCR2.1-TOPO vector containing the left arm of homology and the pDGloxP$^{DEL}$ plasmid with the right arm of homology were digested with *Sal*1/*Xho*1. The digests were separated by agarose gel electrophoresis and gel purified. The cut pDGloxP$^{DEL}$ vector containing the right arm of homology was ligated to the N2 left arm of homology. The ligation reaction was then electroporated into DH10B *E. coli* and transformants were picked and analyzed by plasmid restriction digest with *Sal*1, *Not*1, and *Kpn*1/*Sal*1. Clones with the correct orientation were sent for sequencing (TAGC University of Alberta).

### 2.2.5. pCR2.1-TOPO_revN2L plasmid

To produce the "repaired" virus, a complete copy of the N2L gene (nucleotides 22047 to 23303) flanked by the same portions of the N1L and M1L genes was amplified by PCR using the N2L KO Left FWD and N2L KO Right REV primers (**Table 2-1**). PCR was carried out using genomic DNA and the *Pfu* high fidelity polymerase. The PCR product size was confirmed agarose gel electrophoresis. Following the PCR, the PCR products were cloned into pCR2.1-TOPO vector creating pCR2.1-TOPO_revN2.

Plasmid DNA was isolated from transformants and confirmed by two separate restriction enzyme digests using *Eco*R1 or *Sal*1. Positive clones were confirmed by DNA sequencing using the M13 forward and M13 reverse primers

(TAGC University of Alberta), as well as N2L inside FWD and N2L inside REV primers (**Table 2-1**).

### 2.2.6. C-terminal GFP tagged KPNα2 and KPNα4

C-terminal GFP tagged KPNα2 and KPNα4 fusions were cloned into pcDNA6.2_EmGFP/TOPO vector following the Vivid Colors Mammalian Expression Kit (Invitrogen). Primers are described in **Table 2-1**. Positive clones were identified by restriction digests with *Sac*1 and *Pst*1 for GFP-KPNα2 and *Sac*1 and *Hind*III for GFP-KPNα4.

### 2.3. CREATION OF A N2 POLYCLONAL ANTI-SERUM

### 2.3.1. Western blotting

Protein lysates were fractionated by SDS-PAGE gels (8-12%). The SDS-PAGE gels were then subjected to coomassie staining or the proteins were transferred to a nitrocellulose membrane. The nitrocellulose membrane was then treated with Odyssey blocking buffer diluted 1:1 with PBS (140mM NaCl; 3mM KCl; 10mM $Na_2HPO_4$-$7H_2O$; 2mM $KH_2PO_4$), and then stained with a primary antibody (see **Table 2-3**) for 2-4 hours at room temperature or left overnight at 4˚C. Following the primary antibody staining, the membrane was washed three times with PBS-T (150mM NaCl; 10mM $KPO_4$; 0.1% Tween-20) and then incubated with an appropriate secondary antibody (see **Table 2-3**) for 1 hour at room temperature. The membrane was then washed 2 times in PBS-T and once in PBS, and then scanned on a LiCor Odyssey imager.

### 2.3.2. Expression of N2L-His$_6$ protein

Dr. Bart Hazes (University of Alberta) provided an aliquot of the plasmid containing the N2L N-terminal His$_6$ tag in pET21a (+) which was constructed by GeneArt and codon optimized for expression in *E. coli*. This plasmid was then transformed into DHE 142 (BL21 DE3 *recA pLysS*) [108] *E. coli* for expression.

Colonies containing the N2L N-terminal His$_6$ tagged plasmid were grown up overnight in lysogeny broth (LB) supplemented with chloramphenicol (25μg/mL) and ampicillin (100μg/mL). The following day, the cultures were diluted 1/20 and grown at 37˚C until they reached an OD$_{600}$ of 0.6. The cultures were then induced with 1mM IPTG (Fisher) and incubated at 37˚C or room temperature until point of harvest. The harvested bacterial pellets were then mixed with Bug Buster (Novagen), lysozyme (0.8 mg/mL) (USB Corporation), DNase (0.02mg/mL) (Fermentas), and 1X reaction buffer. The lysate was incubated at room temperature for 20 minutes and then centrifuged for 5 minutes at 14,000g. The supernatant was separated from the pellet. SDS-PAGE loading buffer was added to both the pellet and the supernatant, and the protein samples were then fractionated on a 12% SDS-PAGE gel. One gel was stained with coomassie blue while the other was transferred to a nitrocellulose membrane. The nitrocellulose membrane was western blotted with a monoclonal anti-His antibody (see **Table 2-3**) and then stained with a goat anti-mouse secondary (see **Table 2-3**).

### 2.3.3. Purification of N2L-His$_6$ protein

One colony from the DHE142 *E. coli* streaked plate was picked and grown up overnight in 5mL LB supplemented with chloramphenicol (25μg/mL) and ampicillin (100μg/mL). This culture was then used to inoculate two 150mL flasks of LB supplemented with chloramphenicol (25μg/mL) and ampicillin (100μg/mL) and grown overnight at 37˚C. Five liters of the same media were then inoculated with 25mL of the overnight culture and grown to an $OD_{600}$ of 0.6 at 37˚C in a shaking incubator. The cultures were then induced with 1mM IPTG and incubated for 1 hour at 37˚C before adding rifampicin to a final concentration of 50μg/mL. Cultures were then allowed to grow for 3 more hours and then the bacteria were harvested by centrifugation at 6000g for 10 minutes at 4˚C.

Pellets were resuspended in 200mL of resuspension buffer (20mM Tris-HCl pH 8.0) before sonication with 10 second pulses for 2 minutes. Inclusion bodies were collected by centrifugation at 10,000g for 15 minutes at 4˚C. The supernatant was removed and the pellet was washed twice following these steps: resuspended in 3mL of cold isolation buffer (2M urea, 20mM Tris-HCl pH 8.0, 0.5M NaCl, 2% Triton-X 100), sonication with 10 second pulses for 1 minute, and then centrifuged at 15,000g for 10 minutes at 4˚C. The washed pellet was resuspended in 250mL binding buffer (6M guanidine hydrochloride. 20mM Tris-HCl pH 8.0, 0.5M NaCl, 5mM imidazole, 1mM β-mercaptoethanol) and then stirred at room temperature for 1 hour. The sample was then centrifuged at 15,000g for 15 minutes at 4˚C. Finally, the protein sample was further clarified by filtration through Millipore SteriFlip 0.45μm Filter units. The filtered supernatant was then loaded onto a 5mL nickel column (GE Healthcare) using an AKTA

HPLC. The protein was eluted off the column using imidazole in a stepwise gradient of increasing concentrations of imidazole (5 column volumes of each of the following: 50mM, 100mM, 200mM, 300mM, 400mM, and 500mM imidazole). Fractions were collected and a sample of each fraction was precipitated with trichloroacetic acid (TCA) to rid the sample of guanidium hydrochloride for analysis on SDS-PAGE gels. The TCA precipitation protocol took the $15\mu L$ fraction sample and diluted it with water to a final volume of $100\mu L$. This sample was then mixed in a 1:1 ratio with 10% TCA and incubated on ice for 20 minutes. The protein sample was pelleted by centrifugation at 15,000g for 15 minutes. The protein pellet was washed with ice cold 95% ethanol and centrifuged for 5 minutes at 14,000g. The pellet was dried and then resuspended in SDS-PAGE loading buffer. Proteins were fractionated on a 12% SDS-PAGE gel and coomassie stained. Fractions containing the highest amount of protein were pooled and dialyzed overnight at 4°C in 4L of 1/10X PBS with two buffer changes.

### 2.3.4. Generation of the N2 polyclonal anti-serum

N2L His$_6$ tagged recombinant protein (1.5 mg/mL) was sent to ProSci Incorporated (Poway, CA) to produce anti-sera in rabbits. Pre-immune serum was collected prior to immunization. Rabbits were immunized a total of four times, with 14 days in between each immunization. Serum was first collected between the third and fourth immunizations. Additional serum was collected another three times, 7, 14, and 22 days after the final immunizations. Serum was collected a

final time from the two rabbits with the highest signal 25 days after the final immunization.

### 2.3.5. Preparation of acetone dehydrated cells

To remove the background signal from the N2 anti-serum detected in all bleeds, the sera was incubated with acetone dehydrated BSC40 cells infected with the ΔN2L virus. BSC40 cells were infected at an MOI of 5 with the ΔN2L virus and allowed to infect for 20 hours. The infected cells were scraped into cold PBS and then 2 volumes of acetone were added. Cells were incubated at 0˚C for 30 minutes with occasional mixing and then centrifuged at 10,000g for 10 minutes. The pellet was resuspended in fresh acetone and incubated at 0˚C for 10 minutes and then centrifuged again for 10 minutes at 10,000g. The pellet was transferred to filter paper and air dried at room temperature. The air dried cell pellet was then added to the anti-sera and incubated at 4˚C overnight with constant rotation. The following day, the cell debris was pelleted by centrifugation at 14,000g for 5 minutes, and the supernatant was transferred to a clean tube. The pre-cleared anti-serum was then tested in western blotting.

### 2.4. CELL CULTURE AND VIRUSES

### 2.4.1. Cells and viruses

Human embryonic kidney 293 (HEK293), STO mouse embryonic fibroblasts, and HeLa cells were obtained from the American type culture collection (ATCC) and grown in Dulbecco's modified Eagle's medium (DMEM)

supplemented with 1% L-glutamine, 1% non-essential amino acids, and 1% antibiotic/antimycotic (all from Invitrogen) plus 10% fetal bovine serum (Sigma). African green monkey cells (BSC40) were purchased from ATCC and maintained in minimum essential medium (MEM) supplemented with 1% L-glutamine, 1% non-essential amino acids, and 1% antibiotic/antimycotic plus 5% fetal bovine serum. All cells tested negative for mycoplasma by PCR assay (Invitrogen).

VACV (strain Western Reserve) was also purchased from ATCC. Two clones of Dryvax (DPP15 and DPP17) [109] and two clones of Tian Tan (TP03 and TP11) [110] were used in these studies and were cloned by Dr. Li Qin (University of Alberta).

### 2.4.2. Cloning the N2L deletion virus (ΔN2L)

To delete the N2L gene, BSC40 cells were infected with VACV WT at MOI = 2 and then transfected, two hours later, with 2μg of linearized pDGloxPΔN2 (**section 2.2.5.**) using Lipofectamine 2000. The progeny were harvested after 72 hours and the recombinant viruses VACVΔN2L were isolated using two rounds of mycophenolic (MPA) drug selection [111] in liquid culture, followed by four rounds of plaque purification under agar. For drug selection the media was supplemented with MPA (25mg/mL), hypoxanthine (15mg/mL), and xanthine (250mg/mL). PCR was used to confirm the purity of the viruses using primers N2L KO Right REV and N2L KO Left FWD (**Table 2-1**).

### 2.4.3. Cloning the N2L revertant virus (rN2L)

To re-introduce the N2L gene, BSC40 cells were infected with VACV ΔN2L at MOI = 2 and then transfected, two hours later, with 2μg of linearized Topo-PCR_2.1_N2L_revertant (**Table 2-2**) plasmid using Lipofectamine 2000. The progeny were harvested after 48 hours and the recombinant viruses VACV rN2L were isolated on mouse STO cells in the presence of 0.1 mM 6-thioguanine (6-TG) (Sigma) [112] in liquid culture, followed by three rounds of plaque purification under agar on BSC40 cells. PCR was used to confirm the purity of the viruses using primers N2L KO Right REV and N2L KO Left FWD (**Table 2-1**).

### 2.4.4. Sucrose purification of virus particles

BSC40 cells were infected with the ΔN2L, rN2L, or WT viruses at a MOI of 5. After 48 hours, cells were harvested into 50 mL conical tubes and pelleted by centrifugation at 2000g for 5 minutes at 4°C. The pellet was resuspended in 10mM Tris pH 8.0 and the virus was released from the cells by Dounce homogenization. Lysates were then centrifuged for 10 minutes at 3000g. The supernatant was set aside and the pellet was resuspended in 10mM Tris pH 8.0 and subject to a second round of Dounce homogenization and centrifugation. The supernatants were pooled together and layered over a 36% sucrose cushion and centrifuged at 13,000rpm for 80 minutes at 4°C. The supernatant was discarded and the virus pellet was resuspended in PBS A and titered on BSC40 cells.

### 2.5. VIRUS CULTURE AND PLAQUE ASSAYS

### 2.5.1. Multi-step growth curves

For multi step growth curves, BSC40 cells were infected at an MOI of 0.01. The viruses were harvested at 0, 3, 6, 12, 18, 24, 48, and 72 hours post infection and the virus was released by three consecutive freeze-thaws. Viral titers were then determined by titration on BSC40 cells.

### 2.5.2. Plaque Morphology

BSC40 cell monolayers were infected at 60 pfu per dish for 48 hours. The cells were washed with PBS then fixed and stained with crystal violet (15% ethanol; 2% glacial acetic acid; 2% formaldehyde; 0.5% crystal violet). The dishes were imaged with a HP ScanJet 6300 scanner and plaque areas calculated using Image J v1.45s (http://imagej.nih.gov/ij).

### 2.5.3. Cytosine arabinoside (AraC)

BSC-40 cells were infected with VACV WT at an MOI of 5 for 1 hour, and then cells were either left untreated (MEM only) or treated with 80μg/mL cytosine arabinoside (AraC). Proteins were harvested at set time points, size fractionated using SDS-PAGE, and western blotted using antibodies directed against N2, I3 (an early VACV gene product), A34 (a late VACV gene product), and cellular β-actin.

### 2.5.4. α-amanitin resistance

We tested the growth of different VACV strains (WT, ΔN2L, rN2L, Tian Tan, and Dryvax) in the presence of 0, 2, and 6 μg/mL α-amanitin, or in cells

pretreated with 2 or 6 µg/mL drug for different amounts of time. BSC40 cells were infected with ~80 pfu per 60 mm dish for 1 hour and then treated with 0, 2, 6, and 18 µg/mL α-amanitin. The cells were incubated at 37°C or 39.5°C for 48 hours and then washed with PBS and then fixed and stained with crystal violet. The dishes were imaged with a HP ScanJet 6300 scanner and plaque areas calculated using Image J. In a separate assay, BSC40 cells were pretreated with 2 or 6 µg/mL drug for different amounts of time (12, 6, 3, or 0 hours) and then infected with the same viruses mentioned above for 48 hours. The plates were washed with PBS and then fixed and stained with crystal violet. The dishes were imaged with a HP ScanJet 6300 scanner and plaque areas calculated using Image J.

## 2.6. WESTERN BLOTTING

Protein samples were prepared by infecting BSC40 cells with WT, ΔN2L, and rN2L viruses at an MOI of 5. Before harvesting the total protein, cell monolayers were washed with PBS, then RIPA buffer supplemented with a protease inhibitor tablet (Roche) was added and the lysates were incubated on ice for 30 minutes. Total cell lysates were centrifuged for 30 minutes at 14,000g and the DNA pellet was removed leaving the protein sample behind.

Protein lysates were then fractionated by SDS-PAGE gels as described in **section 2.3.1.**.

## 2.7. IMMUNOFLUORESCENCE MICROSCOPY

### 2.7.1. Fixed cell immunofluorescence microscopy

BSC40 cells were cultured on glass coverslips in 24 well plates, infected with virus at an MOI of 5. Infection times varied from 6-24 hours post infection, and then the cells were fixed on ice for 30 min in 4% paraformaldehyde in PBS. For transfection studies, cells were transfected with 150ng of DNA per well using Lipofectamine 2000 at 2 hours post infection. Fixed cells were permeabilized using 100 mM glycine in 0.1% Tween-20 in PBS (PBS-T). Cells were incubated in blocking buffer (3% BSA, 0.1% Tween 20 in PBS) and then stained for either 3h at room temperature or they were left at 4°C overnight in primary antibody (see **Table 2-3** for antibody dilutions). The cells were then stained for 1hr with the appropriate secondary antibodies (see **Table 2-3**). Cells were then stained with 5 ng/ml DAPI for DNA and 0.3 U/mL rhodamine phalliodin for actin. Coverslips were mounted in Mowoil mounting media (25% glycerol, 10% Mowoil, 0.1M Tris HCl pH 6.8). Cells were imaged using a widefield Delta-vision deconvolution microscope at 60X (N.A. = 1.42) and the files processed using a SoftWorx deconvolution algorithm and conservative ratio settings (SoftWorx v 4.1.2). Cells were also imaged using a Quorum WaveFX (Olympus IX-81/Yokagawa CSUX1) spinning disk confocal microscope (PerkinElmer) and images processed using velocity (v 6.0.1) software.

### 2.7.1. Fluorescence recovery after photobleaching (FRAP)

BSC40 cells were cultured on glass bottom dishes. Plasmids encoding either the C-terminal tagged GFP-KPNα2 or GFP-KPNα4 were transfected into

BSC40 cells using 1 μg or 2 μg of DNA respectively. After ~24 hrs, the cells were left uninfected (Mock) or infected with either the WT or ΔN2L virus at an MOI of 5. At 4.5 hrs post-infection, cells were imaged using the PERKIN ELMER Spinning Disk ERS Confocal microscope with the 63X objective lens. Images were taken twice every second prior to photobleaching, whereas post photobleaching, images were taken once every three seconds. Cells were photobleached using the 488 laser.

## 2.8. PROTEIN CO-IMMUNOPRECIPITATION

### 2.8.1. N-terminal FLAG-tagged karyopherins α1-6

Plasmids encoding FLAG-tagged karyopherins α1 to α6 were kindly provided by Dr. M. Shaw (Mt. Sinai School of Medicine, New York [113]). Primers were designed to each karyopherin and all plasmids were confirmed by sequencing (see **section 2.7.1.**).

### 2.8.2. Immunoprecipitation

Plasmids encoding FLAG-tagged forms of karyopherins α1 to α6 (**section 2.8.1.**) were transfected into BSC40 cells, in 150mm dishes, using 20 μg DNA per dish and Lipofectamine 2000. The cells were cultured for 24 hr and then infected with VACV at MOI of 5 and cultured for another 6 hr. The cells were harvested by centrifugation for 10 minutes at 4°C at 800 g. The cell pellet was washed once in PBS A (137 mM NaCl, 2.7 mM KCl, 8.1 mM $Na_2HPO_4$, 1.5mM $KH_2PO_4$) and centrifuged as mentioned above. The cells were then lysed by passage through a

21.5 gauge needle in 0.5 mL IP lysis buffer (150 mM NaCl, 20 mM Tris pH 8, 1mM EDTA, 0.5% NP-40) supplemented with one protease-inhibitor tablet per 20 mL buffer and then incubated on ice for 90 minutes. The extract was cleared by centrifugation for 10 min at 10,000 g and transferred to a new tube. A 50% slurry of mouse monoclonal anti-FLAG magnetic beads (50 μL) (Sigma) was added to each tube and incubated overnight at 4°C with gentle mixing. The beads were harvested using a magnetic tube rack and washed three times with TBS (50mM Tris HCl pH 7.4, 150mM NaCl). The proteins were then boiled in 2X sample buffer (125mM Tris HCl pH 6.8, 4% SDS, 20% glycerol (v/v), 0.004% bromophenol blue) for 3 minutes and then fractionated using an SDS PAGE gel and then subjected to western blotting.

### 2.8.3. Reciprocal immunoprecipitations

For the reciprocal IP, BSC40 cells were grown in 150mm dishes until they became confluent. The cells were then infected with VACV WT for 6 hours. Cells were harvested into 50 mL conical tubes and centrifuged for 10 minutes at 800 rpm at 4°C. The cell pellet was washed once in PBS A and centrifuged for 10 minutes at 800 rpm at 4°C. Cells were lysed by passage through a 21.5 gauge needle in 0.5 mL IP lysis buffer supplemented with one protease-inhibitor tablet per 20 mL buffer. The lysates were incubated on ice for 90 minutes, centrifuged for 10 minutes at 10,000 g, and then incubated for 30 minutes with 40 μL Protein G Sepharose beads (GE Healthcare). The beads were removed by centrifugation at 2000 g and then 10μL of the N2 polyclonal anti-serum was added to the lysate

and incubate overnight at 4°C. Protein G Sepharose beads (40μL) were then added to each tube and gently mixed for 2-4 hours at 4°C. The beads were recovered by centrifugation at 2000 g for 2 minutes and then washed as follows: remove supernatant from the beads, add 1 mL IP lysis buffer, gently mix for 5 minutes, centrifuge at 2000 g for 2 minutes and repeat 5 times. The beads were then boiled in 4X SDS PAGE loading buffer (3.7% SDS; 4% β-mercaptoethanol; 40% glycerol (v/v); 50mM Tris HCl pH 6.8; 0.1% Bromophenol blue) for 10 minutes and then fractionated on an SDS PAGE gel. The lysates were western blotted for N2 and KPNα2.

## 2.9. REPORTER GENE ASSAYS

### 2.9.1. pNFκB-TA & renilla reporter plasmids

Plasmids encoding an NFκB-regulated promoter driving firefly luciferase (pNFκB-TA-Luc, Clontech), and a *Renilla* luciferase gene under HSV-TK promoter control (phRL-TK, Promega), were obtained from Dr. R. Ingham (University of Alberta).

### 2.9.2. NLS-BFP-GFP & NLS-GFP plasmids

A plasmid encoding an N-terminal SV40 NLS fused to enhanced blue and green fluorescent protein (NLS-BFP-GFP) and a plasmid encoding the same N-terminal SV40 NLS fused to enhanced green fluorescent protein (NLS-GFP) was obtained from Dr. T. Hobman (University of Alberta) and was originally a gift of Dr. F. Beltram [114].

### 2.9.3. pNFκB-TA luciferase assay

Plasmids encoding an NFκB-regulated promoter driving firefly luciferase and a *Renilla* luciferase gene under HSV-TK promoter control were co-transfected into HEK293 cells ($5x10^4$ cells/well in 24 well plates) using 60 ng of the NFκB reporter plasmid, 10 ng of the *Renilla* control plasmid, and 30, 60, or 120ng of C-terminal N2-MYC plasmid (CMV promoter) or the empty vector control (pcDNA3.0) and Lipofectamine 2000. After incubating the cells for 18-24 hours, the cells were stimulated with 50 ng/mL TNFα for six hours and then lysed with passive lysis buffer (Promega). The amount of firefly luciferase relative to the *Renilla* luciferase activity was determined as directed by the manufacturer. These experiments were performed in triplicate and repeated three times.

This assay was also performed using the N2L recombinant viruses. In this experiment, HEK293 cells ($5x10^4$ cells/well in 24 well plates) were transfected with 60 ng of the NFκB reporter plasmid and 10 ng of the *Renilla* control plasmid. The cells were incubated with the plasmids overnight. Before the cells were infected, they were treated with 5, 16.7, or 50 ng/mL TNFα for 30 minutes and then infected with WT, ΔN2L or rN2L at an MOI of 5. The TNFα was present throughout the infection. Six hours post infection the cells were lysed and assayed for luciferase as previously described.

### 2.9.4. Nuclear transport of NLS-BFP-GFP and NLS-GFP reporter proteins

HeLa cells were transfected with 150 ng of each NLS-BFP-GFP plasmid (see **section 2.9.2**) and the CMV C-terminal N2-MYC (see **section 2.2.3.**) for 18-24 hours. The cells were then processed for immunofluorescence (see **section 2.7.**).

To test if the viruses had an effect on the reporter proteins localization, the HeLa cells were transfected with 150 ng of either the NLS-BFP-GFP or NLS-GFP (see **section 2.9.2**), and then infected with WT, ΔN2L, and rN2L at an MOI of 5 for 6 hours. The cells were then fixed and processed for immunofluorescence (see **section 2.7.**).

## 2.10. SINGLE STRANDED DNA CELLULOSE ELUTION ASSAY

Single stranded DNA cellulose from calf thymus DNA (Sigma) was prepared by Ms. Melissa Harrison (University of Alberta) as follows: 10g ssDNA cellulose was resuspended in 10 mL ddH$_2$O to make a 50% slurry.

BSC40 cells were grown in 150 mm dishes and infected with VACV WT for 6 hours. Cells were harvested into 50 mL conical tubes and centrifuged for 10 minutes at 800 rpm at 4°C. The cell pellet was washed once in PBS A and centrifuged for 10 minutes at 800 rpm at 4°C. Cells were lysed by passage through a 21.5 gauge needle in 0.5 mL lysis buffer (50mM NaCl, 20mM Tris pH 8.0, 1mM EDTA pH 8.0, 0.5% NP-40) supplemented with one protease-inhibitor tablet (Roche) per 20 mL buffer. The lysates were incubated on ice for 90 minutes, and then centrifuged for 10 minutes at 10,000 g. The ssDNA cellulose was prepared as follows: a 500 μL aliquot of the 50% slurry was transferred to a

new microfuge tube and centrifuged 1000 g for 1 minute. The supernatant was removed and the cellulose was resuspended in 1 mL ddH$_2$O. The ssDNA cellulose was then washed in lysis buffer, twice. After the final supernatant was removed, the cell lysate was added to the microfuge tube containing the ssDNA cellulose. The proteins were allowed to bind overnight at 4˚C with gentle rotation. The samples were then centrifuged at 1000 g for 1 minute and the supernatant was removed. The cellulose was then washed with lysis buffer (50 mM NaCl) three times, each time the supernatant was collected. Following the washes, the ssDNA cellulose was incubated with lysis buffer containing 150 mM NaCl for 5 minutes with gentle rotation. The sample was centrifuged at 1000 g for 1 minute and the supernatant was collected. This process was repeated using lysis buffer containing 250mM, 500mM, and 2M NaCl.

The protein in the supernatants was then precipitated with 50% (w/v) trichloroacetic acid (TCA) (Acros). Two volumes of 50% TCA was added to four volumes of protein sample and incubated on ice for 10 minutes. The sample was centrifuged at 14,000 g for 5 minutes, the supernatant was removed, and the protein pellet was washed with cold acetone. The centrifuge and the acetone wash steps were repeated for a total of two washes. The pellet was then dried in a 60°C heating block and resuspended in SDS PAGE loading buffer. The protein sample was then boiled for 10 minutes and fractionated on an SDS PAGE gel and then subjected to western blotting. The nitrocellulose membranes were stained for both N2 and I3 (SSB).

## 2.11. VIRULENCE IN BALB/C MICE

This work was done with the special help of Ms. Nicole Favis (University of Alberta). The Balb/c mice (Charles River) were acclimatized to their environment for 1 week before virus administration. All procedures and daily monitoring were performed in a biosafety cabinet. The mice were anesthetized by an intraperitoneal injection of a ketamine/xylazine cocktail (100mg/kg ketamine; 20mg/kg xylazine) (dispensed from HSLAS, University of Alberta). While under anesthesia, the mice were then given a single intranasal (10μL) dose of the respective virus (virus treatment groups were divided in two, with half of the mice receiving a dose of $1x10^5$ pfu/mL [$1x10^3$/inoculation] and the other half receiving a higher dose of $1x10^6$ pfu/mL [$1x10^4$/inoculation]). The mice were then monitored daily, up to 30 days, for signs of infection and weight loss. All virus treated mice will be compared to a control group of mice inoculated with PBS. Mice that lost more than 20% of their body weight were euthanized. All mice were euthanized after 30 days of the initial virus administration.

## 2.12. PREPARATION OF VIRUS DNA FROM PURIFIED VIRIONS

### 2.12.1. Viral DNA preparation

BSC40 cells were grown in 150 mm dishes (10x150mm dishes per virus) and infected with VACV ΔN2L or rN2L at an MOI of 0.01 for three days [115]. Cells were harvested into 50 mL conical tubes and centrifuged for 5 minutes at 500 rpm at 4°C. The pellet was resuspended in 10mM Tris pH 9.0 and the virus was released from the cells by Dounce homogenization. The lysed cells were

centrifuged for 10 minutes at 1100g at 4°C and the supernatant was collected. The pellet was resuspended in 10mM Tris and subjected to a second Dounce homogenization and centrifugation.

Step gradients (layer 3mL of 40% sucrose, 2.2mL of 36% sucrose, 2mL of 28% sucrose, and 1mL 24% sucrose (each in 1mM Tris HCl pH 9.0)) were prepared (two per virus) in SW41 tubes ~2 hours before use. The supernatants containing the virus were sonicated on ice for 5-10 minutes. Six sucrose cushions (6mL 36% (w/v) sucrose in 10mM Tris HCl pH 9.0) were prepared and the sonicated virus was added to each tube and centrifuged for 80 minutes at 33,000g at 4°C. After centrifugation, the virus pellet was resuspended in 1mM Tris pH 9.0 and sonicated as above. The sonicated virus was then overlayed onto the first sucrose step gradient and centrifuged for 50 minutes at 26,000g at 4°C. The milky band of virus was collected and set aside. The pellets were once again resuspended in 1mM Tris pH 9.0, sonicated as above, and re-banded on the second set of step gradients. Both sets of virus bands were pooled together in a centrifuge tube and two volumes of 1mM Tris pH 9.0 was added. The purified virus was pelleted by centrifuging for 30 minutes at 33,000g at 4°C. Finally, the purified virus pellet was resuspended in 1mM Tris pH 9.0.

The virus suspension is then mixed with virion lysis buffer (0.4 mg/mL Proteinase K, 1,2% sodium dodecyl sulfate, 50 mM Tris-HCl pH 8.0, 4 mM EDTA pH 8.0, and 4mM NaCl) and incubated overnight at 37°C. The virus DNA is then gently extracted with phenol/chloroform/isoamyl by gentle rotation and centrifugation at 15,000g for 10 minutes at room temperature. The aqueous

solution is transferred to a new tube and mixed with chloroform/isoamyl and then centrifuged again as the previous step. The chloroform/isoamyl extraction is repeated once more. The DNA is then precipitated with 95% ethanol and 3M NaOAC pH 5.2, incubated at -80°C for 15 minutes, and centrifuged at 15,000g for 10 minutes at room temperature. The supernatant was poured off and the DNA was dried and then resuspended in elution buffer (Fermentas). The DNA concentration and quality is checked using spectrophotometry.

## 2.12.2. Sequencing

A total of 500ng of DNA from each virus was sequenced using a high-throughput pyrosequencing approach on a Roche 454 GS FLX Titanium sequencer platform.

**Table 2-1: List of primers used in these studies**

| Primer | Sequence 5'-3' |
| --- | --- |
| N2L C-term Tag FWD (Sal1) | GTCGACATGACGTCCTCTGCAATGGATAATAATGAACC |
| N2L C-term Myc Tag REV (Not1) | GCGGCCGCTTACAGATCTTCTTCAGAAATAAGTTTTTGTTCGAAATACTTAGTTTCCACG |
| N2L N-term Myc Tag FWD | GTCGACATGGAACAAAAACTTATTTCTGAAGAAGATCTGATGACGTCCTCTGCAATGGAT |
| N2L N-term Flag Tag FWD | GTCGACATGGACTACAAGGACGACGATGACAAGATGACGTCCTCTGCAATGGATAATAAT |
| N2L N-term Tag REV | GCGGCCGCTTAGAAATACTTAGTTTCCACGTAGTTAATGAAACAT |
| N2L KO Left FWD (Spe1) | ACTAGTGAAGTGGGATCCATAAGATGC |
| N2L KO Left REV (Sal1) | GTCGACTTGTTAAAAATAATCATCGAA |
| N2L KO Right FWD (BamH1) | GGATCCGAGTTCAAATGTTTCATTAAC |
| N2L KO Right REV (Sac1) | ACTAGTCAATGTACATACATCGCC |
| N2L Inside FWD | CTAGAAATGGTATATGATGCTAC |
| N2L Inside REV | CGAATTCTACGGGATCCACT |
| KPNa2 tag FWD | GCCACCATGTCCACCAACGAGAATGC |
| KPNa2 tag REV | AAAGTTAAAGGTCCCAGGAGCC |
| KPNa4 tag FWD | GCCACCATGGCGGACAACGAGAAACTG |
| KPNa4 tag REV | AAACTGGAACCCTTCTGTTGGTACA |

**Table 2-2: List of plasmids assembled during these studies**

| Plasmid Name | Plasmid Backbone | Tag |
|---|---|---|
| N2L_N-terminal_His6 | pET21a(+) | His6 |
| pDGloxPΔN2 | pDGloxP | N/A |
| pCR2.1-TOPO_revN2L | Topo-PCR-2.1 | N/A |
| N2L_C-terminal_MYC | pSC66 | MYC |
| N2L_N-terminal_MYC | pSC66 | MYC |
| N2L_N-terminal_FLAG | pSC66 | FLAG |
| GeneART_N2L_C-terminal_MYC | pcDNA3.0 | MYC |
| GFP-KPNα2 | pcDNA6.2_EmGFP/TOPO | GFP |
| GFP-KPNα4 | pcDNA6.2_EmGFP/TOPO | GFP |

**Table 2-3: List of antibodies used in these studies**

| Antibody | Species | Source | Catalog number | WB dilution | IF dilution |
|---|---|---|---|---|---|
| **Commercial Primary Antibodies** | | | | | |
| β-actin | Mouse | Sigma | A5441 | 1/20,000 | |
| DNA topoisomerase II α/β | Rabbit | Stressen | KAM-CC215 | | 1/500 |
| FLAG | Mouse | Sigma | F1804 | 1/1000 | |
| FLAG | Rabbit | Sigma | F7425 | | 1/500 |
| His6 | Mouse | Roche | 11 922 416 001 | 1/2000 | |
| Karyopherin α2 | Mouse | Santa Cruz | sc-55538 | 1/1000 | 1/500 |
| Karyopherin α4/importin α3 | Rabbit | ProteinTech Group, Inc. | 12463-1-AP | 1/500 | 1/500 |
| Myc-tag | Mouse | Cell Signaling | 2276 | 1/1000 | 1/500-1/1000 |
| NFκB p65 | Rabbit | Santa Cruz | sc-372 | | 1/1000 |
| NPI-1 (KPNA1) | Mouse | ZYMED | 37-0800 | | 1/500 |
| Pol II (RNA Polymerase II) | Mouse | Santa Cruz | sc-71917 | | 1/1000 |
| **VACV Primary Antibodies** | | | | | |
| VACV N2L | Rabbit | ProSci | | 1/1000 | N/A |
| VACV I3L (10D11) | Mouse | ProSci | | 1/10,000 | 1/1000 |
| VACV A34 | Rabbit | ProSci | | 1/10,000 | |
| **WB Secondary Antibodies** | | | | | |
| IRDye 800CW | Mouse | LiCor | | 1/20,000 | |
| IRDye 680CW | Mouse | LiCor | | 1/20,000 | |
| IRDye 680CW | Rabbit | LiCor | | 1/20,000 | |
| IRDye 800CW | Rabbit | LiCor | | 1/20,000 | |
| **IF Secondary Antibodies** | | | | | |
| Alexa Fluor 488 | Mouse | Molecular Probes | | | 1/10,000 |
| Alexa Fluor 488 | Rabbit | Molecular Probes | | | 1/10,000 |
| GAM Cy5 | Mouse | Molecular Probes | | | 1/10,000 |
| GAR Cy5 | Rabbit | Molecular Probes | | | 1/10,000 |

**CHAPTER 3 – RESULTS**

**VACV N2 POLYCLONAL ANTI-SERA PRODUCTION AND CHARACTERIZATION**

**3.1. INTRODUCTION**

Vaccinia virus (VACV) is a large, double stranded DNA virus that replicates within the cytoplasm [77]. The central region of the genome is more conserved and encodes for proteins essential for viral replication [70]. The genes encoded outside of the central region are more variable and, although not required for viral replication, play important roles in modulating the host immune response [70]. As poxviruses replicate, it is inevitable that they will produce immunostimulatory nucleic acids that can activate the innate immune response [77]. To combat the host from initiating an effective immune response, numerous proteins are encoded by poxviruses to modulate the host immune response [70, 77]. For example, one group of VACV proteins, A46, A52, B15, K7, and N1, interfere non-redundantly in the toll-like receptor (TLR) signaling pathway [116].

Based on sequence homology, other VACV proteins that currently have no known functions are predicted to play roles in immune evasion [116], including N2, C1, C6, and C16/B22 [116]. VACV C6 has recently been characterized as a virulence factor that inhibits IRF3 and IRF7 activation by binding to the TBK-1 adaptor proteins TANK, SINTBAD, and NAP1 [47]. The C16 protein has also been characterized as another virulence factor, inhibiting IRF3 [32, 48]. The N2 protein is predicted to be a 21kDa protein expressed early in infection [117]. It is

highly conserved in the Orthopox genus while no obvious homologs are found in other organisms. The role of N2 will be discussed further throughout this thesis.

Antibodies are powerful research tools. In the presence of a foreign molecule, the host produces a collection of antibodies which can then be used to in downstream applications [118, 119]. Antibodies can be used for many research applications, including mapping the distribution of the virus antigen in cells, isolating the antigen from a mixture, or determining if the antigen binds any other macromolecules [118, 119]. Yet, there is no antibody available against the VACV N2 protein. In this chapter, the generation and characteristics of a new N2 polyclonal anti-serum is described. This anti-serum should be useful to determine the role N2 plays in the VACV lifecycle.

## 3.2. RESULTS

### 3.2.1. Expression and purification of the N2-His$_6$ protein

To generate recombinant His-tagged N2 protein for the generation of a polyclonal anti-serum, *E. coli* DHE 142 were transformed with N2L_ pET21a(+) (**Figure 3-1**) (described in **section 2.3.1.**). Bacteria were induced with IPTG and then grown at the optimal temperature of 37°C as well as at room temperature. *E. coli* can tolerate lower temperatures however protein synthesis occurs at a slower rate than at 37°C. In regards to inclusion bodies, lower temperatures can result in more soluble recombinant proteins. Protein samples from both the supernatant and the pellet were then fractionated by SDS-PAGE gels. As seen in **Figure 3-2**, both the coomassie blue stained gel and the nitrocellulose membrane stained with the
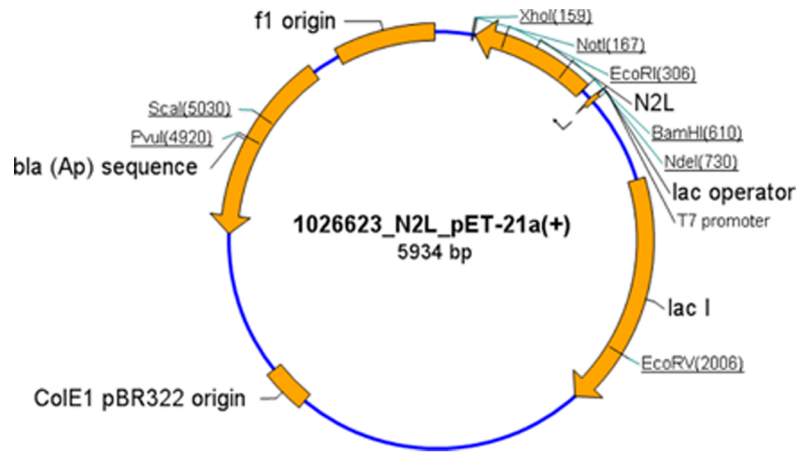
**Figure 3-1: N2L_pET-21a(+)**. An *E.coli* codon optimized N2L gene was synthesised by GeneART and cloned into pET21a(+) using Nde1 and Not1 cloning sites. This allows for inducible expression of N2 in frame with a N-terminal His tag. The final construct was verified through sequencing by GeneART.
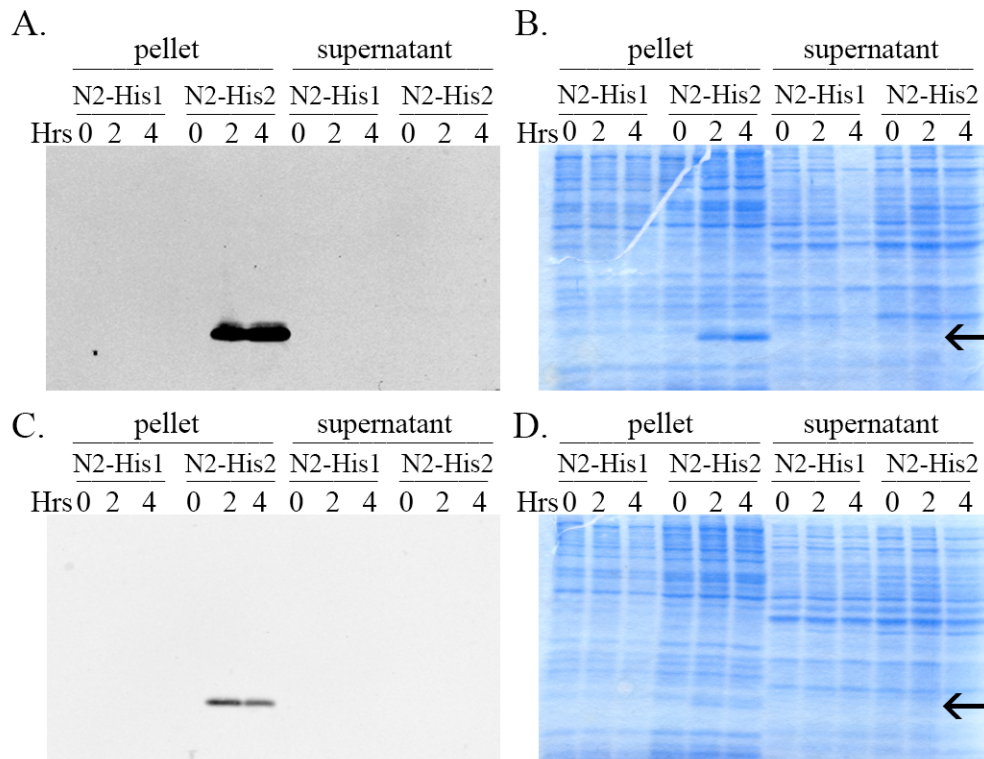
**Figure 3-2: Expression of N2-His protein**. Two separate isolates of DHE142 *E. coli* transformed with the N2L_pET21a(+) were grown to an OD600 of 0.6. Protein expression was induced with 1mM IPTG after which the bacteria were incubated at either 37°C (A+B) or room temperature (C+D). Bacteria were harvested, lysed, and the supernatant was separated from the pellet by centrifugation and the proteins were separated by SDS-PAGE gel electrophoresis. The gels were either stained with coomassie blue (B+D) or transferred to a nitrocellulose membrane and immunoblotted with a monoclonal anti-His antibody(A+C). The arrows indicate the position of the induced protein consistent with full length N2-His.

monoclonal anti-His$_6$ antibody show that the N2-His$_6$ tagged protein is expressed very well, however the protein was insoluble and formed inclusion bodies. Temperature did not increase the recombinant N2 protein solubility. However, greater expression was observed at 37°C then at room temperature.

Although the N2-His$_6$ tagged protein was insoluble and formed inclusion bodies, this protein could still be used to generate a polyclonal antibody. A large scale expression (described in **section 2.3.1.**) was performed to increase the amount of protein for purification. The inclusion bodies were isolated, washed, and then resuspended in binding buffer before being subjected to filtration for further purification and loaded onto a nickel column using the AKTA HPLC. The bound protein was then eluted off the column using a stepwise gradient of increasing concentrations of imidazole and 2 mL fractions were collected. A sample from each fraction was resolved by a SDS-PAGE gel and stained with coomassie blue. Two separate peaks appeared in the HPLC graph (**Figure 3-3**). These data are consistent with the coomassie blue stained gels, where the N2-His$_6$ protein eluted off the column in fractions A9-A12 and B1-B2. These fractions were pooled together and dialyzed in 1/10X PBS. Because the Bradford assay can only measure the concentrations of a protein in solution, we could not determine the concentration of the insoluble recombinant N2 protein through a Bradford assay. Instead, we compared the amount of recombinant protein to the VACV I3 (SSB) protein. The VACV I3 protein is a soluble protein whose concentration was determined through a Bradford assay. Both protein samples were diluted and

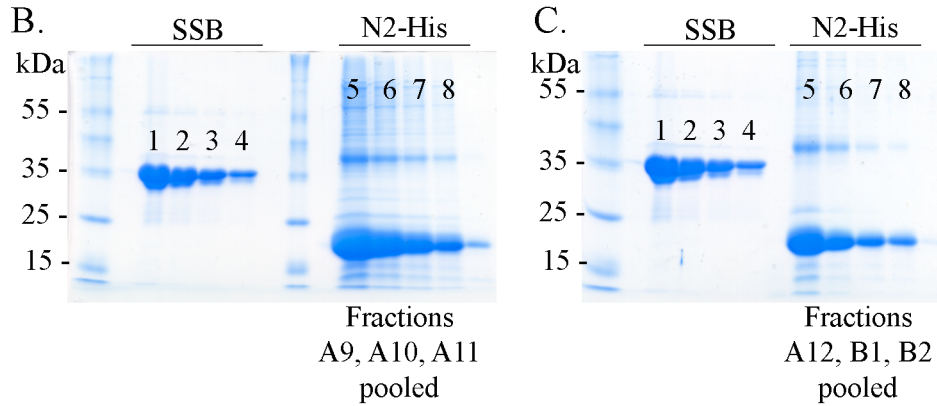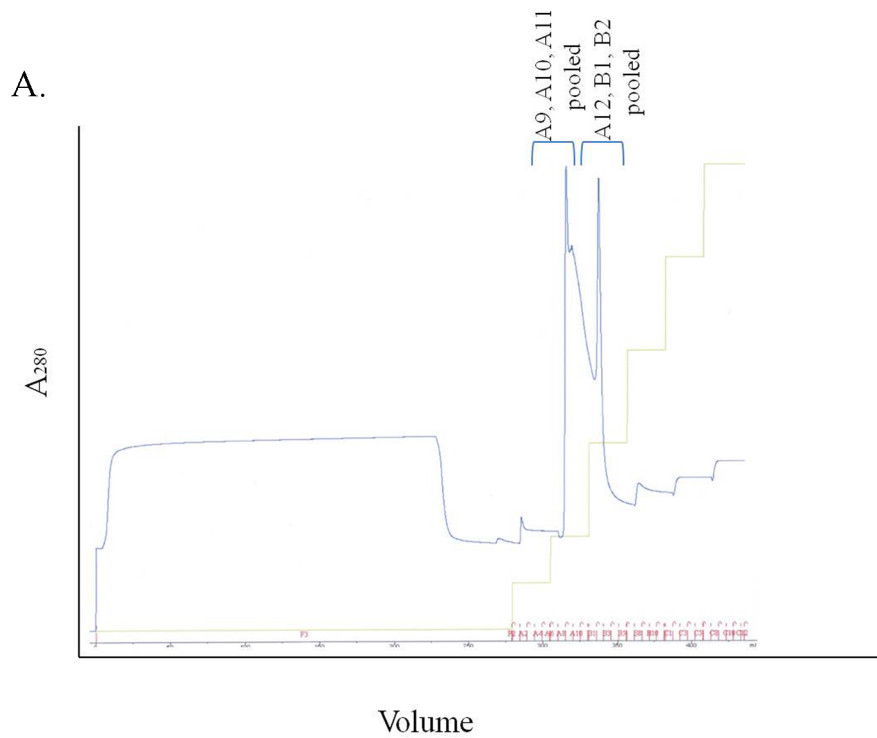**Figure 3-3: HPLC Tracings and SDS-PAGE gels from the N2-His protein purification.** (A) HPLC tracings for the N2-His protein elution from the AKTA. (B) SDS-PAGE gel of recombinant N2-His fractions A9-11 combined. The N2-His protein is diluted 10-fold per dilution (Lanes 5-8) and compared to a known SSB concentration of 1.5mg/mL (Lanes 1-4). (C) SDS-PAGE gel of recombinant N2-His for fractions A12, B1-2 pooled together.

fractionated on SDS-PAGE gels and the band intensities were compared to determine the concentration of the recombinant N2 (**Figure 3-3**).

### 3.2.2. Generation and optimization of the N2 polyclonal anti-serum

To generate the polyclonal anti-sera, the purified N2-His$_6$ tagged protein was sent to ProSci Incorporated (as described in **section 2.3.3.**) where four rabbits were immunized with the recombinant N2.

All pre-immune serum was tested for cross-reactivity with viral lysates in western blots (**Figure 3-4**). Rabbits 1 and 4 had very low cross-reactivity to the VACV infected lysates. Rabbit 3 reacted with some high molecular weight proteins present in both VACV infected cells and mock infected cells. Finally, rabbit 2 also had low cross–reactivity to the mock infected and VACV infected cells. However, at later times in infection, the pre-immune sera reacted with a ~35 kDa band. Still, no anti-sera picked up any signal related to N2.

All bleeds received from ProSci Incorporated were tested against protein samples prepared from BSC40 cells infected with WT virus. Proteins were fractionated by SDS-PAGE gel and western blotted using the rabbit serum (**Figure 3-5**).  No detectable signal was observed until the second bleed, after all three initial and the booster immunizations were given. Two rabbits with the strongest signal, rabbit 2 and 4, were selected for further analysis. Serum from these two rabbits strongly detected N2 in VACV-infected BSC40 cells. The fourth bleed produces a slightly stronger signal then the fifth bleed. It was therefore selected to be optimized and used in future experiments (**Figure 3-5**).
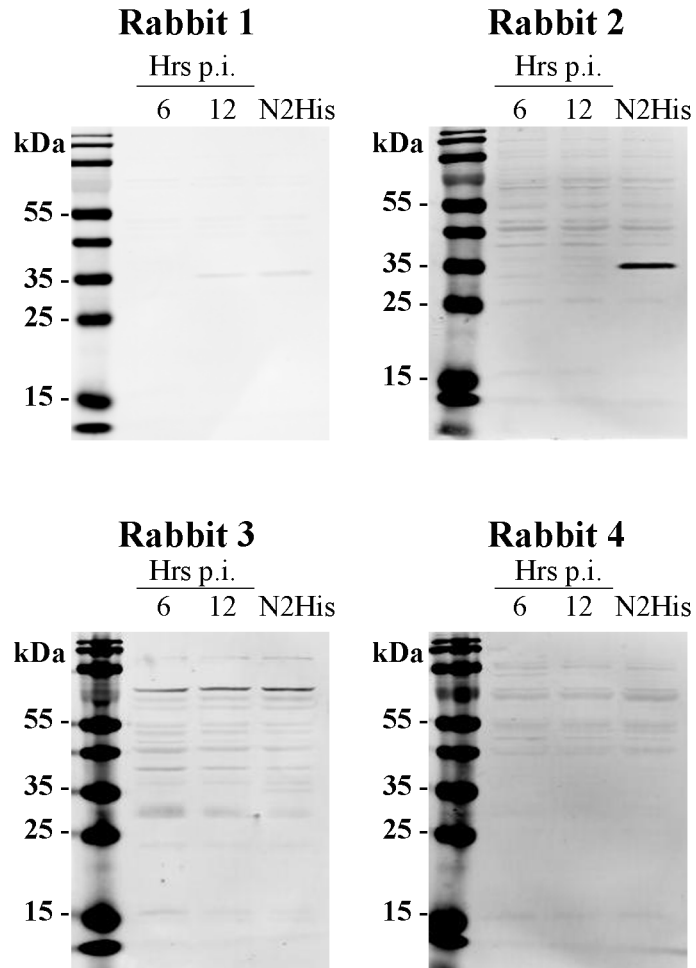
**Figure 3-4: Rabbit anti-serum prior to immunization with the recombinant N2-His protein.** Protein samples were fractionated by SDS-PAGE gel electrophoresis. Nitrocellulose membranes were stained with the pre-immunization bleeds at a 1 in 1000 dilution. Membranes were imaged on the LiCor Odyssey scanner.
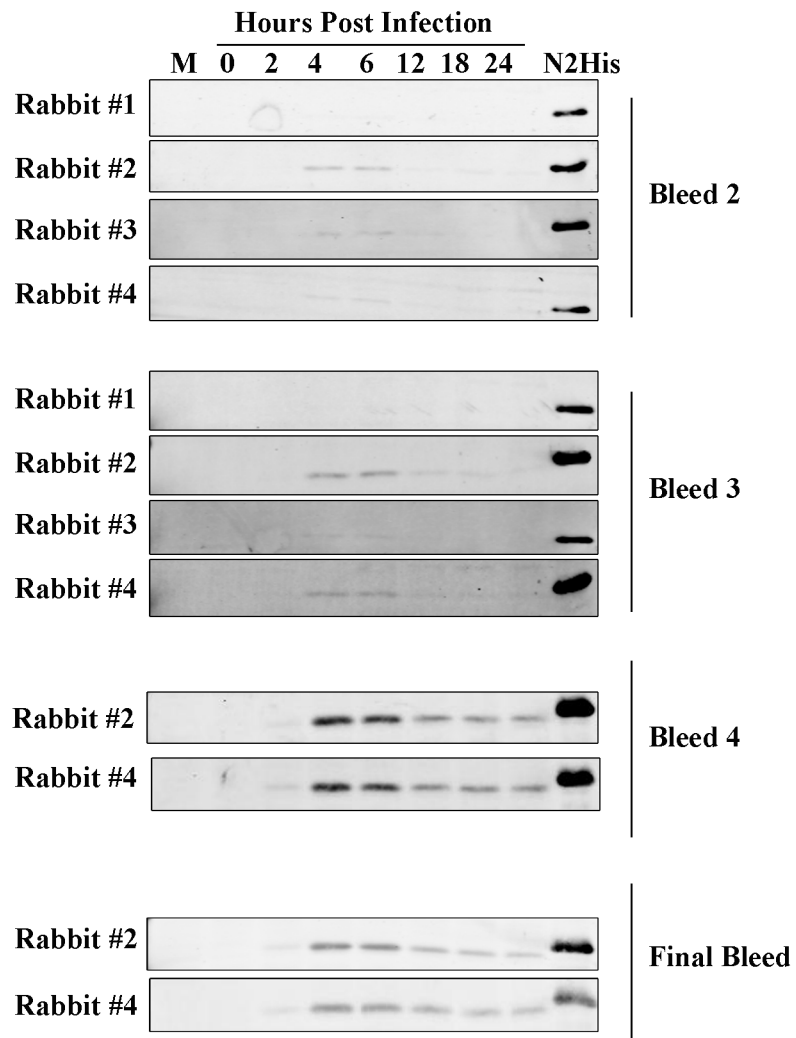
**Figure 3-5: Rabbit Anti-serum to N2-His protein.** The purified N2-His protein was injected into four separate rabbits by ProSci Inc. The anti-serum was tested against VACV infected BSC40 protein lysates at the indicated times. The N2-His protein was also incuded as a positive control. Note that the final bleed refers to the exsanguinations and only two rabbits were chosen for exsanguination.

Different dilutions were tested to further optimize the polyclonal anti-serum. As seen in **Figure 3-6**, all dilutions gave a detectable signal. The 1/1000 dilution was chosen to use in further experiments. A combination of the bleeds from both rabbits was also tested to see if the combination of both antibodies would produce a stronger signal. As seen in **Figure 3-6**, the combination of both antibodies does produce a stronger signal.

Since the N2 polyclonal anti-serum had some cross-reactivity with non-specific bands (**Figure 3-7**), we tried to reduce the detection of the non-specific bands by incubating the N2 anti-serum with acetone dehydrated BSC40 cells infected with the VACV N2L deletion virus (described in **section 2.4.2.**). As seen in **Figure 3-7**, after incubating the N2 polyclonal anti-sera with ΔN2L infected dehydrated cells, the background signal was significantly reduced without affecting the N2 signal.

### 3.2.3. Testing the N2 polyclonal antibody in immunoprecipitation

To determine if the N2 polyclonal anti-serum can be used to immunoprecipate the VACV N2 protein, BSC40 cells were either mock infected or infected with WT virus. Cells were collected 6 hours post-infection and then incubated with the N2 polyclonal anti-serum. Protein G Sepharose beads were used to pull down the N2 antibody as described in **section 2.8.3.** Bound proteins were then size fractionated by SDS-PAGE gel and subjected to western blot analysis using the N2 polyclonal anti-serum. As seen in **Figure 3-8**, the N2

A.



B.
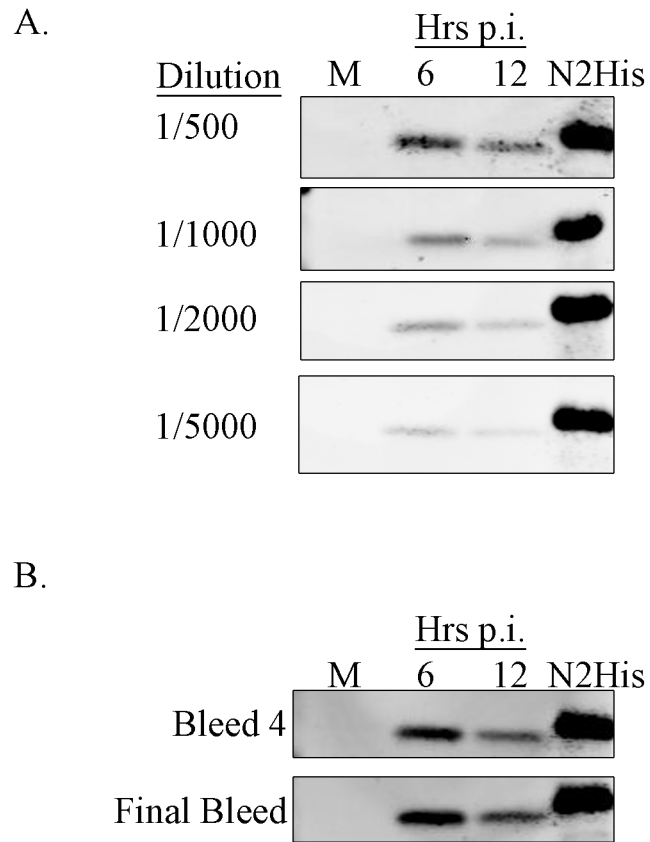


**Figure 3-6: Optimization of the N2 polyclonal antibody.** Protein samples harvested at the indicated time points were fractionated by SDS-PAGE. The nitrocellulose membranes were stained with several different dilutions of the anti-serum (A). Protein samples harvested at the indicated times were fractionated by SDS-PAGE gel. The nitrocellulose membranes were blotted with a mixture of the two anti-serums produced by rabbits #2 and #4 for Bleed 4 and the Final Bleed (B). The anti-sera from each rabbit was diluted 1 in 1000.
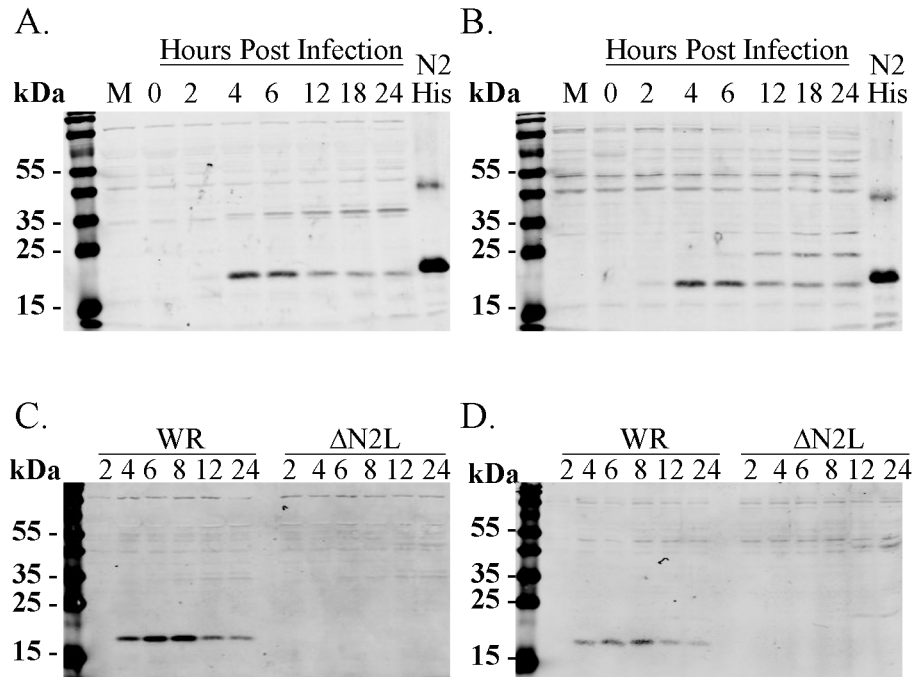
**Figure 3-7: Reducing the cross reactivity of the N2 anti-serum to non-specific proteins.** BSC40 cells were infected with the ΔN2L virus at an MOI of 5. Cells were harvested and then dried with acetone. The dried cell pellets were then incubated with the anti-serum overnight. Following the incubation, the cell debris was removed by centrifugation and the remaining anti-serum was tested in western blotting. Anti-serum from rabbit 2 bleed #4 (A) or rabbit 4 bleed #4 (B) before incubation with the dried cell pellet. Anti-serum from rabbit 2 bleed #4 (C) or rabbit 4 bleed #4 (D) after incubating with the dried cell pellet.
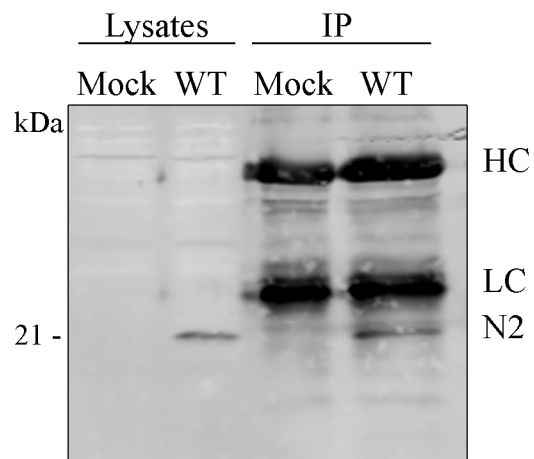
**Figure 3-8: The N2 polyclonal antibody can be used in immunoprecipitations.** BSC40 cells were either mock infected or infected with WT VACV for 6 hours. Cells were harvested and the N2 polyclonal antibody was incubated with the lysates. The antibody was pulled out with protein G sepharose beads. The proteins were then western blotted and stained using the N2 polyclonal antibody. The light (LC) and heavy (HC) chains are highlighted on the blot.

polyclonal anti-serum can successfully pull-down the ~21 kDa N2 protein in infected cells.

### 3.2.4. Testing the N2 polyclonal antibody in immunofluorescence

To determine if the N2 polyclonal anti-serum can be useful in immunofluorescence, BSC40 cells were seeded on coverslips and were either mock infected or infected with WT, ΔN2L, or rN2L viruses (described in **section 2.7.**). Cells were fixed 6, 12, 18, and 24 hours later, and then blocked and immunostained with either the untreated N2 anti-serum or the anti-serum treated with acetone dehydrated BSC40 cells. All time points showed the same staining pattern. Only 24 hours is depicted in **Figure 3-9**. The N2 protein is known to have a nuclear localization, discussed in Chapter 5 (**Figure 5-2**) [81, 120], and this N2 polyclonal anti-serum exhibited an non-specific staining pattern seen throughout the cytoplasm in cells regardless of the presence or absence of N2. These results indicate that the N2 polyclonal anti-serum is not specific in immunofluorescence.

### 3.3. DISCUSSION

Antibodies are useful tools in studying proteins. They can be used to determine cellular localization or isolate the protein from a mixture and determine any potential interactions with other proteins [118, 119]. Producing an antibody involves injecting the antigen into a laboratory animal, allowing the animal to mount an immune response, and finally, collecting the serum which contains the
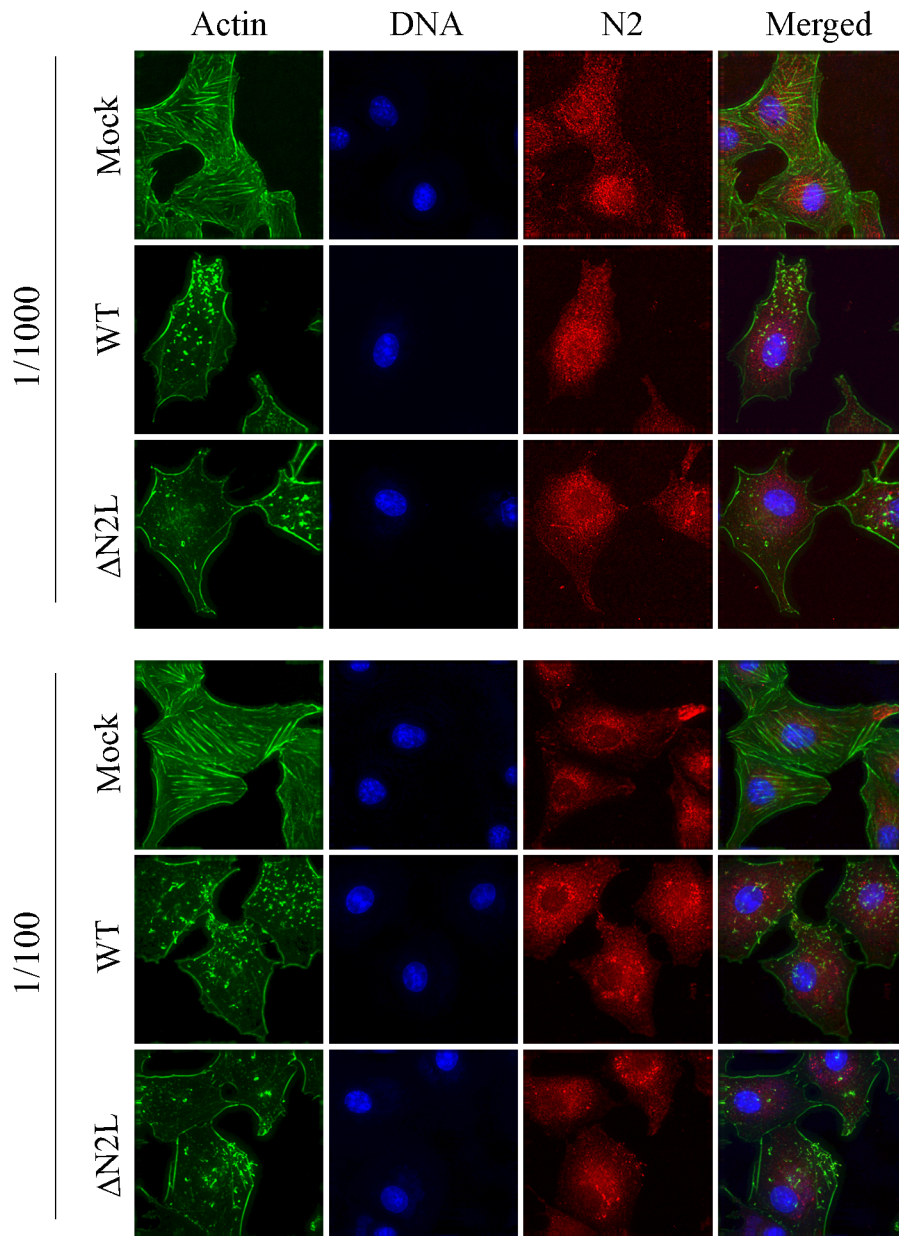
**Figure 3-9: Testing the N2 anti-serum in immunofluorescence.** BSC40 cells were either mock infected or infected with WT virus or the ΔN2L virus. Cells were fixed 24 hours post infection and stain with the N2 anti-serum at either a 1/1000 dilution or 1/100 dilution and counterstained with DAPI and rhodamine phalloidin to visualize DNA and actin respectively. Images were taken on a Deltavision microscope at 60X.

antibodies that will recognize the antigen [118]. Here we discuss how the N2 antigen was produced and how the polyclonal anti-serum was optimized.

Codon optimization of the N2L gene for expression in *E. coli* was used in an attempt to express a soluble protein to produce an antibody to N2. Although the N-terminal His$_6$-tagged N2 protein expressed well in *E. coli*, it formed inclusion bodies. It is not uncommon for recombinant proteins to form inclusion bodies in *E. coli* when expressed at such high levels [121]. Lowering the temperature after the bacteria were induced with IPTG did not increase the solubility of the protein. However, it did result in a lower yield of inclusion bodies produced. This is most likely due to the bacteria growing at a lower temperature resulting in slower growth of the bacteria which results in less protein being made. Even though the N2 protein formed inclusion bodies, we were still able to use it as an antigen in rabbits to produce a polyclonal anti-serum.

Western blot applications were used to test the polyclonal anti-sera produced by the four separate rabbits immunized with the N2 inclusion bodies. First, the pre-bleeds were screened for background activity and all rabbits exhibited a low cross-reactivity to the VACV infected lysates at the position of N2 (21 kDa). Next we examined the serum samples post-immunization. The first bleed was taken before the booster immunization, and did not detect any signal for N2 in VACV infected lysates. After the booster immunization, however, the sera began to detect N2 in VACV infected lysates. Rabbits #2 and #4 were chosen for further analysis since they produced the stronger signal against N2 in VACV infected lysates from the third bleed. Fourth and fifth bleeds were performed on

these two selected rabbits, as shown in **Figure 3-5**, and the fourth bleed produced a stronger signal to N2. Therefore it was selected to be optimized further.

Several high molecular weight bands were detected in uninfected and infected BSC40 lysates. This background was notably reduced by incubating the serum with acetone dehydrated BSC40 cells that were infected with the N2L deletion virus (**Figure 3-7**). The anti-serum from rabbit 2 (bleed 4) was then chosen for further experiments.

We successfully produced a polyclonal anti-serum against VACV N2 and determined that it could be used at a 1 in 1000 dilution in western blot applications. Next, we examined if the N2 polyclonal anti-serum could be used in immunoprecipitations or immunofluorescence assays. N2 is successfully pulled down from VACV infected lysates with the N2 anti-serum (**Figure 3-8**). However the polyclonal anti-serum was unable to detect N2 in immunofluorescence microscopy. The polyclonal anti-serum did not show any specificity to the nucleus in VACV infected cells, where N2 is known to localize (discussed further in **Chapter 5**). Instead, the polyclonal anti-serum stained the cytoplasm of the cells with no particular pattern. Moreover, the same staining pattern was observed in cells that were infected with WT or ΔN2L viruses, as well as those that were mock infected.

The new polyclonal anti-serum generated against VACV N2 proved to be very successful in western blotting techniques as well as immunoprecipitations. However, it proved to be unsuccessful in immunofluorescence. Nevertheless, this anti-serum will prove useful in studying the role of N2.

**CHAPTER 4 – RESULTS**

**EXPLORING THE ROLE OF N2L IN POXVIRUS BIOLOGY**

**4.1. INTRODUCTION**

Vaccinia virus is a large DNA virus that encodes for more than 200 genes [122]. The central region is highly conserved and encodes for proteins required for viral replication while the variable terminal regions encode for proteins that affect virulence or host range [32]. A subset of proteins encoded by the variable regions target the innate immune system [32]. In order to suppress the innate immune response, the majority of these proteins are expressed early in infection [32]. Another notable feature of these immunomodulatory proteins is that several proteins target the same cellular signaling pathway [32].

Signal transduction networks play a critical role in the innate immune response to virus infection, integrating and translating various markers of infection into an array of protective responses, including new patterns of gene expression. The sophistication and complexity of these systems is illustrated through VACVs ability to interfere in the activation of a nuclear factor kappa B (NFκB) dependent inflammatory response (reviewed in [32, 65, 66]).

There are at least thirteen VACV proteins identified that collectively suppress the NFκB signaling pathway [32]. Ten of these VACV proteins are intracellular and act at different stages in the signaling cascade to inhibit NFκB [32]. However, it has been speculated that there may be additional proteins with an unknown function that target this pathway [116]. In this chapter, we investigate N2's role in replication and spread of the virus, as well as virulence properties.

**4.2. RESULTS**

**4.2.1. N2L is an early gene and is not required for VACV replication in cell culture**

We started this work by examining what role N2 had on VACV replication. For this, we needed to create an N2-deficient virus. We had no problems constructing viruses lacking N2L (**Figure 4-1**), immediately suggesting that the gene is not essential for growth in tissue culture. To measure these effects more quantitatively, we compared the effects of the ΔN2L mutation on plaque size 48 hours post-infection, and on virus yield in multi-step growth curves. Deleting N2L had no significant effects on the sizes of the plaques formed on BSC40 cells (**Figure 4-2**) and plating virus at MOI of 0.01 on BSC40 cells yielded similar levels of WT, ΔN2L and rN2L viruses when measured 48 or 72 hr post-infection. The kinetics of virus production were also very similar (**Figure 4-2**). We concluded that N2L is not required for VACV spread or replication *in vitro*.

Promoter analysis and deep sequencing of VACV RNA transcripts suggests N2 is an early gene [123]. We wanted to confirm this by analyzing protein lysates. For this, BSC40 cells were infected with WT, ΔN2L, or the N2L revertant (rN2L) virus were the N2L gene is restored in the ΔN2L virus. Proteins were extracted at different times post-infection, size fractionated using SDS-PAGE, and western blotted using the polyclonal N2L antibody (**Figure 4-3**). The protein is first detected around 4 hours. The protein levels are highest between 6 and 12 hours. However, N2 can still be detected at 24 hours post infection. These
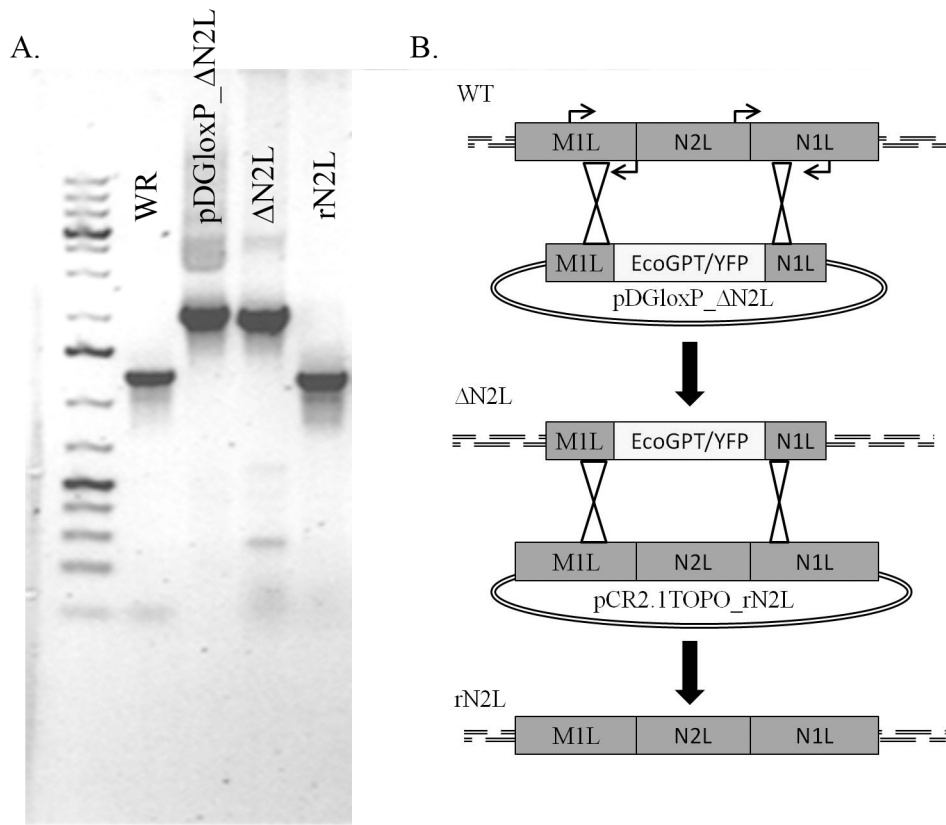
**Figure 4-1: PCR analysis on the N2L locus.** PCR was used to amplify the N2L locus in the WR virus strain, the pDGloxP_ΔN2L plasmid used to create the ΔN2L virus, the purified ΔN2L virus, and the rN2L virus using the N2L KO Left FWD and N2L KO Right REV primers (A). Strategy used to assemble the recombinant viruses (B).

A.



B.
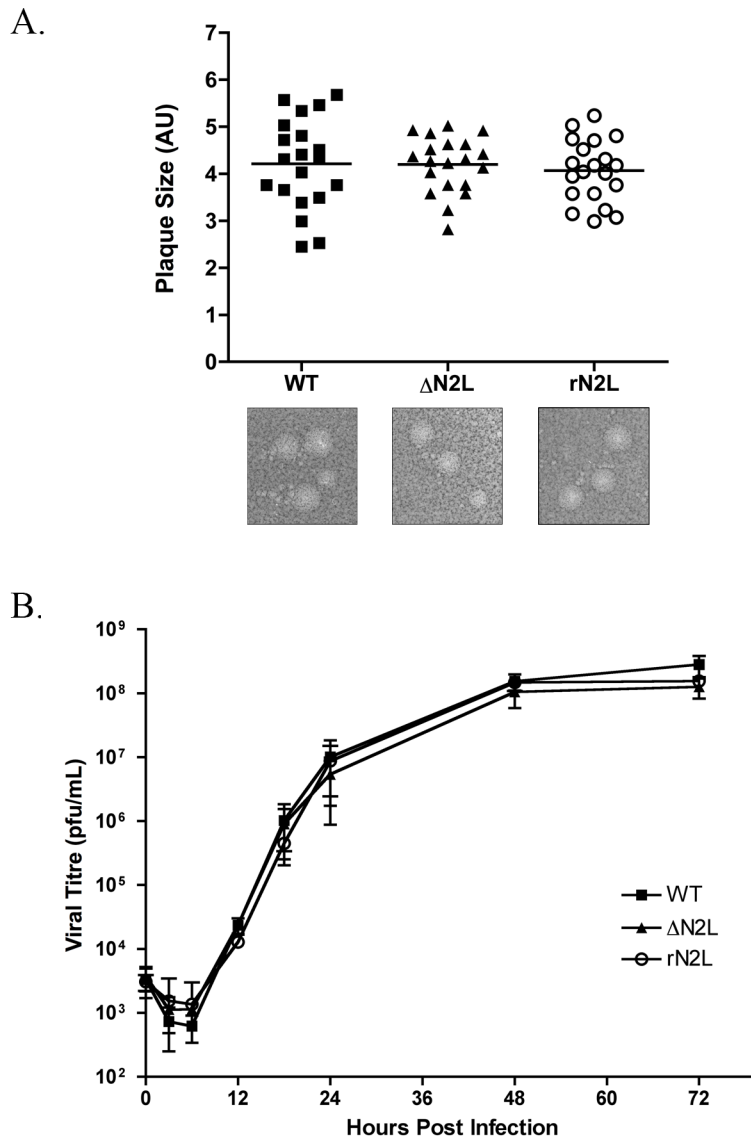


**Figure 4-2: VACV N2L is not required for viral spread or replication *in vitro*.** BSC40 cells were infected with the indicated viruses and stained with crystal violet 48 hours post infection. Plaque sizes were measured using Image J and plotted with Prism (AU = Aribitrary Units). Plaque images are displayed below the graph (A). BSC40 cells were infected at an MOI of 0.01 with the WT, ΔN2L, or rN2L viruses. Cells were harvested at the indicated time points and titered on BSC40 cells (B). The mean plus S.E.M. are shown from three separate experiments.
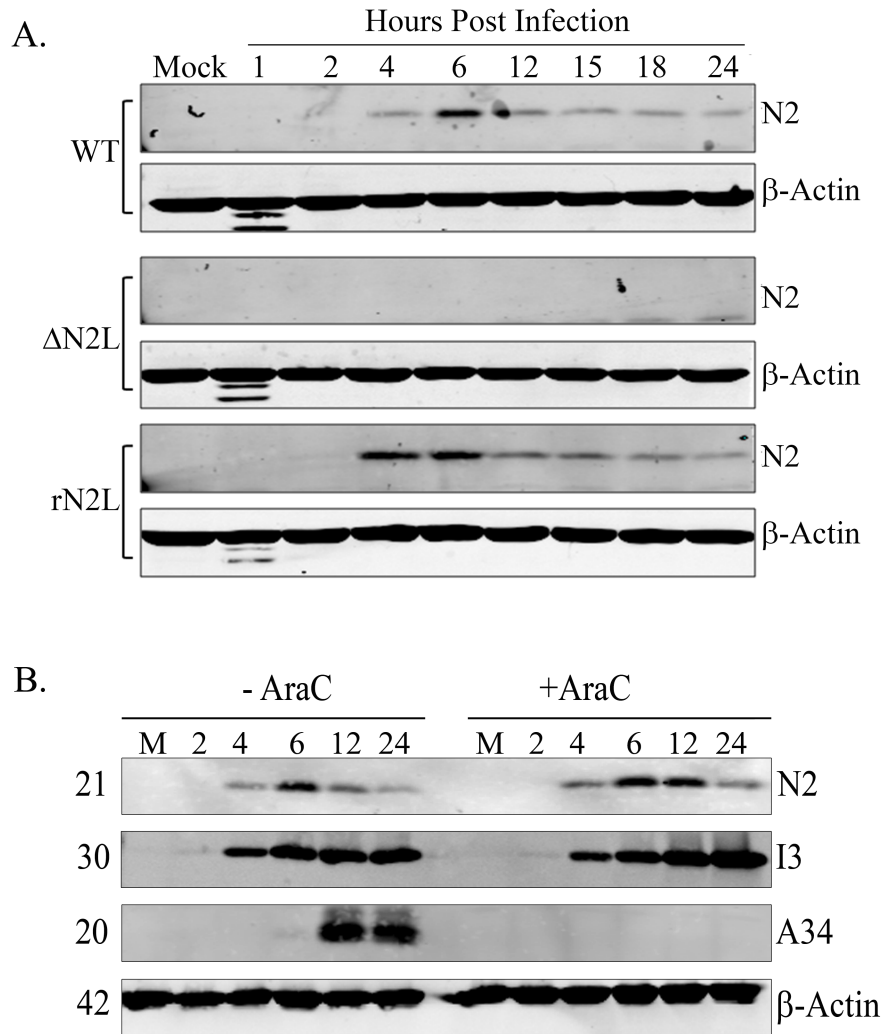
**Figure 4-3: N2L is an early protein.** BSC40 cells were infected with WT, ΔN2L, or rN2L at an MOI of 5. Cells were harvested throughout the infection and total protein was extracted then fractionated by SDS-PAGE. N2 was detected with the polyclonal antibody (A). BSC40 cells were infected at an MOI of 5 with WT. The cells were then left untreated or treated with 80μg/mL araC to inhibit late gene expression. Proteins were extracted and western blotted. 13L and A34R are known early and late genes, respectively (B).

results suggest that N2 is an early protein. To further test if N2 is a *bona fide* early protein, BSC-40 cells were infected with VACV WT and treated with cytosine arabinoside (araC) to inhibit replication and consequently late gene expression. The proteins were extracted, size fractionated using SDS-PAGE, and western blotted using antibodies directed against N2, I3 (an early VACV gene product), A34 (a late VACV gene product), and cellular β-actin (**Figure 4-3**). N2 was still synthesized even in cells treated with araC, showing that it, like VACV I3, is an early gene product.

### 4.2.2. N2 does not confer α-amanitin resistance or temperature sensitivity

It has previously been suggested that a G-to-T transversion mutation at the -10 position in the leader sequence of N2L is responsible for creating α-amanitin resistance and temperature sensitivity [103]. We wanted to test if our N2L deletion virus also behaved in the same manner. We infected BSC40 cells with the WT, ΔN2L, or rN2L viruses, as well we included two clones of Dryvax (DP15 and DP17) and two clones of Tian Tan (TP11 and TP3). The Dryvax and Tian Tan virus strains were cloned by Dr. Li Qin (as described in **section 2.4.1.**) and were include as controls. At the -10 position in the leader sequence of N2L, Dryvax encodes a 'T' whereas Tian Tan and our lab WR strain encodes for a 'G'. Infection inoculums were replaced with MEM containing 0, 2, or 6 μg/mL α-amanitin and incubated at 37°C or 39.5°C for 48 hours. Plaque sizes for each virus increased slightly when cells were treated with 2 μg/mL α-amanitin at either temperature whereas they decreased when treated with 6 μg/mL α-amanitin when

incubated at either temperature (**Figure 4-4**). The number of plaques for each virus treatment remained constant between the different treatment conditions (**Figure 4-5**). We also tested the virus ability to grow on BSC40 cells that were pre-treated with α-amanitin for different periods. BSC40 cells were pretreated with either 2 or 6 μg/mL α-amanitin for 12, 6, or 3 hours and then infected. After the infection, the α-amanitin was replaced with the MEM for already treated cells. Plaque sizes displayed similar effects to the first experiment, where 2 μg/mL increased the plaque size and 6 μg/mL decrease the plaque size (**Figure 4-6**). Once again, total number of plaques on each plate for each virus treatment remained constant throughout the different drug treatments (**Figure 4-7**). With this data however, we saw no effects of the ΔN2L mutation on virus growth on BSC40 cells in the presence of α-amanitin.

### 4.2.3. N2 inhibits the activation NFκB sensitive promoters

To investigate if N2 inhibits NFκB activity, we used a TNF-α sensitive transfection-reporter system comprising of a plasmid encoding a firefly luciferase gene regulated by an NFκB dependent promoter, and a transfection/transcription control plasmid encoding a *Renilla reniformis* luciferase gene regulated by a herpes simplex virus thymidine kinase promoter. The *Renilla reniformis* luciferase gene is always expressed while the firefly luciferase is only expressed when the NFκB pathway is activated. Once the cells are stimulated with TNFα, the firefly luciferase will be expressed, and if N2 blocks this pathway, we will see a decreased level of firefly luciferase activity. HEK293 cells were co-transfected
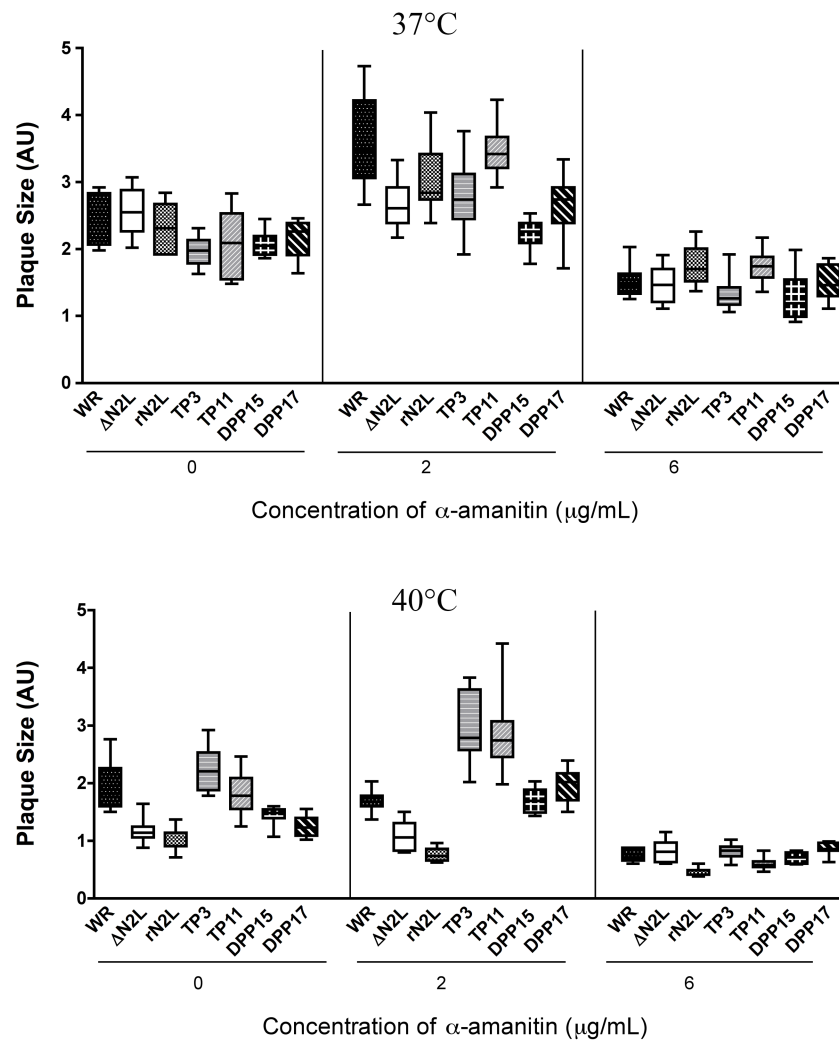
**Figure 4-4: The N2L mutants can grow in the presence of α-amanitin at both the permissive and non-permissive temperatures.** BSC40 cells were infected with the indicated viruses at ~80 pfu/dish and were either treated with 2μg, 6μg or left untreated. The cells were left for 48 hours and then stained with crystal violet. Plaque measurements were captured using Image J.
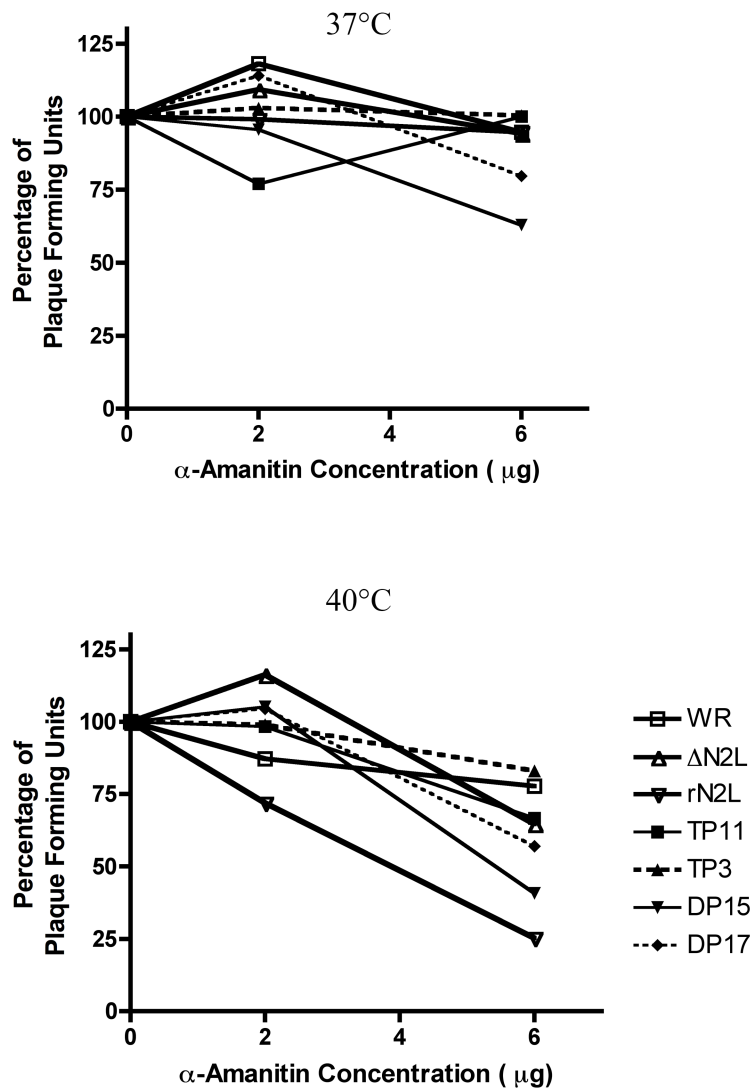
**Figure 4-5: The N2L mutants can grow in the presence of α-amanitin at both the permissive and non-permissive temperatures.** BSC40 cells were infected with the indicated viruses at ~80 pfu/dish and were either treated with 2μg, 6μg or left untreated. The cells were left for 48 hours and then stained with crystal violet. The number of plaques in each well were counted and then graphed.
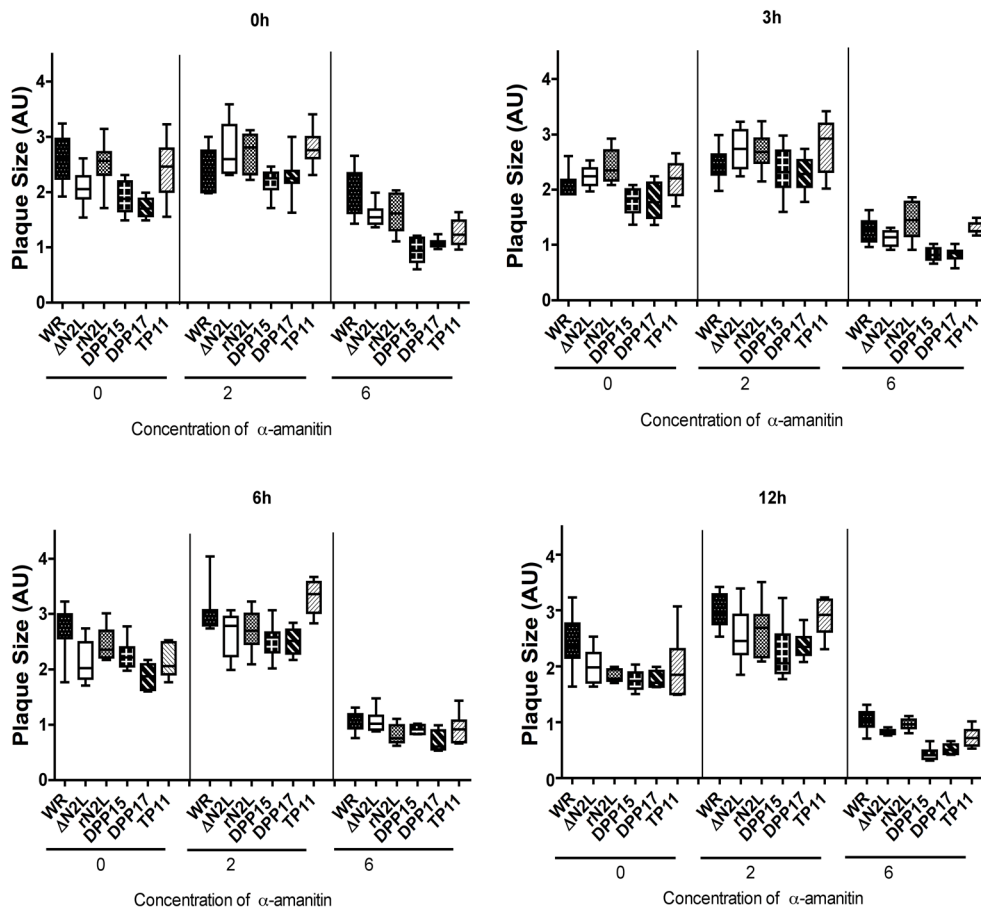
**Figure 4-6: The N2L mutants can grow on BSC40 cells pretreated with α-amanitin.** BSC40 cells were pretreated with either 2μg or 6 μg, or left untreated for 12, 6, or 3 hours and then infected with the indicated viruses. The cells were stained 48 hours post infection with crystal violet and the plaques were measured with Image J.
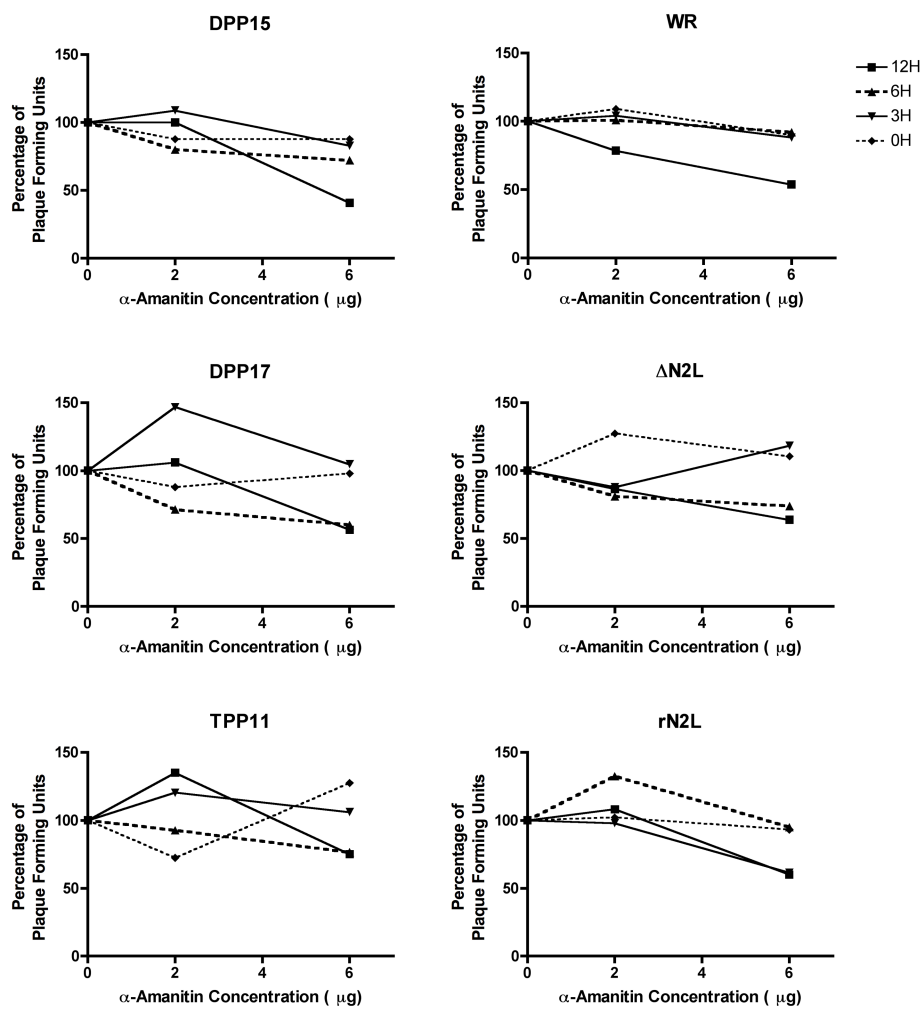
**Figure 4-7: The VACV N2L mutants are able to grow on BSC40 cells pre-treated with α-amanitin.** BSC40 cells were treated with 2μg or 6 μg for 0, 3, 6, or 12 hours and then infected with ~80 pfu for 48 hours. Cells were then stained with crystal violet and the number of plaques were counted.

with these two reporter plasmids along with a plasmid encoding the CMV promoter-regulated MYC tagged N2 (see **section 2.2.3.**) or the pcDNA3.0 vector. Twenty-four hours later, the cells were treated (or mock-treated) with 50 ng/mL TNF$\alpha$ and then assayed for the levels of firefly luciferase relative to the expression of *Renilla* luciferase to normalize the expression for transfection efficiency. The results are shown in **Figure 4-8**. The reporter system readily detects TNF-$\alpha$-dependent activation of the NF-$\kappa$B-regulated firefly luciferase gene, and the level of expression of firefly luciferase is significantly reduced in cells transfected with plasmids encoding MYC tagged N2 protein. However, even in the presence of N2, there is still a significant increase in the NF$\kappa$B activity. We also tested the WT, $\Delta$N2L and rN2L viruses ability to inhibit the NF$\kappa$B pathway (**Figure 4-9**). Here, cells were transfected with the two reporter plasmids. Twenty-four hours later the cells were stimulated with 5, 16.7, or 50 ng/mL TNF$\alpha$ for 30 minutes and then infected with WT, $\Delta$N2L, or rN2L. Cells were lysed 6 hours post infection and then assayed for levels of firefly luciferase relative to the expression of *Renilla* luciferase. We saw no difference in levels of luciferase expression between the different virus groups or mock infected cells.

### 4.2.4. N2 does not affect the localization of NF$\kappa$B p65.

With the help of Dr. M. Barry and Ms. Kristen Burles (University of Alberta), we examined the N2 deletion virus ability to phosphorylate I$\kappa$B, which is upstream in the pathway of NF$\kappa$B activation. Upon phosphorylation, the I$\kappa$B protein is degraded and releases the NF$\kappa$B proteins. HeLa cells were infected with
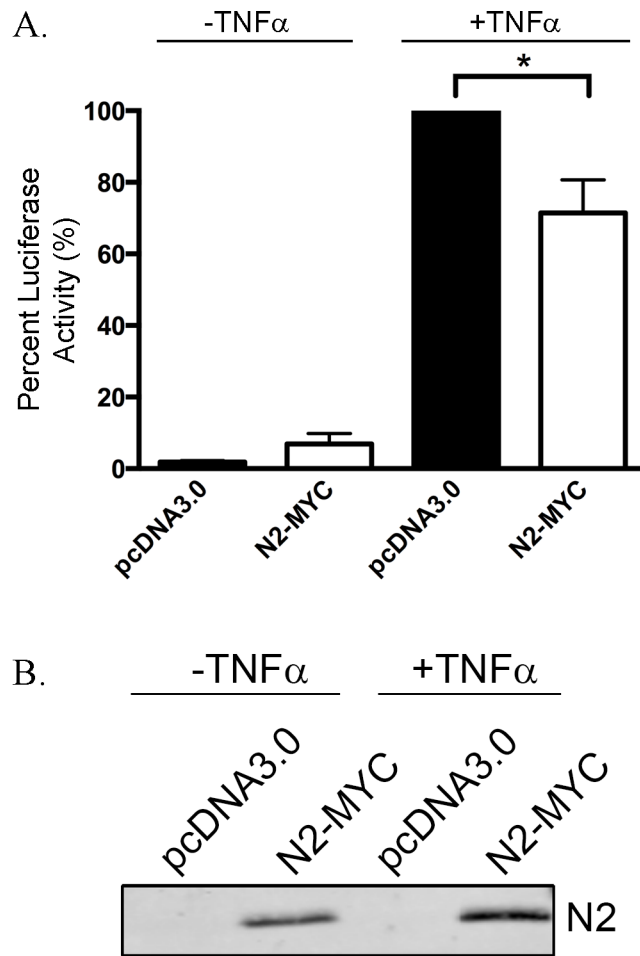
**Figure 4-8: N2 inhibits the NFκB promoter.** HEK 293 cells were transfected with 60 ng of the empty vector plasmid (EV) pcDNA3.0 or the C-terminal tagged N2-MYC plasmid. The cells were left untreated or were treated with TNFα. Six hours after stimulation, the cells were washed, lysed, and then measured for luciferase activity (A). Western blot of the lysed proteins (B).
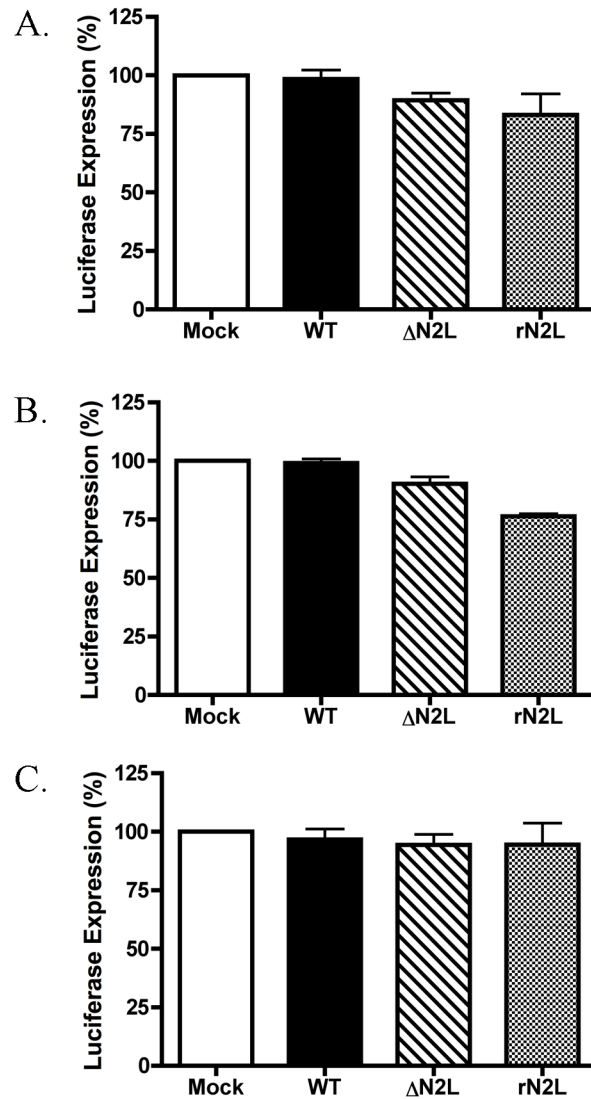
**Figure 4-9: N2L has no affect on the NFκB promoter during a virus infection.** HEK 293 cells were infected with the indicated viruses for 6 of hours and treated with varying amounts of TNFα throughout the infection. (A) 50 ng/mL TNFα, (B) 16.7 ng/mL TNFα, and (C) 5 ng/mL TNFα.

WT, ΔN2L, or rN2L at an MOI of 5. At 12 hours post infection, the cells were treated with 50 ng/mL TNFα and harvested at specific time points (**Figure 4-10**). Proteins were fractionated by SDS-PAGE gels and blotted for either total IκBα or phosphorylated IκBα. Once again, there were no differences between the viruses induction of IκB phosphorylation as all virus treatment groups were unable to prevent the phosphorylation of IκB. Interestingly, the phosphorylated IκBα protein is not degraded during infection, unlike the case in the mock infected samples.

We also examined the localization of the NFκB p65 subunit in HEK 293 cells that were either mock treated or treated with TNFα. In the untreated cells, p65 is predominantly cytoplasmic for the WT, ΔN2L and rN2L viruses whereas in cells treated with TNFα, the p65 subunit re-localizes to the nucleus (**Figure 4-11**). We observed no differences in p65 localization in cells infected with either WT, ΔN2L or rN2L viruses when the cells are treated with TNFα.

### 4.2.5. Examining the role of N2L in VACV pathogenesis

To test whether N2L is a virulence gene, Balb/c mice were infected at a low dose ($1x10^3$ pfu/mouse) or a high dose ($1x10^4$ pfu/mouse). The animal weights were measured daily throughout the course of infection (**Figure 4-12**). The low dose of virus had little effect on the mice. Only the WT treated group had a mild sign of illness. The high dose of virus had a greater effect on the mice, where all treatment groups except the PBS mice lost weight. The ΔN2L group

| Mock | WT | ΔN2L | rN2L | |
|---|---|---|---|---|
| | | | | TNFα |
| 0  10 20 30  60 120 | 0  10 20 30  60 120 | 0  10 20 30  60 120 | 0  10 20 30  60 120 | (min) |

IκBα

P-IκBα

I3L

β-Actin
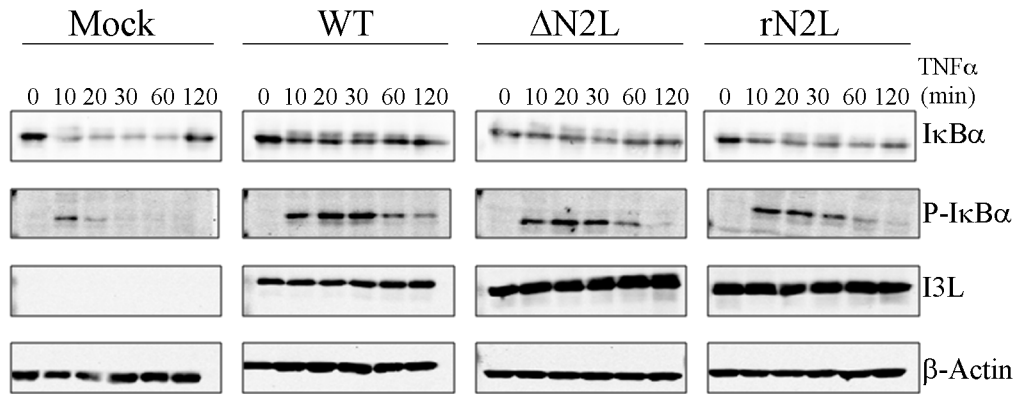
**Figure 4-10: N2 does not affect IκBα degradation.** HeLa cells were infected with the indicated viruses for 12 hours. TNFα was then added to the cells and the cells were harvested at the indicated times. Proteins were fractionated by SDS-PAGE and western blotted for IκBα, P-IκBα, I3L and β-actin.
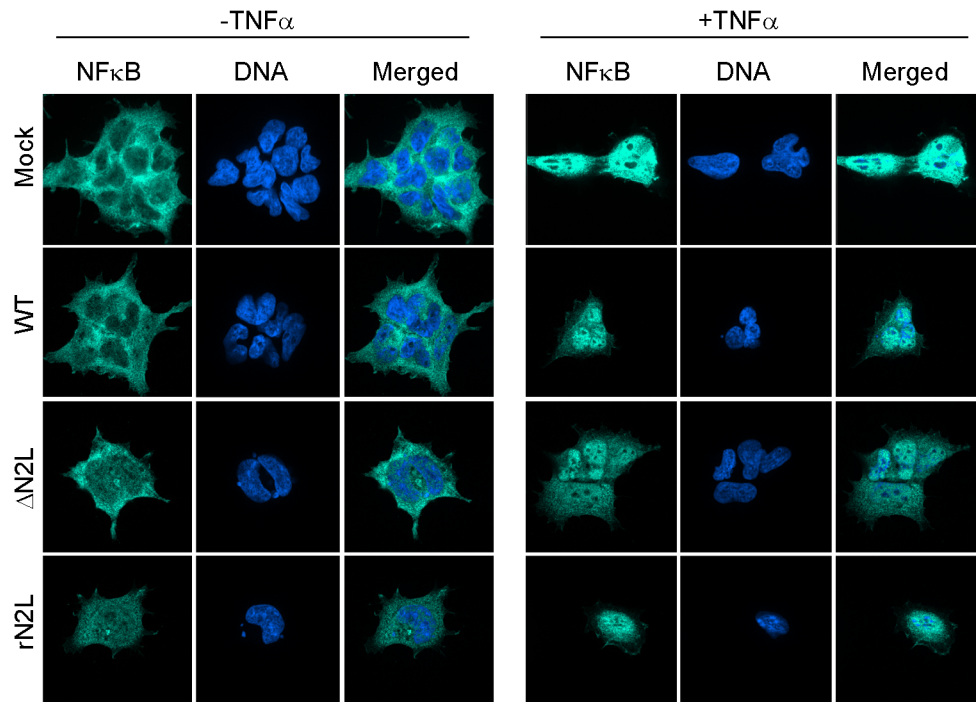
**Figure 4-11: N2 does not alter the localization of the NFκB p65 subunit.** HEK 293 cells were infected with the indicated viruses at an MOI of 5 for 6 hours. Thirty minutes prior to fixation the cells either stimulated with TNFα or left unstimulated.The cells were then fixed and stained with DAPI and the NFκB p65 antibody to visualize DNA and the NFκB p65 subunit. Images were taken on a Quorum WaveFX spinning disk confocal microscope.

A.



B.
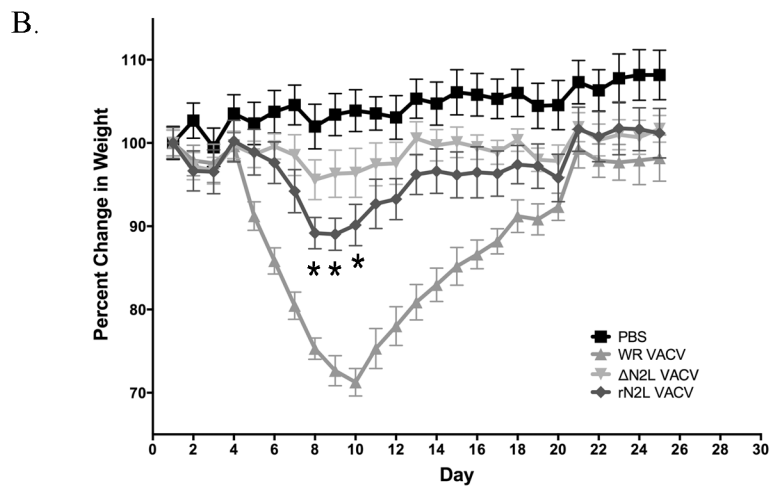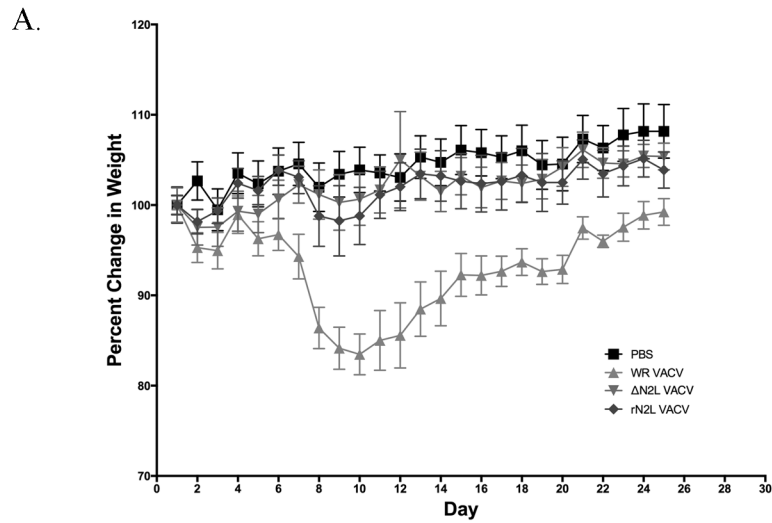


**Figure 4-12: Percent change in body weights.** Balb/c mice were infected with WT, ΔN2L, or rN2L viruses or treated with PBS. The animal were weighed daily and the data is plotted as the percent change in body weight. Weight differences in low dose group (A). Differences in the high dose group (B). (* = significant difference between ΔN2L and rN2L virus groups)

displays a similar trend to the PBS group. Even though the rN2L group lost weight, the group does not drop in weight similar to the WT virus.

Due to the differences in the virulence between the rN2L and WT viruses, we decided to sequence the ΔN2L and rN2L virus genomes to examine if the rN2L might have had a second site mutation, relative to the WT virus. The N2L locus is successfully disrupted in the ΔN2L virus and present in the rN2L virus. However, there is a single nucleotide substitution at position 89977 in the H4L gene (RNA polymerase associated protein RAP94) that changes the sequence from an arginine (ΔN2L) to an isoleucine (rN2L). It is unclear what impact this substitution has on the virus.

## 4.3. DISCUSSION

VACV encodes for a large number of proteins that suppress the activity of the innate immune system [32, 65]. Many of these proteins target steps involved in the upstream activation and nuclear translocation of the NFκB family transcription factors. Because N2 is predicted to be part of A46-related family [116], which is a family of VACV proteins that target the TLR signaling pathway, this led us to test what effect N2 might have on the TNF-α dependent activation of an NFκB regulated promoter.

We were able to create a complete N2L deletion mutant, which immediately suggests that the N2L gene is not required for growth in tissue culture. Knocking out the N2L gene had no effect on the plaque size of the virus and we saw no significant difference to the amount of virus produced at 48 and 72

hours post infection in the multi-step growth curve. We were also able to confirm that N2 is an early protein since it was still produced in the presence of AraC. Interestingly, the N2 protein levels decrease throughout the infection whereas the I3 protein levels do not. This is due to I3 being expressed at both early and intermediate times during infection.

Looking more closely at the proposed G-to-T transversion mutation, we noted that this site (-10 with respect to the N2L start codon) is associated with a sequence polymorphism, being a 'G' in VACV strain WR and some Tian Tan strains [110], and a 'T' in strains Lister, Copenhagen and in all of the Dryvax clones we have recently sequenced [109]. None of these strains are naturally temperature sensitive, including our Dryvax clones. In our experience, the N2L deletion mutant was still capable of growing in the presence of α-amanitin and it did not show signs of temperature sensitivity. Whether temperature sensitivity, defects in core protein cleavage, replication in enucleated cells, and α-amanitin resistance are all manifestations of mutations linked to N2L [103] should probably be revisited.

To determine if N2 plays a part in inhibiting the NFκB pathway, we examined if N2 can inhibit the activity of a firefly luciferase reporter plasmid. From our data, N2 did not inhibit the activity of the NFκB promoter driving luciferase expression. We also examined at the viruses ability to inhibit the NFκB reporter plasmid. Three different concentrations of TNFα were used to stimulate the cells. At 5 ng/mL and 50 ng/mL, there is no difference between the WT, ΔN2L, and rN2L viruses. At 16.7 ng/mL however, the rN2L signal is lower than

the WT and ΔN2L wells. This can be due to an experimental error when adding the reagents. These data show that during a virus infection, N2 does not have an effect on the NFκB promoter. However, in the absence of infection, N2 is capable of inhibiting the NFκB promoter.

We also examined the localization of NFκB subunit p65. The p65 subunit under normal cellular conditions is cytoplasmic, while when a cell undergoes a stress response, the p65 subunit is translocated into the nucleus. First, we looked at if deleting N2 had any effect on the phosphorylation of the IκBα protein. IκBα inhibits NFκB by masking the NLS of the subunits such as p65 and holding it in the cytoplasm, preventing it from being transported to the nucleus. Once the IκBα is phosphorylated, the protein gets degraded and releases the NFκB subunits. No differences are observed when comparing the phosphorylation of IκBα amongst WT, ΔN2L, and rN2L. The phosphorylation of IκBα peaks around 30 minutes after TNFα treatment in all virus groups, and then starts to decline 60 minutes post treatment. Interestingly, in the mock infection, we observe a rapid decrease in the amount of phoshporylated IκBα which is not observed during virus infection. This may indicate that VACV is somehow blocking the degradation of IκBα once it becomes phosphorylated. When looking at the localization of NFκB p65 subunit during the infection, it remains in the cytoplasm for all virus treatments (WT, ΔN2L, or rN2L). However, if we stimulate the cells with TNFα 30 minutes prior to fixation, we see p65 localize to the nucleus in all virus treatments (WT, ΔN2L, and rN2L). However, as discussed in the **Chapter 1**, VACV encodes for

ten intracellular NFκB inhibitors. Our immunofluorescence data shows that even in the WT infection, treatment with TNFα still results in the translocation of the p65 subunit. From these data we can conclude that N2 is not altering the localization of the NFκB p65 subunit. These results are not surprising since N2 has a nuclear localization while the p65 unit is held in the cytoplasm. If N2 inhibits NFκB activity, it should do so in the nucleus, downstream of p65 subunits translocation into the nucleus.

There have been numerous instances where a VACV protein is not required for growth in tissue culture but it is still needed *in vivo*. To determine if N2 is a virulence factor, we infected Balb/c mice through the intranasal route with the WT, ΔN2L, and rN2L viruses. Interestingly, the outcome of ΔN2L virus infection tends to follow that of the PBS control group. The mice show little signs of illness and do not lose a significant amount of weight. In the WT treatment group the mice fell very ill, which was determined by total weight loss as well as signs of illness. Surprisingly, the rN2L group didn't behave exactly like the WT group. This group did become sick however, the WT group displayed greater signs of illness. It is unclear why there is a difference between the two viruses. Therefore, to determine if there was an alternate mutation, we sequenced the recombinant viruses. From sequencing the ΔN2L and rN2L viruses, we can see that the N2 locus is completely deleted in the ΔN2L virus while it is present, with no errors, in the rN2L virus strain. Further investigation of the sequence led us to find 1 amino acid substitution between the 2 viruses in the H4L gene. The impact that this mutation has on the virus is unknown. An alternate explanation that could

account for the difference seen between the WT and rN2L groups is that the rN2L virus was plaque purified whereas our WT virus stock was not.

In conclusion, we have shown that N2 is not necessary for growth in tissue culture as we were able to delete the gene without affecting the growth of the virus. However *in vivo* it appears to be a virulence factor. We were unable to reproduce the results claiming that N2 is responsible for $\alpha$-amanitin resistance and temperature sensitivity. Our luciferase reporter assays did show that N2 can inhibit the activity of the NF$\kappa$B promoter. This effect is occurring after the translocation of the p65 subunit into the nucleus since N2 had no effect of the phosphorylation of I$\kappa$B$\alpha$, as well it does not have any effect on the localization of the NF$\kappa$B p65 subunit.

**CHAPTER 5 – RESULTS**

**VACV N2L IS A CONSERVED ORTHOPOX GENE THAT INTERACTS WITH KPNα2 AND KPNα4**

**5.1. INTRODUCTION**

An often-noted feature of poxvirus biology is that these large DNA viruses are replicated and assembled in the cytoplasm of infected cells [29]. Due to their cytoplasmic nature, poxviruses were traditionally thought to encode their own replication machinery and require little contribution of host nuclear proteins [28]. However, in recent years host nuclear proteins have been found to be either present in viral factories or contribute to viral replication. These include a host-encoded inhibitor of viral DNA replication called BAF, which is countered by the VACV B1 kinase [124], and cellular topoisomerase II, which is stabilized within virus replication sites through an interaction with the VACV DNA ligase [44]. Furthermore, several poxvirus proteins have been shown to localize with the cell nucleus, including C4 [46], C6 [47], C16 [48], B14 [49], E3 [50], and F16 [51]. This chapter examines whether N2 is another VACV protein that localizes to the cell nucleus.

Entrance and exit of large proteins to the nucleus is controlled by nuclear pores [82]. Large proteins, which cannot diffuse into the nucleus, encode a nuclear localization signal (NLS) which allows them to be recognized by transport proteins [82]. In the classical nuclear import pathway, a protein encoding a NLS interacts with a family of adaptor and transport proteins called karyopherins (KPNs) [87]. Proteins belonging to the KPN α family serve as adaptor molecules,

linking the NLS-bearing proteins (cargos) to importin β [87]. This interaction promotes the translocation of the cargo through the nuclear pore [87].

Bioinformatics analysis of the VACV proteome identifies only two proteins, N2 and O1, which encode classic bipartite NLS sequences. O1 has recently been reported to play a role in enhancing Raf/MEK/ERK signaling [125], but our examination of the localization of this protein suggests it has a cytoplasmic localization (**Figure 5-1**). In contrast, as we show here, N2 localizes to the nucleus.

The function of the VACV N2L gene has recently been shown to be an inhibitor of IRF3. However, the mechanism of action remains unclear [81]. The protein belongs to a large family of poxvirus proteins that are predicted to share a common Bcl-2-like structure and many suppress TLR signaling [116]. Here we show that N2 is a nuclear protein, and it co-immunoprecipitates with KPNs $\alpha$2 and $\alpha$4, and appears to associate with DNA. However the purpose served by this association remains uncertain.

## 5.2. RESULTS

### 5.2.1. N2L is conserved amongst orthopoxviruses

Analysis of published sequence data showed that the N2L gene is highly conserved amongst orthopoxviruses (www.poxvirus.org) (**Figure 5-2**). Using the Sequences Identities and Similarities tool (SIAS) (http://imed.med.ucm.es/Tools/sias.html), it was determined that the different full length genes share between 88-97% amino acid identity. Only portions of the
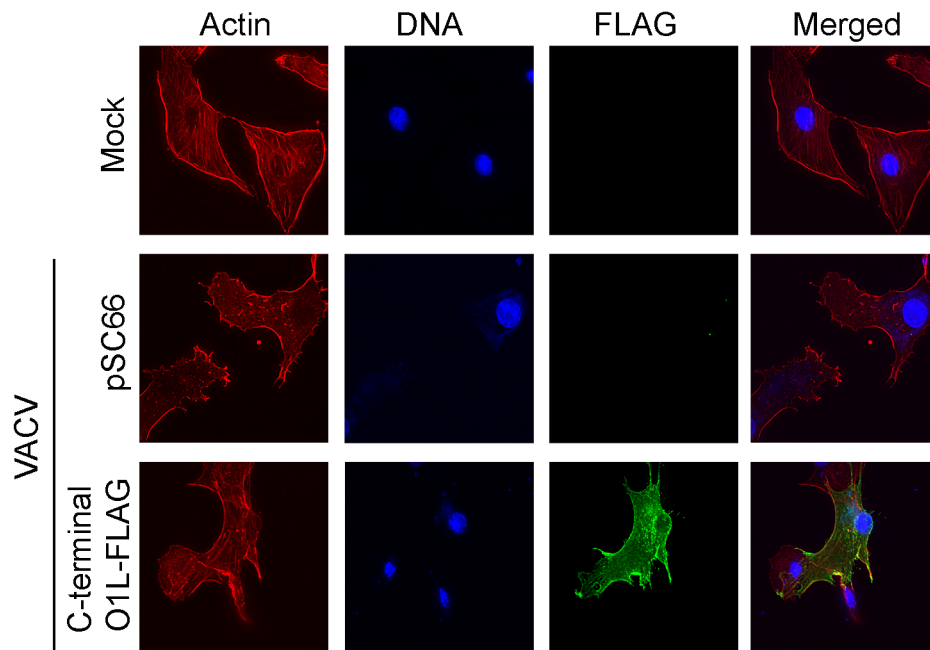
**Figure 5-1: Localization of VACV O1L C-terminal FLAG tagged protein.**
BSC40 cells were either mock infected or infected with WT virus at an MOI of 5. The cells were then transfected 2 hours post infection with either the pSC66 empty vector or the O1L C-terminal FLAG tagged construct. Cells were fixed at 24 hpi and stained with rhodamine phalloidin, DAPI, and anti-FLAG to view actin, DNA, and the Flag tagged O1 protein respectively. Cells were imaged using a Deltavision microscope at 60X.

```
Vaccinia     MTSSAMDNNEPKVLEMVYDATILPEGSSMDPNIMDCIN-RHINMCIQR-TY 49
Variola      MSSSTMDNNEPKVLEMVYDSPILPEGSSMDPNIINCIN-RHINMCLQH-TY 49
Ectromelia   MTSSAMDNNEPKVLEMVYDATILPEGSGMDPSIIDCIN-RHINMCTQR-SY 49
Monkeypox    MTSSAMDNNEPKVLEMVYDATILPECSGMDPSIIDCIN-RHINMRIQR-SY 49
Cowpox       MTSSTMGNDEPNVLE-VYDATFLPEGSSMDPNIIDCIN-RHIDMCIQRRSY 49
Camelpox     MSSSAMDNNEPKVLEMVYYSPILPEGSSMDPNIINCIN-RHINICIQR-TY 49
Taterapox    --------------------------MDPNIINCINRRHINMCIQR-TY 22
                                      ***.*::*** ***::   *: :*

Vaccinia     SSSIIAILDRFLMMNKDELNNTQCHIIKEFMTYEQMAIDHYGGYVNAILY 99
Variola      SSSIIAILDRFLMMNKDELNNTQCHIIKEFMTYEQMAIDHYGGYVNAILY 99
Ectromelia   SSSNIIAILDRFLMMNKDELNNTQCHIIKEFMTYEQMAIDHYGGYVNAILY 99
Monkeypox    SSSNIIAILDRFLMMNKDELNNTQCHIIKEFMTYEQMAIDYYGGYVNAILY 99
Cowpox       SSSIIAILDRFLTMNKDELNNTCHIIKEFMTYEQMAIDHYGGYVNAILY 99
Camelpox     SSSIIAILDRFLMMNKDELNNTQFHIIKEFMTYEQMAIDH---------- 89
Taterapox    SSSIIAILDRFLMI-KDELNNTQCHIIKEFMTYEQMAIDHYGGYVNAILY 71
                **.********* : ******* **************:

Vaccinia     QIRKRPNQHHTIDLFKRIKRTRYDTFKVDPVEFVKKVIGFVSILNKYKPV 149
Variola      QIRKRPNQHHTIDLFKKIKRTRYDTFKVDPVEFVKKVIGFVSILNKYKPV 149
Ectromelia   QIRKRPNKHHTIDLFKRIKRTRYDTFKVDPVEFVKKVIGFVSILNKYKPI 149
Monkeypox    QIRKRPNQHHTIDLFKRIKRTRYDTFKVNPVEFVKKVIGFVSILNKYKPI 149
Cowpox       QIRKRPNQHHTIDLFKRIKRTRYDTFKVDPVDFVKKVIGFVSILNKYKPV 149
Camelpox     ------------------------------------------------- 89
Taterapox    QIRKRPNQHHTLICLKE--------------------------------- 88

Vaccinia     YSYVLYENVLYDEFKCFINYVETKYF-- 175
Variola      YSYVLYENVLYDELKCFIDYVETKYFQN 177
Ectromelia   YSYVLYENVLYDELKCFIDYVETKYFQN 177
Monkeypox    YSYVLYENVLYDELKCFIDYVETKYFQN 177
Cowpox       YNYVLFENVLYDELKCFIDYVETKYFQN 177
Camelpox     --------------------------- 89
Taterapox    --------------------------- 88
```

**Figure 5-2: Sequence alignment of N2 homologs amongst Orthopoxviruses.**
The sequence alignment of N2L shows that N2 is a highly conserved protein in the Orthopoxvirus genus. The putative bipartite nuclear localization signal, identified by ScanProsite, is highlighted in grey. Residues highlighted in dark grey are necessary for the bipartite nuclear localization signal. This sequence alignment was generated with Clustal W. (* = conserved residue; : = conservation between groups of strongly similar properties; . = conservation between groups of weakly similar properties)

gene appear to have been retained by taterapox and camelpox viruses. The N2L gene in taterapox is truncated at both the 5' and 3' ends and camelpox virus is missing the 3' end. The putative bipartite nuclear localization signal (NLS), identified by the ScanProsite tool (prosite.expasy.org/**scanprosite/***)*, is conserved in all of the full-length Orthopoxvirus proteins however, it is partially or completely eliminated by the deletions in taterapox and camelpox viruses.

## 5.2.2. N2 localizes to the nucleus during a viral infection

The presence of the NLS suggests that N2 might normally traffic to the nucleus, and we wanted to determine if this is the case. Since the polyclonal N2 antibody proved unsuitable for immunofluorescence purposes (as discussed in **Chapter 3** (**Figure 3-9**)), we generated a series of N2-MYC constructs that allowed us to examine its localization. These constructs were placed under a synthetic E/L pox promoter (see **section 2.2.1.** and **2.2.2.**) or a CMV promoter (see **section 2.2.3.**), which allowed us to examine N2 localization in either the presence or absence of viral infection.

The N2-MYC construct under the CMV promoter was transfected into uninfected BSC40 cells and the location of the MYC-tagged protein determined by immunofluorescence microscopy. Essentially all of the MYC-tagged N2 appeared to be transported to the nucleus as judged by confocal microscopy (**Figure 5-3B**). This method may lead to protein over-expression, and suffers from the fact that the cells are not also infected. To address this concern, we transfected the C-terminal MYC tagged N2 construct under the synthetic early/late pox
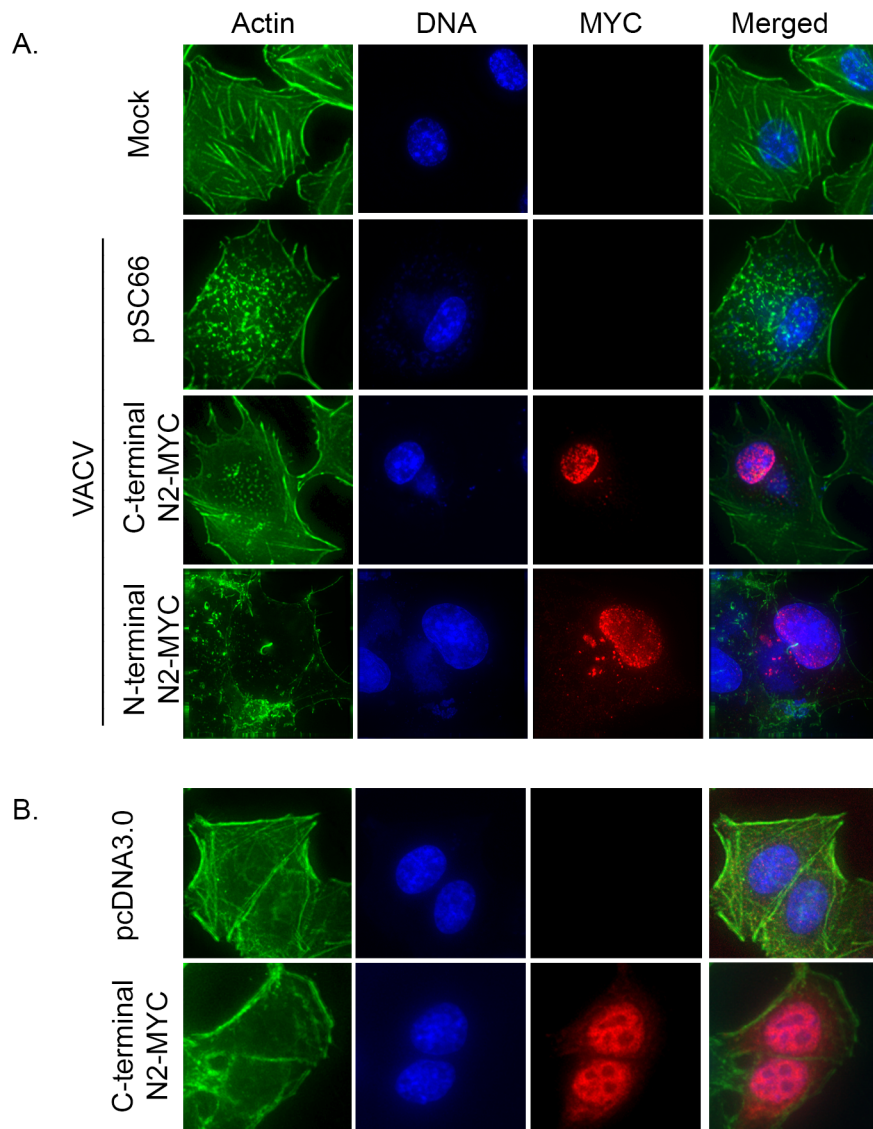
**Figure 5-3: Expression of N2 tagged proteins.** BSC40 cells were either mock infected or infected at an MOI of 5 with WT virus. The cells were then transfected 2 hpi with 150ng of the empty vector pSC66, the N2 C-terminal MYC tagged construct, or the N2 N-terminal MYC tagged construct (A). HeLa cells were transfected with 150ng of the pcDNA3.0 empty vector or with the C-terminal N2-MYC construct expressed from the CMV promoter (B). Both sets of cells were fixed at 18 hpi and stained with rhodamine phalloidin, DAPI, and anti-Myc antibody to view actin, DNA, and the MYC tagged N2 protein, respectively. Cells were imaged using a Deltavision microscope at 60X.

promoter into infected BSC40 cells and the location of the MYC-tagged N2 protein was determined by immunofluorescence microscopy. The protein expressed in this manner was also transported to the nucleus (**Figure 5-3A**). Finally, we transfected DNAs encoding the N-terminal MYC tagged versions of N2 into infected BSC40 cells and the location was determined by immunofluorescence microscopy. Like the C-terminal MYC tagged N2, the N-terminal tagged proteins localize to the nucleus (**Figure 5-3A**).

### 5.2.3. N2 associates with cellular karyopherin proteins KPNα2 and KPNα4

Proteins bearing NLS tags are usually trafficked to the nucleus through an interaction with one or more karyopherin proteins [87]. Furthermore, it was previously shown through a yeast-two-hybrid screen that N2 interacts with two KPN α isoforms [126]. To investigate whether N2 uses these karyopherin import proteins to enter the nucleus, protein interactions between N2 and host KPN proteins were determined though protein immunoprecipitations. BSC40 cells were transfected with plasmids encoding N-terminal FLAG-tagged KPNα proteins (described in **section 2.8.1.**) and then infected with WT VACV. Immunoprecipitation after six hours of infection with the anti-FLAG antibody co-immunoprecipitated N2 with two of the six tested karyopherin alpha isoforms: KPNα2 and KPNα4 (**Figure 5-4**). A reciprocal immunoprecipitation study was done where BSC40 cells were infected with WT VACV and then immunoprecipitated with the N2L polyclonal anti-serum which co-precipitated with KPNα2 (**Figure 5-4**).

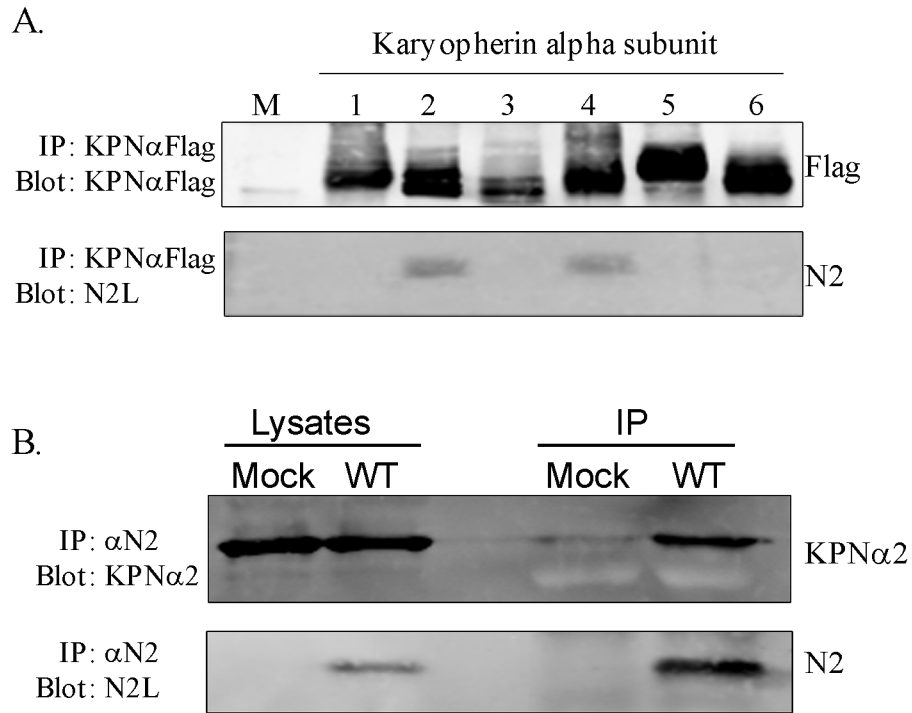**Figure 5-4: N2 interacts with cellular KPNα2 and KPNα4.** BSC40 cells were mock transfected (M) or transfected with plasmids encoding FLAG-tagged KPNα proteins and then infected with WT VACV. Immunoprecipitation with an anti-FLAG antibody co-precipitated N2 with KPNα2 and KPNα4 (A). For the reciprocal IP, BSC40 cells were infected with WT VACV. Immunoprecipitation with the N2 polyclonal antibody co-precipitated KPNα2 (B).

**5.2.4. Effect of N2 on the distribution of karyopherins and other proteins**

We next wondered whether N2 affects the distribution of KPNα1, KPNα2 and KPNα4 in cells infected with the WT, ΔN2L, and rN2L viruses. We observed that the distributions of KPNα1 and KPNα4 were not altered in the presence or absence of N2 (**Figure 5-5** and **Figure 5-7**). However, we found that the presence of N2 altered the distribution of KPNα2 (**Figure 5-6**). KPNα2 is predominantly in the cytoplasm of uninfected cells, and this distribution was not substantially altered in cells infected with the WT or rN2L viruses. However, KPNα2 relocated to the nuclear periphery in cells infected with the ΔN2L virus forming a ring of antigen that is most clearly seen in the thin sections of the nucleus obtained using confocal microscopy. These data suggest that N2 can somehow suppress a cellular system that is triggered by replicating VACV, and which when activated causes the re-localization of KPNα2. However, the effect seems to be restricted to KPNα2, other KPNs are unaffected.

We also tested what effect N2 had on the distribution of a small selection of other nuclear-targeted proteins. The first was an artificial reporter protein that is not expected to have any special affinity for VACV proteins and consisted of enhanced blue and green fluorescent proteins, fused together, and bearing a bipartite N-terminal SV40 NLS (see **section 2.9.2.**). The fusion creates a large (~57 kDa) protein with unique fluorescent properties that is normally translocated into the nucleus by the nuclear transport machinery. We found that co-expressing this generic reporter protein along with the C-terminal N2-MYC (**section 2.2.3.**)

**Figure 5-5: N2 does not alter the localization for KPNα1.** BSC40 cells were infected with the indicated viruses for 6 hours. The cells were then stained with rhodamine phalloidin, DAPI and KPNα1 antibody to visualize actin, DNA, and KPNα1 respectively. Cells were imaged using a Deltavision microscope at 60X.
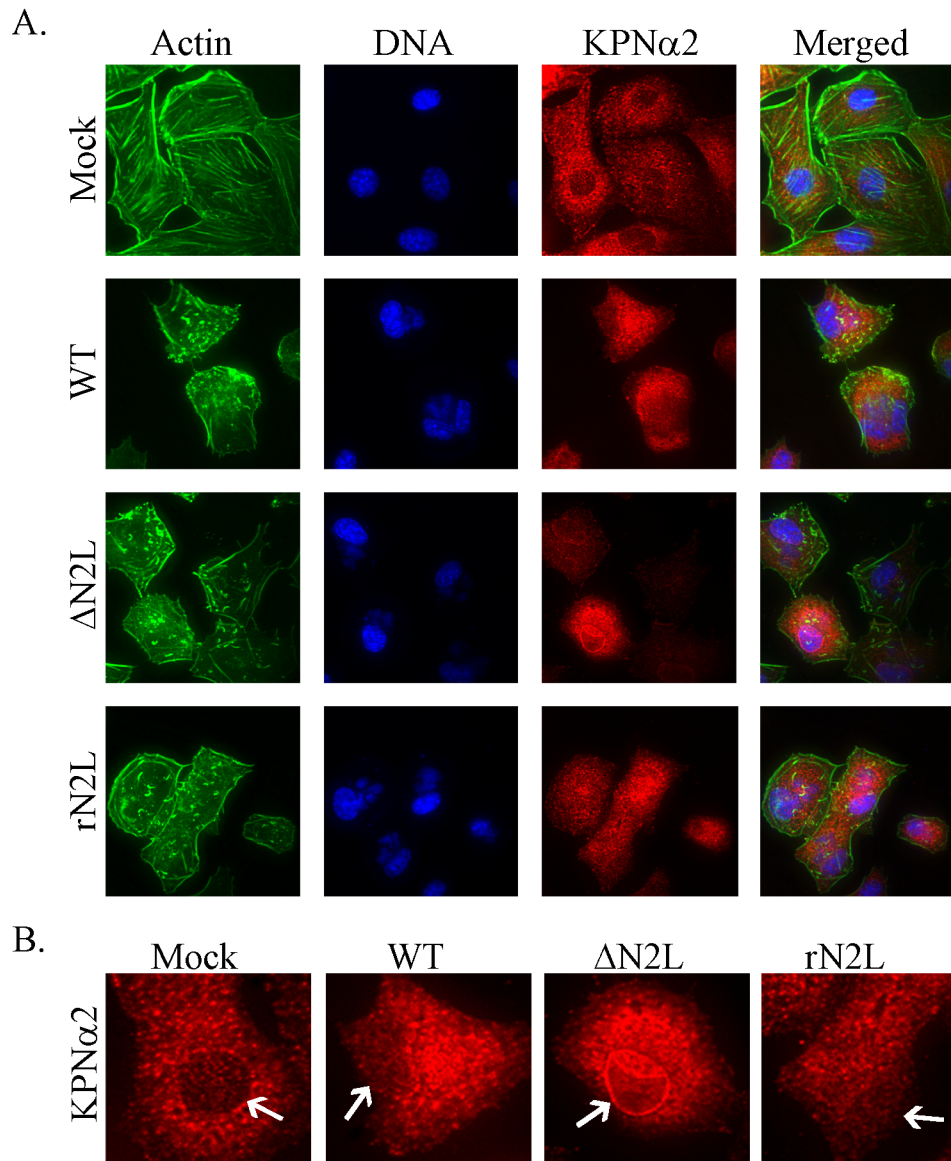
**Figure 5-6: The presence of N2 alters the localization of KPNα2 during VACV infection.** BSC40 cells were infected for 6 hours with the indicated viruses. The cells were then stained with rhodamine phalloidin, DAPI, and the KPNα2 antibody to visualize actin, DNA, and KPNα2 respectively. Cells were imaged using a Deltavision microscope at 60X (A). Enlarged images of KPNα2 staining pattern (B). White arrows indicate the location of the host nucleus.
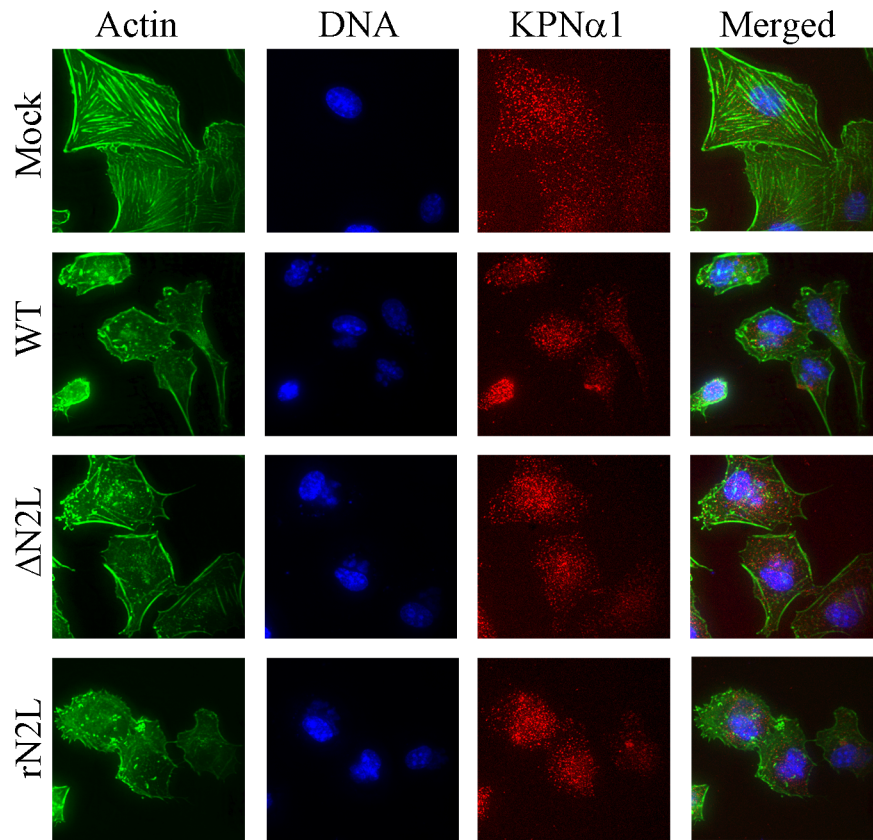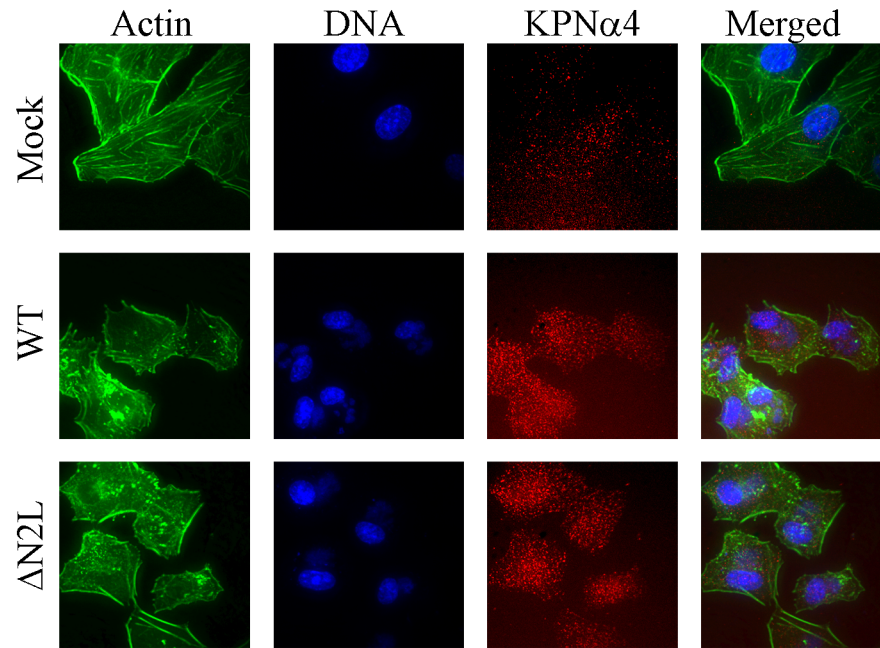
**Figure 5-7: N2 does not alter the localization of KPNα4.** BSC40 cells were infected with the indicated viruses for 6 hours. The cells were then stained with rhodamine phalloidin, DAPI, and the KPNα4 antibody to visualize actin, DNA, and KPNα4 respectively. Cells were images using a Deltavision microscope at 60X.

did not perturb its predominantly nuclear distribution (**Figure 5-8**). We also tested how this protein would behave in cells infected with WT or ΔN2L viruses, and again saw no effects on the distribution of the fluorescence (**Figure 5-9**). Second, this study was stimulated by the original observation that topoisomerase II is recruited to VACV factories [44], and is trafficked into the nucleus using KPNα1, α2 and α4 [127], so we also tested whether N2L affected this process. Again, no obvious differences were seen in the amounts of topoisomerase IIα/β recruited to virus factories in the presence or absence of N2L (**Figure 5-10**). Finally, it is well understood that α-amanitin classically targets cellular RNA polymerase II [128], and we wondered if the postulated link between N2L and α-amanitin resistant viruses might somehow reflect an effect of N2 on levels of cytoplasmic RNA polymerase II. Again, no obvious differences were seen in the distribution of RNA polymerase II in cells infected with WT, ΔN2L, and rN2L viruses (**Figure 5-11**). These observations show that N2 is not affecting the nucleocytoplasmic shuttling of several ordinary proteins, at least one of which is known to use the same KPNs bound by N2.

### 5.2.5. N2 can bind to ssDNA cellulose

Because N2 localizes to the nucleus and inhibits the NFκB sensitive promoter, we wanted to look into any DNA binding properties of N2. Since the recombinant N2-His protein formed inclusion bodies, we used whole cell lysates from BSC40 infected cells. The lysates were obtained after a six hour infection, and were incubated with ssDNA cellulose. After allowing the protein(s) to bind to
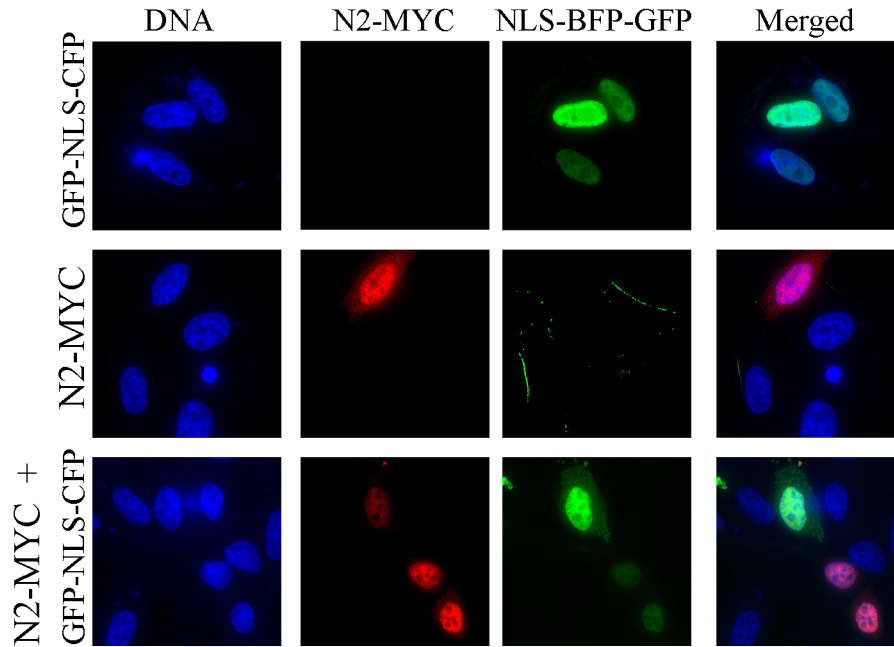
**Figure 5-8: N2 does not alter the localization of a NLS-BFP-GFP reporter protein in the absence of VACV infection.** HeLa cells were transfected with 150ng of either the NLS-BFP-GFP reporter plasmid, the C-terminal N2-MYC tagged construct under the CMV promoter, or they were transfected with a mixture of both plasmids. Cells were fixed 18 hpi then stained with DAPI and the αMYC antibody to visualize DNA and the N2-MYC tagged protein respectively. Images were taken using a Deltavision microscope at 60X.
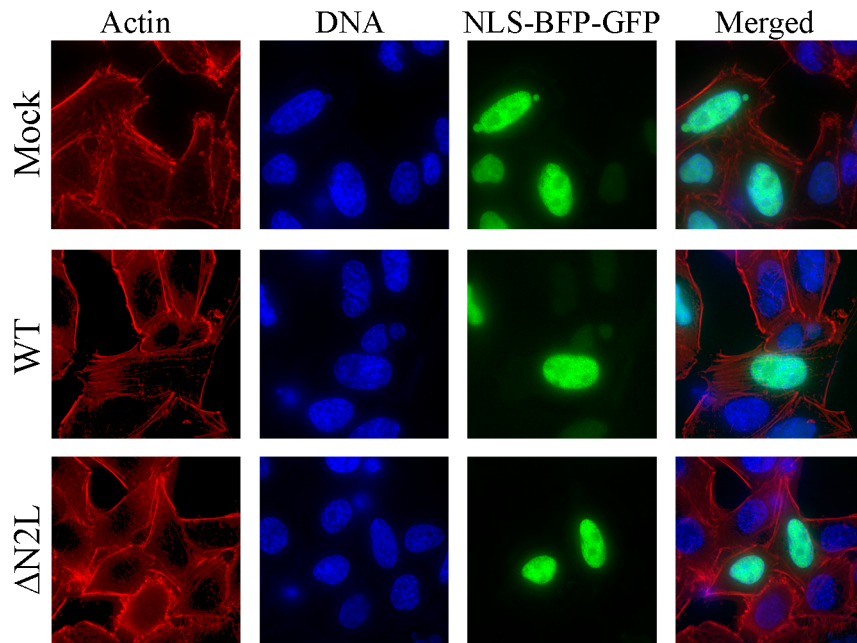
**Figure 5-9: The presence N2 during a VACV infection does not effect the localization of a NLS-BFP-GFP reporter protein.** HeLa cells were transfect with a reporter plasmid that consists of enhanced blue and green fluorescent proteins fused together and bearing a N-terminal bipartite SV40 NLS. After 24 hours, the cells were infected with the indicated viruses for 6 hours. The cells were then fixed and stained with rhodamine phalloidin and DAPI to visualize actin and DNA respectively. Images were taken using a Deltavision microscope at 60X.
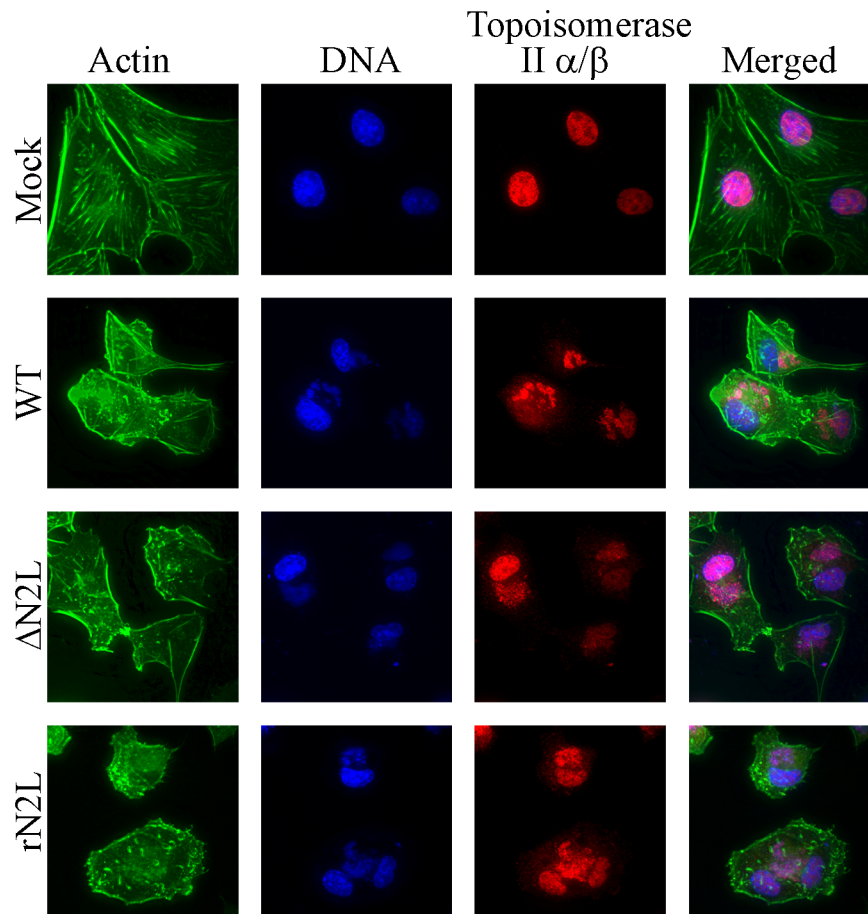
**Figure 5-10: N2 does not alter the localization of Topoisomerase IIα/β.** BSC40 cells were infected with the indicated viruses for 6 hours. The cells were then fixed and stained with rhodamine phalloidin, DAPI, and topoisomerase II α/β to visualize actin, DNA, and topoisomerase II α/β respectively. Images were taken using a Deltavision microscope at 60X.
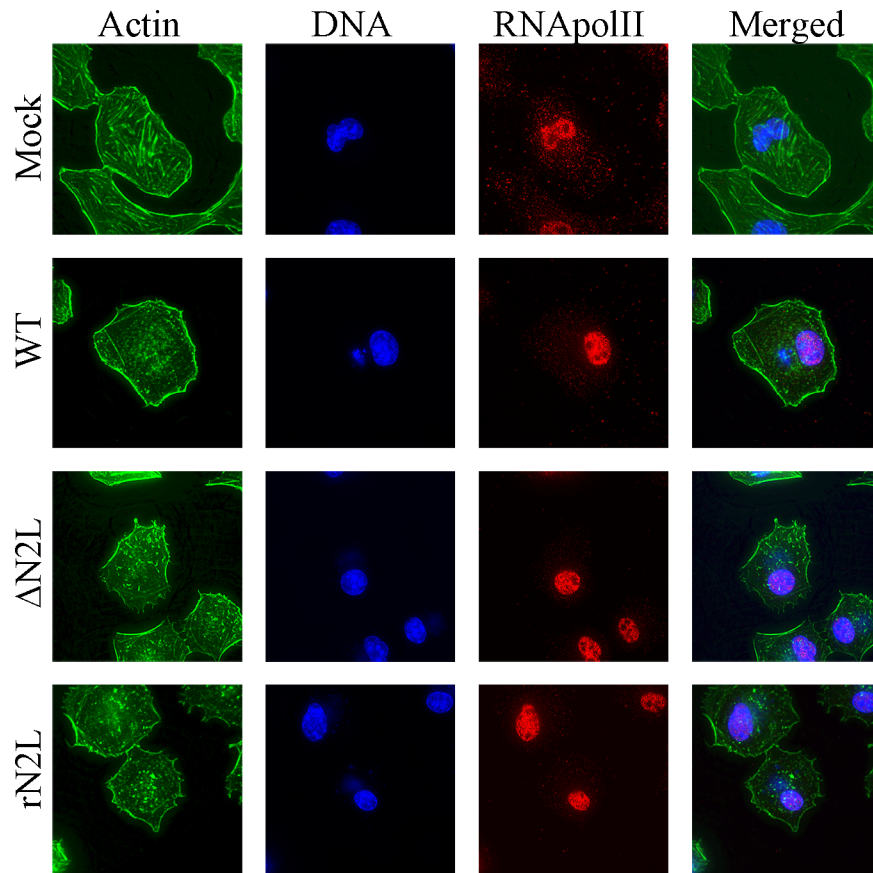
**Figure 5-11: N2 does not effect the localization of RNApolII.** BSC40 cells were infected with the indicated viruses for 8 hours. The cells were then fixed and stained with rhodamine phalloidin, DAPI, and RNApolII antibody to visualize actin, DNA, and RNApolII. Images were taken using a Deltavision microscope at 60X.

the ssDNA cellulose, the lysate was removed and the ssDNA cellulose was washed in a low salt solution. To remove any proteins bound to the ssDNA cellulose, increasing amounts of salt concentrations were used. The VACV I3 (SSB) protein is known to bind DNA and it elutes off the ssDNA cellulose at 2 M NaCl. Interestingly, N2 also associated with the ssDNA cellulose, either directly or indirectly through a protein complex as it was eluted off the ssDNA cellulose at 0.5 M NaCl (**Figure 5-12**).

## 5.2.6. The presence of N2 delays nuclear transport

In light of our observation that during infection with ΔN2L KPNα2 accumulates at the nuclear periphery, we decided to determine if and how N2 is interfering with the nuclear transport system. For this, we expressed GFP tagged KPNα2 or KPNα4 in BSC40 cells and infected the cells with WT, the marker free ΔN2L, or rN2L viruses. In each condition, we photobleached the entire nucleus and measured for the subsequent recovery of the KPN-GFP molecules. Data analysis for the recovery of GFP-KPNα4 did not indicate significant differences despite the presence of absence of N2L. Conversely, when examining GFP-KPNα2, we observed a marked decrease in the rate of nuclear fluorescence recovery when comparing mock and WT infected cells (**Figure 5-13**). The recovery half time (T ½) of KPNα2-GFP in a WT infection is 23.12 seconds, whereas the half time for the Mock and ΔN2L infections was 15.16 and 13.6 seconds respectively (**Figure 5-13**). During WT virus infection, KPNα2 recovery decreases ~ 50%, however, in the absence of N2L (ΔN2L) the rate of recovery
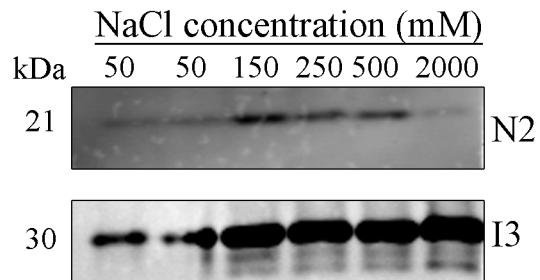
**Figure 5-12: N2 binds to ssDNA cellulose.** BSC40 cells were infected with VACV at an MOI of 5. Monolayers were harvested after 6 hours and whole cell lysates were generated. The lysates were then incubated with ssDNA cellulose. Following the incubation, the lysate was removed and the ssDNA cellulose was washed in a low salt solution. Proteins were removed from the ssDNA cellulose using increasing concentrations of salt. VACV I3 (SSB) is known to bind ssDNA.
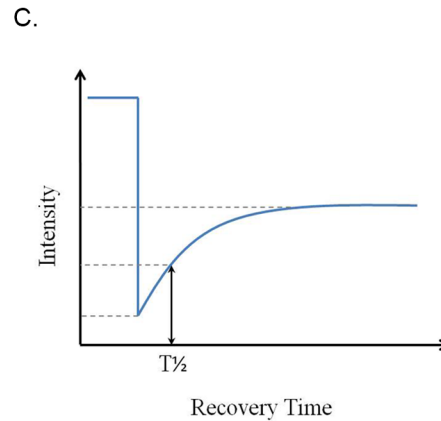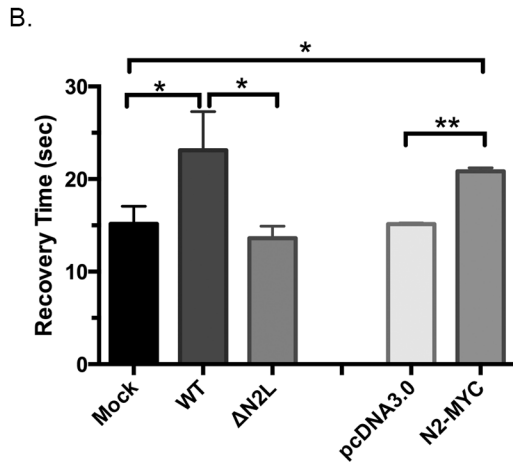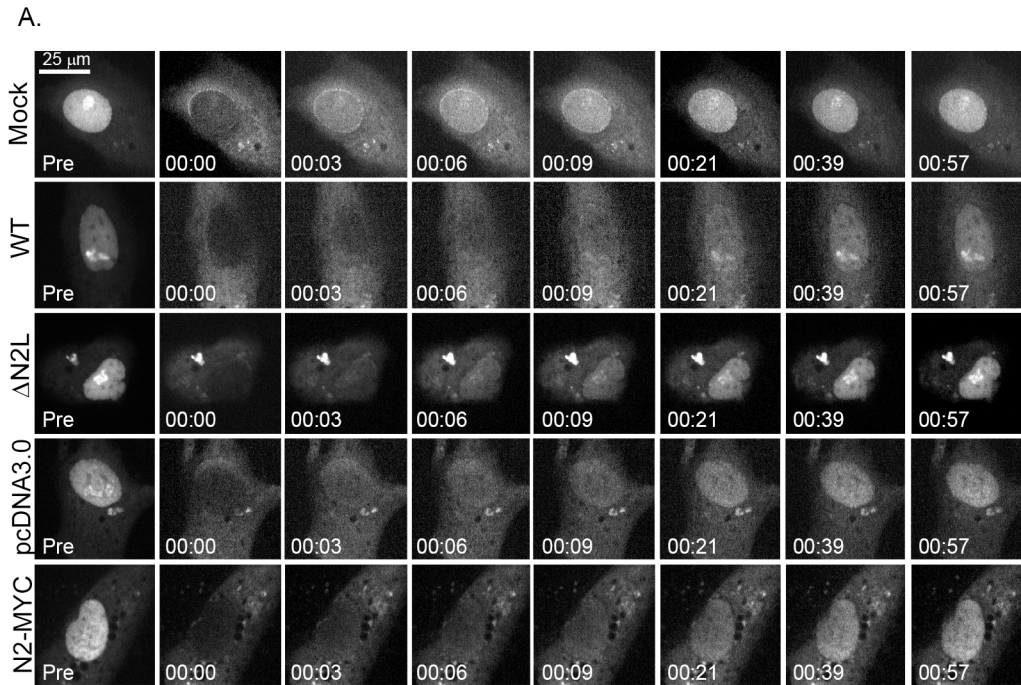
**Figure 5-13: The presense of N2 retards GFP-KPNα2 turnover.** BCS40 cells were transfected with plasmids encoding the GFP-KPNα2 constructs for 20 hours. The cells were then infected with mock, WT, or ΔN2L viruses at an MOI of 5. In parallel, cells were dual transfected with GFP-KPNα2 with either the empty vector pcDNA3.0 or the N2-MYC construct expressed under the CMV promoter. In each case, the presence of N2 delayed the recovery of GFP-KPNα2 into the nucleus (A). The recovery times from three independent experiments (8-10 nuclei per experiment) were measured and the $T_{1/2}$ was calculated and plotted (B). Recovery curve showing how the $T_{1/2}$ is measured (C).

mirrors that of mock infected cells. A similar effect is observed when N2-MYC is expressed in the cells in absence of an infection; the recovery half time mirrors that of a WT infection, whereas the empty vector control behaves like mock infected cells. Analysis of the recovery curves shows that there is a marked difference between the mock and the VACV infected curves indicating that N2 is not the only factor modulating KPNα2 nuclear turnover during infection (**Figure 5-14**).

## 5.3. DISCUSSION

We detected a putative bi-partite NLS in both the VACV O1 and N2 proteins. By tagging the C-terminal ends of both proteins with a FLAG (O1) or MYC (N2) tag, we determined that O1 localized to the cytoplasm whereas N2 localized to the nucleus. Analysis of the published sequence data showed that VACV N2L is highly conserved in the Orthopoxvirus genus with the exceptions of camelpox and taterapox which encoded a truncated version of N2. The NLS is highly conserved in the full length proteins, however the NLS in taterapox and camelpox is either partially or completely disrupted. The presence of the bipartite NLS implies that N2 may normally localize to the nucleus. By generating both the N- and C- terminal tagged N2 proteins, we were able to confirm that N2 does localize to the nucleus. This is also true when N2 is expressed both with the synthetic pox E/L promoter as well as in the absence of infection using a CMV promoter.

Because N2 has an NLS, it may use the host KPN proteins to translocate
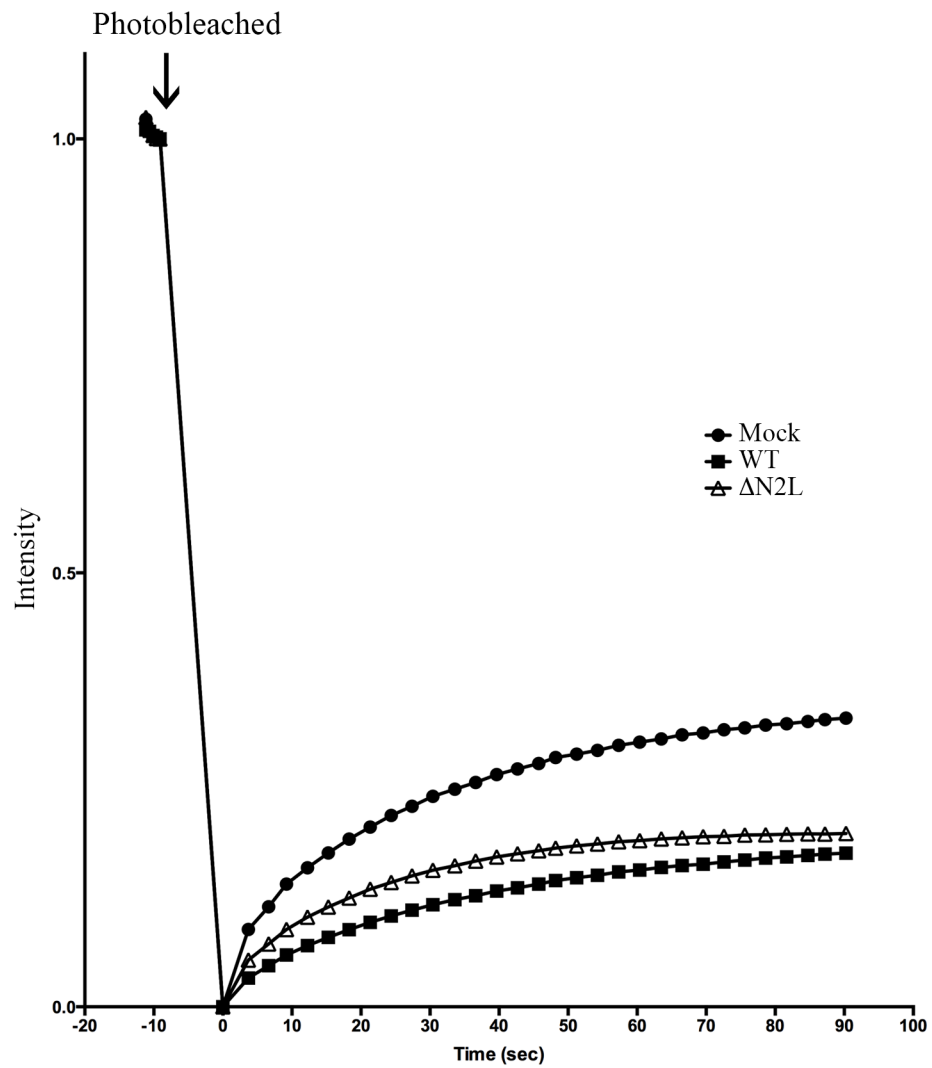
**Figure 5-14: VACV has additional N2-independent mechanisms for disrupting host nuclear transport.** The total recovery curves show a large difference between mock infected samples and ΔN2L virus infected samples. This difference suggests that there are additional N2-independent mechanism(s) that VACV uses to inhibit host nuclear transport.

into the nucleus. Furthermore, it was predicted that N2 interacted with KPNα2 and KPNα5 through a yeast-two hybrid screen [129]. Zhang *et al*. were able to confirm the interaction with KPNα2 but not KPNα5 through a GST pull-down [126]. To determine if N2 uses this machinery, protein interactions were tested by immunoprecipitation. N2 co-precipitated with two of the six KPN alpha proteins, KPNα2 and KPNα4. Our data confirms that N2 interacts with KPNα2 during infection and further extends this interaction to include KPNα4. False positive hits are common in yeast-two hybrid screens. The discrepancy between KPN molecules is likely due to the nomenclature of KPNs or the similarity between the proteins. This observation that N2 binds KPNα2 and KPNα4 could support at least two, not mutually exclusive, models for N2 function. First it may just reflect the fact that N2 employs KPNα2 and KPNα4 transport partners to translocate into the nucleus. Alternatively, it may indicate that N2 binding to karyopherins plays some role in modulating or interfering with the activities of protein nuclear transport systems, a function that would have obvious advantages for VACV, given that nuclear promoters are the ultimate targets of many antiviral signal transduction networks.

We also examined how the KPN alpha isoforms and certain host proteins would behave in the presence or absence of N2. In terms of KPNs α1 and α4, we saw no effect on the proteins localization between different virus treatments. However, we saw that KPNα2 accumulated around the nucleus when N2 is absent from the infection. These data suggest that N2 can somehow suppress a cellular system that is triggered by replicating VACV, and which when activated causes

the re-localization of KPNα2. We also looked at the effects N2 had on NLS-BFP-GFP (described in **section 2.9.2.**), topoisomerase IIα/β, and RNA polymerase II. In each case, N2 did not affect the localization of any of these proteins. The NLS-BFP-GFP reporter still localized to the nucleus, topoisomerase IIα/β was still recruited to the viral factories, and RNA polymerase II was still predominantly found in the nucleus.

To further investigate how N2 affects nuclear transport, we employed FRAP. We photobleached the entire nucleus in either mock, WT or ΔN2L infected samples and measured the recovery of GFP-KPNα2. We discovered that in the absence of N2, GFP-KPNα2 recovers at a faster rate and to higher quantities when compared to the WT infected samples. This is also true in the absence of infection, while N2 is expressed from a CMV promoter. These data provide us with two potential hypotheses. The first hypothesis suggests that N2 is simply using the host nuclear transport machinery to enter the nucleus. Under this assumption, there is a greater amount of KPNs inside the nucleus in WT infected cells as opposed to when N2 is absent from infection. Therefore, when the nucleus is photobleached, a greater proportion of the total cellular KPN-GFP signal is bleached and results in a slower recovery of GFP-KPN. The second hypothesis is that N2 is directly interfering with nuclear transport. Because the KPNα2 recovers faster in the absence of N2, one can reason that N2 functions to delay nuclear transport. We also examined the effects myxoma virus had on the GFP-KPNα2 molecules since it lacks an N2 homology (**Figure 5-15**). Surprisingly, myxoma virus behaved like the WT virus opposed to the ΔN2L virus. This suggests that
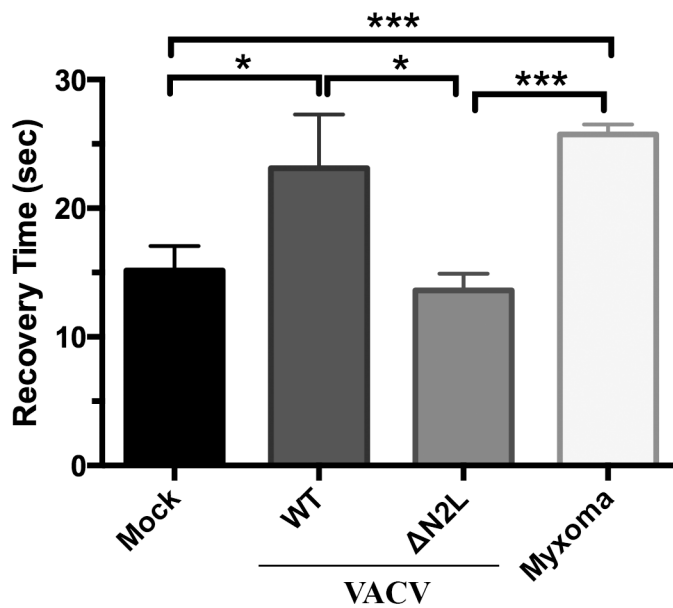
**Figure 5-15: Inhibition of nuclear transport is not specific to Orthopoxviruses.** We also tested what effects myxoma virus would have on the GFP-KPNα2 molecule since it lacks an N2 homolog. Surprisingly, myxoma behaved like the WT VACV virus. This data suggests that Orthopoxviruses are not the only genera that inhibit host nuclear transport. (Note: Data from Figure 5-13B is replotted for comparison).

there are additional mechanisms that poxviruses use to inhibit host nuclear transport. It is also important to note that these experiments were done using tranfections and over expression may affect the outcome of the experiment. As well, the KPNs were tagged with GFP and GFP on its own is known to localize to the nucleus to some extent. This GFP fusion may affect the natural localization of the KPN proteins.

In summary, we have shown that N2 localizes to the host nucleus, as well it interacts with two host KPN alpha proteins. Although N2 does not alter the localization of several host nuclear proteins, we found that it does change the localization of KPNα2. Furthermore, we demonstrated through FRAP that N2 delays the recovery of KPNα2-GFP. Our FRAP also uncovered an alternate N2 independent mechanism that poxviruses use to inhibit host nuclear transport.

# CHAPTER 6 – CONCLUSIONS AND FUTURE DIRECTIONS

## 6.1. OVERVIEW

Earlier findings that the cellular topoisomerase II$\alpha$/$\beta$ localized to viral factories [44] led us to investigate the VACV N2 protein, which was identified in a bioinformatic screen of VACV proteins that contained an NLS. We hypothesized that because N2 had a NLS and localized to the nucleus, it may play a role in interfering or regulating host nuclear transport. A yeast-two hybrid screen identified KPN$\alpha$2 and KPN$\alpha$5 as potential binding partners of N2, amongst others [129]. To determine if N2 interacted with these karyopherin molecules, we performed co-immunoprecipitions with KPN alpha subunits 1-6. Through this experiment we confirmed that N2 interacted with KPN$\alpha$2 and extended this finding to include KPN$\alpha$4. Our data is consistent with Zhang *et al*. in showing that N2 co-immunoprecipitates with KPN$\alpha$2 but not KPN$\alpha$5 [126]. Further examination of KPN$\alpha$2 through immunofluorescence revealed that during infection with the N2L deletion mutant, KPN$\alpha$2 relocalized and accumulated around the nuclear membrane. Because this phenotype was observed in a fixed sample, we were unable to determine if the KPN$\alpha$2 was trapped at the nuclear membrane, or if was rapidly moving in and out of the nucleus. To investigate how the KPN$\alpha$2 proteins were behaving during the $\Delta$N2L infection, we employed FRAP to study the dynamics of the KPN$\alpha$2 molecules. We discovered that the presence of N2 delayed the recovery of KPN$\alpha$2. Based on our results, we propose that during VACV infection N2 modulates nuclear transport by competing for available KPN in the cell. Our model (**Figure 6-1**) depicts that in the absence of
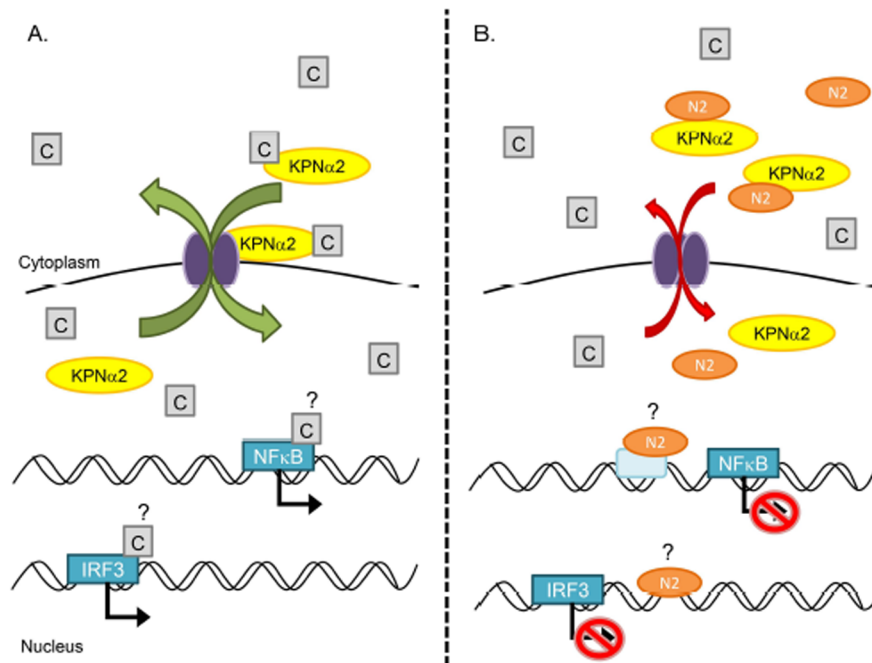
**Figure 6-1: Model of VACV N2 role in disrupting host nuclear transport.** Our model depicts that in the absence of N2 (Panel A) KPNα2 can bind to its cargo, localizes to the nuclear periphery, and transports in and out of the nucleus at a regular rate. In Panel B, when N2 is present during infection, N2 overwhelms KPNα2 preventing it from binding to its regular cargo. N2 is then relocated into the nucleus. This association between N2 and KPNα2 delays the exchange rate of KPNα2. Because N2 is an early protein, its expression peaks between 4 and 6 hours post infection and begins to decline after 12 hrs post infection. It is possible that N2 outcompetes KPN cargoes early in infection to prevent host transcription factors from entering the nucleus. While later in infection, once the virus has started packaging new virions, the amount of N2 is reduced and host nuclear transport is no longer a threat to the virus. Furthermore, once inside the nucleus, N2 may play an additional role. Since N2 associates with DNA, it could be that N2 is binding to DNA directly or indirectly through a transcriton complex, preventing host transcription.

N2, KPNα2 can bind to its cargo, localizes to the nuclear periphery, and transports in and out of the nucleus at a regular rate. When N2 is present during infection, N2 competes for the available KPNα2 to relocate into the nucleus. This association delays the exchange rate of KPNα2. Because N2 is an early protein, its expression peaks between 4 and 6 hours post infection and begins to decline after 12 hrs post infection. It is possible that N2 outcompetes KPN cargoes early in infection to prevent host transcription factors from entering the nucleus. While later in infection, once the virus has started packaging new virions, the amount of N2 is reduced and host nuclear transport is no longer a threat to the virus.

## 6.2. THE ROLE OF N2 DURING VACV INFECTION

When I began this thesis project, little was known about VACV N2. Earlier reports linked N2 to α-amanitin resistance and temperature sensitivity [103, 130, 131], while bioinformatics analysis predicted that N2 belonged to the VACV A46/N1 protein families which target the TLR pathway [116].

To determine if N2 had a role in spread of the virus, we performed a multi-step growth curve and analyzed the plaque morphology of the N2 deletion virus. In the absence of the N2L gene, there was no significant difference in the amount of virus produced during infection. We also determined that N2 had no effect on the plaque morphology. Using the N2 polyclonal anti-serum (described in **Chapter 3**) we were able to confirm that N2 is expressed early during infection since it was still produced in the presence of AraC, which is an inhibitor of VACV late gene expression.

Before further investigation into the function of N2, we revisited an earlier report suggesting that the N2L gene was responsible for temperature sensitivity and α-amanitin resistance [103]. It was proposed that a G-to-T transversion mutation at the -10 position upstream of the N2L start codon was responsible for this phenotype [103]. Looking more closely at the proposed G-to-T transversion mutation, we noted that this site is associated with a sequence polymorphism, being a 'G' in VACV strain WR and some Tian Tan strains [110], and a 'T' in strains Lister, Copenhagen and in all of the Dryvax clones we have recently sequenced [109]. First we analyzed how our N2L mutant viruses along with clones from Dryvax and Tian Tan behaved in the presence of various concentrations of α-amanitin at a permissive and high temperature. We also pre-treated the cells with various concentrations of α-amanitin for different amounts of time before infection with the N2L mutant viruses. In either case, the N2L deletion mutant was still capable of growing in the presence of α-amanitin and it did not show signs of temperature sensitivity. Whether temperature sensitivity, defects in core protein cleavage, replication in enucleated cells, and α-amanitin resistance [103, 130, 131] are all manifestations of mutations linked to N2L is a question that probably should be revisited.

Next we examined if N2 was involved in inhibition of the NFκB pathway. First, we examined if the N2L deletion mutant had any effect on the phosphorylation of the NFkB inhibitor IκBα. No differences were observed when comparing the phosphorylation of IκBα amongst WT, ΔN2L, and rN2L viruses. The phosphorylation of IκBα peaks around 30 minutes after TNFα treatment in

all virus groups, and then starts to decline 60 minutes post treatment. We next examined if N2 had an effect on the translocation of p65 into the nucleus. When the cells were left untreated, the NFκB p65 subunit was found in the cytoplasm during infection with WT, ΔN2L, and rN2L viruses. When we treated the cells with TNFα 30 minutes prior to fixation, we observed p65 localizing to the nucleus in all treatment groups (WT, ΔN2L, and rN2L). From our results, we can conclude that N2 does not affect the phosphorylation of IκBα or the translocation of p65 into the nucleus. This is not surprising since N2 has a nuclear localization while the NFκB p65 subunit is held in the cytoplasm. If N2 inhibits the NFκB activity, it is likely occurring in the nucleus, downstream of p65 subunits translocation into the nucleus.

To determine if N2 inhibits the activity of NFκB in the nucleus, we performed firefly luciferase reporter assays. In absence of a VACV infection, N2 is capable of inhibiting the activity of NFκB. However, Ferguson *et al.* also performed this assay and saw no significant effect of N2 on NFκB activity [81]. We also looked into the virus ability to inhibit the NFκB reporter plasmid and saw no difference between the mock infected wells and the WT, ΔN2L and rN2L viruses. This is likely due to the presence of TNFα during the infection. As previously discussed, in the absence of TNFα, the NFκB subunit p65 remains in the cytoplasm, however upon stimulation with TNFα, p65 localizes to the nucleus. The nuclear localization of p65 was observed all samples (mock infected or WT, ΔN2L, and rN2L viruses infected). Although we did observe a significant

reduction in the activity of the NFκB promoter in the absence of infection, we predict that this is an off target effect from the true function of N2.

Although we determined that N2 is not required for growth in tissue culture, it may be needed *in vivo*. To determine if N2 is a virulence factor, we infected Balb/c mice with the WT, ΔN2L, and rN2L viruses. The mice that were infected with the ΔN2L virus displayed less signs of illness and did not lose a significant amount of weight when compared to the WT group where the mice were very sick. Surprisingly, the rN2L group didn't follow the same infection pattern as the WT group. Although this group did display signs of illness that were significantly different from the ΔN2L group on days 8-10, they did not become as sick as the WT group. This difference between the WT and revertant viruses led us to sequence our recombinant viruses to ensure no additional mutations were introduced. Through our sequencing data, we can clearly see that the N2 locus is completely absent from the ΔN2L virus while it is present, with no errors in the rN2L virus. Further investigation of the sequence led us to identify a single amino acid substitution between the two viruses. The mutation is in the H4L gene, however the impact this mutation has on the virus remains unknown.

In **Chapter 4**, we have shown that N2 is not necessary for growth in tissue culture, however *in vivo* it appears to be a virulence factor. In contrast to publications claiming that N2 is responsible for α-amanitin resistance and temperature sensitivity, we were unable to reproduce these results. We have shown that N2 has no effect of the phosphorylation of IκBα, as well it does not have any effect on the localization of the NFκB p65 subunit. However, N2 is still

able to inhibit the activity of the NFκB promoter.

## 6.3. THE ROLE OF N2 DURING HOST NUCLEAR TRANSPORT

A bioinformatics search of the poxvirus proteome identified VACV N2 amongst a few others of proteins containing a putative bi-partite NLS. Analysis of the N2L gene in the Orthopoxvirus genus showed that N2L is highly conserved in this genus. However both camelpox and taterapox encode a truncated N2. The NLS is highly conserved in the full length proteins but is either partially or completely disrupted in the truncated versions. The presence of the NLS suggests that N2 may normally localize to the nucleus. We confirmed that N2 did localize to the nucleus by generating both N- and C- terminal tagged N2 proteins driven by the synthetic pox E/L promoter. Interestingly, N2 still localized to the nucleus in the absence of infection when expressed from a CMV promoter.

Proteins bearing an NLS are known to translocate to the nucleus through the host KPN proteins [132]. To determine if N2 interacts with these import proteins, we performed immunoprecipitations. We determined that N2 interacted with two of the six tested KPN isoforms, KPNα2 and KPNα4. This data confirms the *in vitro* GST pull-down performed by *Zhang et al*. where they reported N2 interacted with KPNα2 but not with KPNα5 [126], which was the other KPN that came out of the yeast two-hybrid screen [129]. Our data extends their finding to include KPNα4. This observation that N2 binds KPNα2 and KPNα4 could support at least two, not mutually exclusive, models for N2 function. First it may just reflect the fact that N2 employs KPNα2 and KPNα4 transport partners to

translocate into the nucleus. However, the size of the protein renders it unclear why N2 would need to be actively transported by the karyopherin/importin system, as 21 kDa is below the ~60 kDa cut off for spontaneous diffusion through the nuclear pore [133]. Alternatively, it may indicate that N2 binding to KPNs plays some role in modulating or interfering with the activities of protein nuclear transport systems, a function that would have obvious advantages for VACV, given that nuclear promoters are the ultimate targets of many antiviral signal transduction networks.

Because some viruses are known to sequester KPN proteins to cytoplasmic sites to prevent host nuclear transport, we examined whether N2 would alter the localization of the KPNs. We only saw an effect with KPNα2. When N2 is absent from the infection, KPNα2 accumulated around the nucleus. This data suggests that N2 alters the hosts nuclear transport system. Because we were looking at a static data point, we are unable to conclude how transport was being affected. Next we investigated the effects N2 had on reporter proteins (NLS-BFP-GFP) and select host proteins (topoisomerase IIα/β and RNA polymerase II). In each case, N2 did not affect the localization of any of these proteins.

To further investigate if N2 was inhibiting or promoting nuclear transport, we employed FRAP. Our FRAP data shows that in the absence of N2, nuclear KPNα2 recovers at a faster rate and to higher quantities when compared to the WT infected samples. This is also true in the absence of infection, while N2 is expressed from a CMV promoter. Once again, these data provide us with two

potential hypotheses. One being that N2 is using the transport machinery to enter the nucleus and in turn is promoting nuclear transport. Under this assumption, there is a greater amount of KPNs inside the nucleus in WT infected cells as opposed to when N2 is absent from infection. As a result, when photobleaching the nucleus a greater proportion of the total cellular KPN-GFP signal is bleached and therefore leads to a slower recovery of KPN back into the nucleus. The second hypothesis is that N2 is directly interfering with nuclear transport. Because the KPN$\alpha$2 recovers faster in the absence of N2, one can reason that N2 functions to retard nuclear transport.

Because VACV replicates in the cytoplasm, studies focusing on the nucleus and its role in the poxvirus lifecycle have been limited. However, there are numerous instances where other viruses are known to target the nuclear transport pathway to manipulate cellular processes as well as inhibit the host antiviral response to facilitate viral replication (reviewed in **Chapter 1**). Although we have only scratched the surface, our findings are the first to demonstrate how an OPV protein might modulate host nuclear transport. Even though this study is the first to propose a mechanism of how VACV interferes with nuclear transport, we are not the first to show the interplay of the nucleus in the poxvirus lifecycle. Sivan *et al*. recently demonstrated a role for nuclear pore proteins in virion morphogenesis through human genome-wide RNAi screens [43]. Of the six nuclear pore proteins that were identified in this screen, Sivan *et al*. investigated the role of Nup62 [43]. Their results showed that knocking down nuclear pore genes reduced VACV spread, specifically through delaying the formation of

mature virions [43]. However it remains uncertain if this interference with the NPC prevents cellular molecules from exiting the nucleus or prevents access to the nucleus for viral defense proteins [43].

In conclusion, our study demonstrates that the host nuclear transport pathway is yet another pathway VACV targets to reduce the cellular antiviral response. Further research is still necessary for uncovering additional VACV proteins involved in this pathway, as well as the implications this has on the host cell.

## 6.4. FUTURE DIRECTIONS

### 6.4.1. Mechanism in which N2 acts on IRF3

Ferguson *et al*. demonstrated that VACV N2 is a nuclear inhibitor of IRF3 [81]. However, the mechanism of action of N2 on IRF3 remains unknown. Although we've shown that N2 interacts with KPN$\alpha$2 and KPN$\alpha$4, and proposed that N2 competes for KPN cargoes, IRF3 is still translocated into the nucleus. Ferguson *et al*. showed that N2 had no effect on IRF3 phosphorylation or translocation into the nucleus, concluding that N2 inhibits IRF3 downstream of its activation [81]. In our studies we've shown N2 to have a slight association with ssDNA cellulose. From this data we proposed that N2 may be binding directly to the DNA or indirectly to a transcriptional complex. Whether this interaction is responsible for the reduction of IRF3 activity remains unknown. Therefore, further work is still needed to determine if N2 is disrupting the assembly or function of the transcriptional complex inside the nucleus.

To determine if N2 binds to the promoter of the transcription factor IRF3 Chromatin Immunoprecipitation (CHiP) assays can be used. The advantage of this method is that analysis is done in a live cell. In order to perform CHiP, one must have a known target protein (VACV N2) and DNA sequence (IRF3 promoter) that is to be analyzed. This method can also be used to determine if N2 prevents IRF3 from binding to its own promoter sequence.

A DNA pull-down assay can also be used to determine the identity of an unknown DNA sequence. In this scenario, the DNA-protein complex is isolated with the antibody to N2. The unknown DNA sequence can be detected through Southern blot, PCR, or sequencing. One limitation is that the antibodies for the native proteins need to be very specific.

### 6.4.2. Additional protein interactions with host proteins

In the yeast-two hybrid screen performed by Van Vliet *et al*., N2 was reported to interact with 18 cellular proteins [129]. Although this method is prone to false-positives [129], Zhang *et al*. confirmed three of these hits to be true interactions [126]. My study verified the functional consequence of the N2-importin $\alpha$1 (KNP$\alpha$2) interaction. However, it remains unclear how N2 interacts with the other two hits, VCPIP1 and PLSCR4, which were confirmed as a positive hits through GST pull-down assays [126]. Because these experiments were performed *in vitro*, it would be necessary to verify these proteins interact with N2 *in vivo* before further investigation.

VCPIP1 is a deubiquitinating protein that associates with the ER and Golgi [134]. The Golgi is a cellular organelle that plays an important role in intracellular membrane trafficking and it is known that VCPIP1 is required for Golgi assembly and ER network formation [134]. Deubiquitinases (DUBs) have an essential role in several cellular processes including transcription, cell cycle progression, signal transduction pathways, apoptosis, DNA damage repair pathways, as well as others [135]. More recent, DUBs have been reported to play a role in the life cycle of human pathogens, including viruses [135]. Viruses use DUBs to promote their replication, evade the host immune response, and promote the viral infection and its survival [135]. Viruses can either hijack cellular DUBs or they can encode for their own [135]. It remains unclear how N2 interacts with VCPIP1 or how that affects cellular process. As mentioned above, VCPIP1 associates with the ER and Golgi while N2 localizes to the nucleus. In the study done by Ferguson *et al*. N2 localized strictly to the nucleus at early time points during infection while it was found in both the nucleus and cytoplasm during late times post infection [81]. Because these two proteins localize to different cellular structures, the first question to answer would be to determine if they colocalize in the cell or if the presence of N2 alters the localization of VCPIP1.

The PLSCR4 protein is a phospholipid scramblase whose function is yet to be determined [136]. Scrambalases are proteins that span the lipid bilayer and are responsible for translocating phospholipids. The PLSCR4 protein belongs to a family of proteins that are thought to be involved in disrupting the plasma membrane phospholipid asymmetry during critical cellular events such as

apoptosis [136]. Interestingly, this family has a conserved DNA binding motif. However, DNA binding was only demonstrated with the PLSCR1 protein [136]. Additionally, a non-classical NLS was found in PLSCR1 and was found with slight modifications throughout the remaining family proteins [136]. Another region of interest is the cysteine-palmitoylation motif, which regulates its trafficking to the nucleus or plasma membrane [136]. It is thought that members of the PLSCR family play an important role in both the intrinsic and extrinsic apoptotic pathways [136]. For example, the PLSCR3 protein is thought to facilitate mitochondrial targeting of t-Bid, which in turn activates Bax and Bak proteins that aid in the release of cytochrome c [136]. As already mentioned, however, the function of PLSCR4 has yet to be determined. It would be of great interest to examine PLSCR4 cellular localization and biological function. Furthermore, it would be interesting to see if VACV N2 has any effects on the protein, whether altering its localization, binding to DNA through PLSCR4, or preventing the activation of apoptosis.

Finally, from the original list of 18 potential protein interactions [129], only 4 were tested (KPNA2, KPNA5, VCPIP1, and PLSCR4) in GST pull-downs [126]. It would not only be interesting but essential to learn of any additional proteins N2 interacts with to determine its full role in VACV lifecycle.

### 6.4.3. Do any other VACV proteins modulate host nuclear transport?

In this study, we showed that N2 interacted with two host KPN proteins and delayed the turnover rate of KPNα2 during infection. It is also important to

note that the nuclear pore was recently shown to be required for viral morphogenesis [43]. However, it is unknown whether disrupting nuclear pore function restricts cellular proteins from entering or exiting the nucleus or if it prevents viral proteins from entering the nucleus. Regardless, these two studies demonstrate the importance of the nucleus during infection, which leads us to wonder what other viral proteins may take part in this process.

From our FRAP experiment, there is an obvious difference in the total recovery between the Mock and ΔN2L infected samples. This difference suggests that there are additional, N2-independent, mechanisms that exist to modulate nuclear transport. More interestingly, if we reexamine the yeast-two hybrid screen, it is predicted that the VACV D1R gene product, which forms the large subunit of the mRNA capping enzyme [137], interacts with the nuclear pore protein, Nup62 [129]. This interaction has yet to be confirmed through immunoprecipitation studies, however, if it does prove to be a true interaction it would provide more evidence of VACV interacting with the host nucleus.

## 6.5. CONCLUDING REMARKS

In order to promote viral replication and spread, there are a variety of strategies viruses have developed in an attempt to regulate both the nuclear pore complex as well the nuclear transport process [89, 90]. Here, we demonstrated that VACV interferes with the host nuclear transport system through N2 by competing for available KPNα2 and reducing the KPNα2 turnover rate. Our data supports recent findings that the nucleus plays a significant role in the VACV

lifecycle [41, 138] as well as the newly discovered insight that the nuclear pore proteins are essential for virion morphogenesis [43]. Interestingly, analysis of total recovery during the FRAP experiments suggests additional, N2 independent, mechanisms modulating nuclear transport exist. Furthermore, myxoma virus, which lacks an N2 homolog, also exhibited a reduction in the turnover of KPN$\alpha$2 similar to that of WT VACV, suggesting that this mechanism is not exclusive for orthopoxviruses.

# REFERENCES

1.  Riedel, S., *Edward Jenner and the history of smallpox and vaccination.* Proc (Bayl Univ Med Cent), 2005. **18**(1): p. 21-5.
2.  Li, Y., et al., *On the origin of smallpox: correlating variola phylogenics with historical smallpox records.* Proc Natl Acad Sci U S A, 2007. **104**(40): p. 15787-92.
3.  Pauli, G., et al., *Orthopox Viruses: Infections in Humans.* Transfus Med Hemother, 2010. **37**(6): p. 351-364.
4.  Ellner, P.D., *Smallpox: gone but not forgotten.* Infection, 1998. **26**(5): p. 263-9.
5.  Massung, R.F., et al., *Analysis of the complete genome of smallpox variola major virus strain Bangladesh-1975.* Virology, 1994. **201**(2): p. 215-40.
6.  Behbehani, A.M., *The smallpox story: life and death of an old disease.* Microbiol Rev, 1983. **47**(4): p. 455-509.
7.  Langford, R.E., *Introduction to weapons of mass destruction : radiological, chemical, and biological*. 2004, Hoboken, N.J.: Wiley-Interscience. xxv, 394 p.
8.  Janeway, C.A., *Immunobiology : the immune system in health and disease*. 5th ed. 2001, New York: Garland Publ. xviii, 732 p.
9.  Tan, S.Y., *Edward Jenner (1749-1823): conqueror of smallpox.* Singapore Med J, 2004. **45**(11): p. 507-8.
10. Winkelstein, W., *Not just a country doctor: Edward Jenner, scientist.* Epidemiol Rev, 1992. **14**: p. 1-15.
11. Morgan, A.J. and S. Parker, *Translational mini-review series on vaccines: The Edward Jenner Museum and the history of vaccination.* Clin Exp Immunol, 2007. **147**(3): p. 389-94.
12. Lakhani, S., *Early clinical pathologists: Edward Jenner (1749-1823).* J Clin Pathol, 1992. **45**(9): p. 756-8.
13. Smith, K.A., *Smallpox: can we still learn from the journey to eradication?* Indian J Med Res, 2013. **137**(5): p. 895-9.
14. Baxby, D., *The origins of vaccinia virus.* J Infect Dis, 1977. **136**(3): p. 453-5.
15. Emerson, G.L., et al., *The phylogenetics and ecology of the orthopoxviruses endemic to North America.* PLoS One, 2009. **4**(10): p. e7666.
16. Shchelkunov, S.N., *An increasing danger of zoonotic orthopoxvirus infections.* PLoS Pathog, 2013. **9**(12): p. e1003756.
17. Shchelkunov, S.N., *Orthopoxvirus genes that mediate disease virulence and host tropism.* Adv Virol, 2012. **2012**: p. 524743.
18. Baroudy, B.M., S. Venkatesan, and B. Moss, *Structure and replication of vaccinia virus telomeres.* Cold Spring Harb Symp Quant Biol, 1983. **47 Pt 2**: p. 723-9.
19. Roberts, K.L. and G.L. Smith, *Vaccinia virus morphogenesis and dissemination.* Trends Microbiol, 2008. **16**(10): p. 472-9.
20. Schmidt, F.I., C.K. Bleck, and J. Mercer, *Poxvirus host cell entry.* Curr Opin Virol, 2012. **2**(1): p. 20-7.
21. Moss, B., *Poxvirus entry and membrane fusion.* Virology, 2006. **344**(1): p. 48-54.
22. Hsiao, J.C., C.S. Chung, and W. Chang, *Cell surface proteoglycans are necessary for A27L protein-mediated cell fusion: identification of the N-terminal region of A27L protein as the glycosaminoglycan-binding domain.* J Virol, 1998. **72**(10): p. 8374-9.

23. Lin, C.L., et al., *Vaccinia virus envelope H3L protein binds to cell surface heparan sulfate and is important for intracellular mature virion morphogenesis and virus infection in vitro and in vivo.* J Virol, 2000. **74**(7): p. 3353-65.

24. Hsiao, J.C., C.S. Chung, and W. Chang, *Vaccinia virus envelope D8L protein binds to cell surface chondroitin sulfate and mediates the adsorption of intracellular mature virions to cells.* J Virol, 1999. **73**(10): p. 8750-61.

25. Chiu, W.L., et al., *Vaccinia virus 4c (A26L) protein on intracellular mature virus binds to the extracellular cellular matrix laminin.* J Virol, 2007. **81**(5): p. 2149-57.

26. Foo, C.H., et al., *Vaccinia virus L1 binds to cell surfaces and blocks virus entry independently of glycosaminoglycans.* Virology, 2009. **385**(2): p. 368-82.

27. Beaud, G., *Vaccinia virus DNA replication: a short review.* Biochimie, 1995. **77**(10): p. 774-9.

28. Traktman, P., *DNA Replication in Eukaryotic Cells: Poxvirus DNA Replication.* 1996: Cold Spring Harbor Laboratory Press.

29. Schramm, B. and J.K. Locker, *Cytoplasmic organization of POXvirus DNA replication.* Traffic, 2005. **6**(10): p. 839-46.

30. Broyles, S.S., *Vaccinia virus transcription.* J Gen Virol, 2003. **84**(Pt 9): p. 2293-303.

31. Kovacs, G.R., N. Vasilakis, and B. Moss, *Regulation of viral intermediate gene expression by the vaccinia virus B1 protein kinase.* J Virol, 2001. **75**(9): p. 4048-55.

32. Smith, G.L., et al., *Vaccinia virus immune evasion: mechanisms, virulence and immunogenicity.* J Gen Virol, 2013. **94**(Pt 11): p. 2367-92.

33. Banham, A.H. and G.L. Smith, *Vaccinia virus gene B1R encodes a 34-kDa serine/threonine protein kinase that localizes in cytoplasmic factories and is packaged into virions.* Virology, 1992. **191**(2): p. 803-12.

34. Beaud, G., R. Beaud, and D.P. Leader, *Vaccinia virus gene H5R encodes a protein that is phosphorylated by the multisubstrate vaccinia virus B1R protein kinase.* J Virol, 1995. **69**(3): p. 1819-26.

35. Rochester, S.C. and P. Traktman, *Characterization of the single-stranded DNA binding protein encoded by the vaccinia virus I3 gene.* J Virol, 1998. **72**(4): p. 2917-26.

36. Welsch, S., et al., *The vaccinia virus I3L gene product is localized to a complex endoplasmic reticulum-associated structure that contains the viral parental DNA.* J Virol, 2003. **77**(10): p. 6014-28.

37. Doglio, L., et al., *The Vaccinia virus E8R gene product: a viral membrane protein that is made early in infection and packaged into the virions' core.* J Virol, 2002. **76**(19): p. 9773-86.

38. Tolonen, N., et al., *Vaccinia virus DNA replication occurs in endoplasmic reticulum-enclosed cytoplasmic mini-nuclei.* Mol Biol Cell, 2001. **12**(7): p. 2031-46.

39. Smith, G.L. and A. Vanderplasschen, *Extracellular enveloped vaccinia virus. Entry, egress, and evasion.* Adv Exp Med Biol, 1998. **440**: p. 395-414.

40. Smith, G.L., A. Vanderplasschen, and M. Law, *The formation and function of extracellular enveloped vaccinia virus.* J Gen Virol, 2002. **83**(Pt 12): p. 2915-31.

41. Hruby, D.E., L.A. Guarino, and J.R. Kates, *Vaccinia virus replication. I. Requirement for the host-cell nucleus.* J Virol, 1979. **29**(2): p. 705-15.

42.    Hruby, D.E., D.L. Lynn, and J.R. Kates, *Vaccinia virus replication requires active participation of the host cell transcriptional apparatus.* Proc Natl Acad Sci U S A, 1979. **76**(4): p. 1887-90.

43.    Sivan, G., et al., *Human genome-wide RNAi screen reveals a role for nuclear pore proteins in poxvirus morphogenesis.* Proc Natl Acad Sci U S A, 2013. **110**(9): p. 3519-24.

44.    Lin, Y.C., et al., *Vaccinia virus DNA ligase recruits cellular topoisomerase II to sites of viral replication and assembly.* J Virol, 2008. **82**(12): p. 5922-32.

45.    Oh, J. and S.S. Broyles, *Host cell nuclear proteins are recruited to cytoplasmic vaccinia virus replication complexes.* J Virol, 2005. **79**(20): p. 12852-60.

46.    Ember, S.W., et al., *Vaccinia virus protein C4 inhibits NF-κB activation and promotes virus virulence.* J Gen Virol, 2012. **93**(Pt 10): p. 2098-108.

47.    Unterholzner, L., et al., *Vaccinia virus protein C6 is a virulence factor that binds TBK-1 adaptor proteins and inhibits activation of IRF3 and IRF7.* PLoS Pathog, 2011. **7**(9): p. e1002247.

48.    Fahy, A.S., et al., *Vaccinia virus protein C16 acts intracellularly to modulate the host response and promote virulence.* J Gen Virol, 2008. **89**(Pt 10): p. 2377-87.

49.    Benfield, C.T., et al., *Mapping the IkappaB kinase beta (IKKbeta)-binding interface of the B14 protein, a vaccinia virus inhibitor of IKKbeta-mediated activation of nuclear factor kappaB.* J Biol Chem, 2011. **286**(23): p. 20727-35.

50.    Yuwen, H., et al., *Nuclear localization of a double-stranded RNA-binding protein encoded by the vaccinia virus E3L gene.* Virology, 1993. **195**(2): p. 732-44.

51.    Senkevich, T.G., E.V. Koonin, and B. Moss, *Vaccinia virus F16 protein, a predicted catalytically inactive member of the prokaryotic serine recombinase superfamily, is targeted to nucleoli.* Virology, 2011. **417**(2): p. 334-42.

52.    Takeuchi, O. and S. Akira, *Innate immunity to virus infection.* Immunol Rev, 2009. **227**(1): p. 75-86.

53.    Le Negrate, G., *Viral interference with innate immunity by preventing NF-κB activity.* Cell Microbiol, 2012. **14**(2): p. 168-81.

54.    Goodbourn, S., L. Didcock, and R.E. Randall, *Interferons: cell signalling, immune modulation, antiviral response and virus countermeasures.* J Gen Virol, 2000. **81**(Pt 10): p. 2341-64.

55.    Everett, H. and G. McFadden, *Viruses and apoptosis: meddling with mitochondria.* Virology, 2001. **288**(1): p. 1-7.

56.    Haga, I.R. and A.G. Bowie, *Evasion of innate immunity by vaccinia virus.* Parasitology, 2005. **130 Suppl**: p. S11-25.

57.    Benedict, C.A., P.S. Norris, and C.F. Ware, *To kill or be killed: viral evasion of apoptosis.* Nat Immunol, 2002. **3**(11): p. 1013-8.

58.    Cuconati, A. and E. White, *Viral homologs of BCL-2: role of apoptosis in the regulation of virus infection.* Genes Dev, 2002. **16**(19): p. 2465-78.

59.    Dutta, J., et al., *Current insights into the regulation of programmed cell death by NF-kappaB.* Oncogene, 2006. **25**(51): p. 6800-16.

60.    Hayden, M.S. and S. Ghosh, *NF-κB, the first quarter-century: remarkable progress and outstanding questions.* Genes Dev, 2012. **26**(3): p. 203-34.

61.    Le Page, C., et al., *Interferon activation and innate immunity.* Rev Immunogenet, 2000. **2**(3): p. 374-86.

62.    Ivashkiv, L.B. and L.T. Donlin, *Regulation of type I interferon responses.* Nat Rev Immunol, 2014. **14**(1): p. 36-49.

63.     Talon, J., et al., *Activation of interferon regulatory factor 3 is inhibited by the influenza A virus NS1 protein.* J Virol, 2000. **74**(17): p. 7989-96.

64.     Cárdenas, W.B., et al., *Ebola virus VP35 protein binds double-stranded RNA and inhibits alpha/beta interferon production induced by RIG-I signaling.* J Virol, 2006. **80**(11): p. 5168-78.

65.     Mohamed, M.R. and G. McFadden, *NFkB inhibitors: strategies from poxviruses.* Cell Cycle, 2009. **8**(19): p. 3125-32.

66.     Bahar, M.W., et al., *How vaccinia virus has evolved to subvert the host immune response.* J Struct Biol, 2011. **175**(2): p. 127-34.

67.     Ersing, I., K. Bernhardt, and B.E. Gewurz, *NF-κB and IRF7 pathway activation by Epstein-Barr virus Latent Membrane Protein 1.* Viruses, 2013. **5**(6): p. 1587-606.

68.     Jones, J.O. and A.M. Arvin, *Inhibition of the NF-kappaB pathway by varicella-zoster virus in vitro and in human epidermal cells in vivo.* J Virol, 2006. **80**(11): p. 5113-24.

69.     Stack, J., et al., *Vaccinia virus protein A46R targets multiple Toll-like-interleukin-1 receptor adaptors and contributes to virulence.* J Exp Med, 2005. **201**(6): p. 1007-18.

70.     Graham, S.C., et al., *Vaccinia virus proteins A52 and B14 Share a Bcl-2-like fold but have evolved to inhibit NF-kappaB rather than apoptosis.* PLoS Pathog, 2008. **4**(8): p. e1000128.

71.     Benfield, C.T., et al., *Vaccinia virus protein K7 is a virulence factor that alters the acute immune response to infection.* J Gen Virol, 2013. **94**(Pt 7): p. 1647-57.

72.     DiPerna, G., et al., *Poxvirus protein N1L targets the I-kappaB kinase complex, inhibits signaling to NF-kappaB by the tumor necrosis factor superfamily of receptors, and inhibits NF-kappaB and IRF3 signaling by toll-like receptors.* J Biol Chem, 2004. **279**(35): p. 36570-8.

73.     Chen, R.A., et al., *Inhibition of IkappaB kinase by vaccinia virus virulence factor B14.* PLoS Pathog, 2008. **4**(2): p. e22.

74.     Cooray, S., et al., *Functional and structural studies of the vaccinia virus virulence factor N1 reveal a Bcl-2-like anti-apoptotic protein.* J Gen Virol, 2007. **88**(Pt 6): p. 1656-66.

75.     Kibler, K.V., et al., *Double-stranded RNA is a trigger for apoptosis in vaccinia virus-infected cells.* J Virol, 1997. **71**(3): p. 1992-2003.

76.     Chang, H.W., J.C. Watson, and B.L. Jacobs, *The E3L gene of vaccinia virus encodes an inhibitor of the interferon-induced, double-stranded RNA-dependent protein kinase.* Proc Natl Acad Sci U S A, 1992. **89**(11): p. 4825-9.

77.     Valentine, R. and G.L. Smith, *Inhibition of the RNA polymerase III-mediated dsDNA-sensing pathway of innate immunity by vaccinia virus protein E3.* J Gen Virol, 2010. **91**(Pt 9): p. 2221-9.

78.     Mansur, D.S., et al., *Poxvirus targeting of E3 ligase β-TrCP by molecular mimicry: a mechanism to inhibit NF-κB activation and promote immune evasion and virulence.* PLoS Pathog, 2013. **9**(2): p. e1003183.

79.     Shisler, J.L. and X.L. Jin, *The vaccinia virus K1L gene product inhibits host NF-kappaB activation by preventing IkappaBalpha degradation.* J Virol, 2004. **78**(7): p. 3553-60.

80.     Gedey, R., et al., *Poxviral regulation of the host NF-kappaB response: the vaccinia virus M2L protein inhibits induction of NF-kappaB activation via an ERK2*

*pathway in virus-infected human embryonic kidney cells.* J Virol, 2006. **80**(17): p. 8676-85.

81. Ferguson, B.J., et al., *Vaccinia virus protein N2 is a nuclear IRF3 inhibitor that promotes virulence.* J Gen Virol, 2013. **94**(Pt 9): p. 2070-81.

82. Freitas, N. and C. Cunha, *Mechanisms and signals for the nuclear import of proteins.* Curr Genomics, 2009. **10**(8): p. 550-7.

83. Rout, M.P. and J.D. Aitchison, *The nuclear pore complex as a transport machine.* J Biol Chem, 2001. **276**(20): p. 16593-6.

84. Cooper, G., *The Cell: A Molecular Approach.* Second ed. The Nuclear Envelope and Traffic between the Nucleus and Cytoplasm. 2000: Sunderland (MA): Sinauer Associates.

85. Kustanovich, T. and Y. Rabin, *Metastable network model of protein transport through nuclear pores.* Biophys J, 2004. **86**(4): p. 2008-16.

86. Chook, Y.M. and G. Blobel, *Karyopherins and nuclear import.* Curr Opin Struct Biol, 2001. **11**(6): p. 703-15.

87. Lange, A., et al., *Classical nuclear localization signals: definition, function, and interaction with importin alpha.* J Biol Chem, 2007. **282**(8): p. 5101-5.

88. Terry, L.J., E.B. Shows, and S.R. Wente, *Crossing the nuclear envelope: hierarchical regulation of nucleocytoplasmic transport.* Science, 2007. **318**(5855): p. 1412-6.

89. Fontoura, B.M., P.A. Faria, and D.R. Nussenzveig, *Viral interactions with the nuclear transport machinery: discovering and disrupting pathways.* IUBMB Life, 2005. **57**(2): p. 65-72.

90. Yarbrough, M.L., et al., *Viral subversion of nucleocytoplasmic trafficking.* Traffic, 2014. **15**(2): p. 127-40.

91. Gustin, K.E. and P. Sarnow, *Effects of poliovirus infection on nucleo-cytoplasmic trafficking and nuclear pore complex composition.* EMBO J, 2001. **20**(1-2): p. 240-9.

92. Ghildyal, R., et al., *Rhinovirus 3C protease can localize in the nucleus and alter active and passive nucleocytoplasmic transport.* J Virol, 2009. **83**(14): p. 7349-52.

93. Basta, H.A., et al., *Encephalomyocarditis virus leader is phosphorylated by CK2 and syk as a requirement for subsequent phosphorylation of cellular nucleoporins.* J Virol, 2014. **88**(4): p. 2219-26.

94. Bacot-Davis, V.R. and A.C. Palmenberg, *Encephalomyocarditis virus Leader protein hinge domain is responsible for interactions with Ran GTPase.* Virology, 2013. **443**(1): p. 177-85.

95. Frieman, M., et al., *Severe acute respiratory syndrome coronavirus ORF6 antagonizes STAT1 function by sequestering nuclear import factors on the rough endoplasmic reticulum/Golgi membrane.* J Virol, 2007. **81**(18): p. 9812-24.

96. Reid, S.P., et al., *Ebola virus VP24 binds karyopherin alpha1 and blocks STAT1 nuclear accumulation.* J Virol, 2006. **80**(11): p. 5156-67.

97. Mateo, M., et al., *Ebolavirus VP24 binding to karyopherins is required for inhibition of interferon signaling.* J Virol, 2010. **84**(2): p. 1169-75.

98. Shabman, R.S., et al., *The Ebola virus VP24 protein prevents hnRNP C1/C2 binding to karyopherin α1 and partially alters its nuclear import.* J Infect Dis, 2011. **204 Suppl 3**: p. S904-10.

99. Reid, S.P., et al., *Ebola virus VP24 proteins inhibit the interaction of NPI-1 subfamily karyopherin alpha proteins with activated STAT1.* J Virol, 2007. **81**(24): p. 13469-77.

100. Malik, P., et al., *Herpes simplex virus ICP27 protein directly interacts with the nuclear pore complex through Nup62, inhibiting host nucleocytoplasmic transport pathways.* J Biol Chem, 2012. **287**(15): p. 12277-92.

101. McCraith, S., et al., *Genome-wide analysis of vaccinia virus protein-protein interactions.* Proc Natl Acad Sci U S A, 2000. **97**(9): p. 4879-84.

102. Goebel, S.J., et al., *The complete DNA sequence of vaccinia virus.* Virology, 1990. **179**(1): p. 247-66, 517-63.

103. Tamin, A., J. Esposito, and D. Hruby, *A single nucleotide substitution in the 5'-untranslated region of the vaccinia N2L gene is responsible for both alpha-amanitin-resistant and temperature-sensitive phenotypes.* Virology, 1991. **182**(1): p. 393-6.

104. Villarreal, E.C., N.A. Roseman, and D.E. Hruby, *Isolation of vaccinia virus mutants capable of replicating independently of the host cell nucleus.* J Virol, 1984. **51**(2): p. 359-66.

105. Pennington, T.H. and E.A. Follett, *Vaccinia virus replication in enucleate BSC-1 cells: particle production and synthesis of viral DNA and proteins.* J Virol, 1974. **13**(2): p. 488-93.

106. Wasilenko, S.T., et al., *Vaccinia virus encodes a previously uncharacterized mitochondrial-associated inhibitor of apoptosis.* Proc Natl Acad Sci U S A, 2003. **100**(24): p. 14345-50.

107. Rintoul, J.L., et al., *A selectable and excisable marker system for the rapid creation of recombinant poxviruses.* PLoS One, 2011. **6**(9): p. e24643.

108. Zhang, W. and D.H. Evans, *DNA strand transfer catalyzed by the 5'-3' exonuclease domain of Escherichia coli DNA polymerase I.* Nucleic Acids Res, 1995. **23**(22): p. 4620-7.

109. Qin, L., et al., *Genomic analysis of the vaccinia virus strain variants found in Dryvax vaccine.* J Virol, 2011. **85**(24): p. 13049-60.

110. Qin, L., M. Liang, and D.H. Evans, *Genomic analysis of vaccinia virus strain TianTan provides new insights into the evolution and evolutionary relationships between Orthopoxviruses.* Virology, 2013. **442**(1): p. 59-66.

111. Falkner, F.G. and B. Moss, *Escherichia coli gpt gene provides dominant selection for vaccinia virus open reading frame expression vectors.* J Virol, 1988. **62**(6): p. 1849-54.

112. Isaacs, S.N., G.J. Kotwal, and B. Moss, *Reverse guanine phosphoribosyltransferase selection of recombinant vaccinia viruses.* Virology, 1990. **178**(2): p. 626-30.

113. Shaw, M.L., et al., *Nuclear localization of the Nipah virus W protein allows for inhibition of both virus- and toll-like receptor 3-triggered signaling pathways.* J Virol, 2005. **79**(10): p. 6078-88.

114. Cardarelli, F., et al., *In vivo study of HIV-1 Tat arginine-rich motif unveils its transport properties.* Mol Ther, 2007. **15**(7): p. 1313-22.

115. Isaacs, S.N., *Vaccinia virus and poxvirology methods and protocols*, in *Springer protocols*. 2004, Humana Press: Totowa, N.J. p. 1 online resource (xix, 396 p.).

116. Gonzalez, J.M. and M. Esteban, *A poxvirus Bcl-2-like gene family involved in regulation of host immune response: sequence similarity and evolutionary history.* Virol J, 2010. **7**: p. 59.

117. Morgan, J.R. and B.E. Roberts, *Organization of RNA transcripts from a vaccinia virus early gene cluster.* J Virol, 1984. **51**(2): p. 283-97.

118. Harlow, E. and D. Lane, *Using Antibodies: A Laboratory Manual*. 1999: Cold Spring Harbor Laboratory Press. 495.

119. Harlow, E. and D. Lane, *Antibodies : a laboratory manual*. 1988, Cold Spring Harbor, NY: Cold Spring Harbor Laboratory. xiii, 726 p.

120. García-Arriaza, J., et al., *Deletion of the vaccinia virus N2L gene encoding an inhibitor of IRF3 improves the immunogenicity of MVA expressing HIV-1 antigens.* J Virol, 2014.

121. Thomas, J.G. and F. Baneyx, *Protein misfolding and inclusion body formation in recombinant Escherichia coli cells overexpressing Heat-shock proteins.* J Biol Chem, 1996. **271**(19): p. 11141-7.

122. Lefkowitz, E.J., C. Wang, and C. Upton, *Poxviruses: past, present and future.* Virus Res, 2006. **117**(1): p. 105-18.

123. Yang, Z., et al., *Simultaneous high-resolution analysis of vaccinia virus and host cell transcriptomes by deep RNA sequencing.* Proc Natl Acad Sci U S A, 2010. **107**(25): p. 11513-8.

124. Wiebe, M.S. and P. Traktman, *Poxviral B1 kinase overcomes barrier to autointegration factor, a host defense against virus replication.* Cell Host Microbe, 2007. **1**(3): p. 187-97.

125. Schweneker, M., et al., *The vaccinia virus O1 protein is required for sustained activation of extracellular signal-regulated kinase 1/2 and promotes viral virulence.* J Virol, 2012. **86**(4): p. 2323-36.

126. Zhang, L., et al., *Analysis of vaccinia virus-host protein-protein interactions: validations of yeast two-hybrid screenings.* J Proteome Res, 2009. **8**(9): p. 4311-8.

127. Mirski, S.E., et al., *Topoisomerase II binds importin alpha isoforms and exportin/CRM1 but does not shuttle between the nucleus and cytoplasm in proliferating cells.* Exp Cell Res, 2007. **313**(3): p. 627-37.

128. Jacob, S.T., E.M. Sajdel, and H.N. Munro, *Specific action of alpha-amanitin on mammalian RNA polymerase protein.* Nature, 1970. **225**(5227): p. 60-2.

129. Van Vliet, K., et al., *Poxvirus proteomics and virus-host protein interactions.* Microbiol Mol Biol Rev, 2009. **73**(4): p. 730-49.

130. Tamin, A., et al., *Nucleotide sequence and molecular genetic analysis of the vaccinia virus HindIII N/M region encoding the genes responsible for resistance to alpha-amanitin.* Virology, 1988. **165**(1): p. 141-50.

131. Villarreal, E.C. and D.E. Hruby, *Mapping the genomic location of the gene encoding alpha-amanitin resistance in vaccinia virus mutants.* J Virol, 1986. **57**(1): p. 65-70.

132. Sorokin, A.V., E.R. Kim, and L.P. Ovchinnikov, *Nucleocytoplasmic transport of proteins.* Biochemistry (Mosc), 2007. **72**(13): p. 1439-57.

133. Wang, R. and M.G. Brattain, *The maximal size of protein to diffuse through the nuclear pore is larger than 60kDa.* FEBS Lett, 2007. **581**(17): p. 3164-70.

134.     Uchiyama, K., et al., *VCIP135, a novel essential factor for p97/p47-mediated membrane fusion, is required for Golgi and ER assembly in vivo.* J Cell Biol, 2002. **159**(5): p. 855-66.

135.     Saxena, N. and V. Kumar, *Oncogenic viruses: DUBbing their way to cancer.* Virology Discovery, 2013.

136.     Sahu, S.K., et al., *Phospholipid scramblases: an overview.* Arch Biochem Biophys, 2007. **462**(1): p. 103-14.

137.     Shatzer, A.N., S.E. Kato, and R.C. Condit, *Phenotypic analysis of a temperature sensitive mutant in the large subunit of the vaccinia virus mRNA capping enzyme.* Virology, 2008. **375**(1): p. 236-52.

138.     Hruby, D.E., D.L. Lynn, and J.R. Kates, *Identification of a virus-specified protein in the nucleus of vaccinia virus-infected cells.* J Gen Virol, 1980. **47**(2): p. 293-9.